University of Alberta

The role of the Prader-Willi syndrome obesity protein, MAGEL2 in the proper functioning of circadian rhythm

by

Sara Victoria Weselake

A thesis submitted to the Faculty of Graduate Studies and Research
in partial fulfillment of the requirements for the degree of

Master of Science

in

Medical Sciences – Medical Genetics

Fall, 2010
Edmonton, Alberta

Examining Committee

Dr. Rachel Wevrick, Medical Genetics

Dr. Fred Berry, Medical Genetics

Dr. Heather McDermid, Medical Genetics, Biological Sciences

Dr. Rosaline Godbout, Oncology

Abstract

MAGEL2 is one of the five genes inactivated in Prader-Willi Syndrome (PWS), a genetic disorder that manifests with symptoms of developmental delay and morbid obesity. Magel2 is highly expressed in the suprachiasmatic nucleus, which is the location of the central clock or circadian pacemaker. Magel2 knockout mice exhibit defects in circadian rhythm. I hypothesized that Magel2 plays a role in one of the inter-connecting feedback loops that control circadian rhythm in suprachiasmatic neurons. I determined that Magel2 acts as a repressive protein in the cycle's feedback loop using a luciferase assay. Magel2 exerts its repressive effect by restricting the movement of Bmal1 into the nucleus. Magel2 levels are then reduced by increasing Per2, associated with increase movement into the nucleus, as determined by experiments examining subcellular localization and effects on protein levels. Loss of *Magel2* in PWS may contribute to sleep abnormalities in this disorder, specifically the cycling between different sleep stages.

Acknowledgements

Completing my Master's project was an endeavour which would never have been possible without the knowledge, guidance and support of many individuals. Upon completion of my undergraduate degree, I possessed only a meager level of laboratory experience. Over the past two years I have learned a huge amount about both the practical methods and techniques in medical genetics research as well as achieving a comfort level in presenting to audiences that will serve me well in my future endeavors.

Firstly, I would like to thank my supervisor, Dr. Rachel Wevrick. Her tireless and unfaltering support and assistance through all aspects of my project was so greatly appreciated. While I always knew I could tap on her door to ask a question about an experiment or talk over some results, the freedom she afforded me in my daily work to discover and attempt to work problems out by myself have given me invaluable knowledge in independent learning. Additionally, I am hugely greatful her assistance through my post-Masters endeavors into medicine and facilitation of my decision to complete my thesis outside of Edmonton.

Thanks also to the members my supervisory committee, Dr. Fred Berry and Dr. Heather McDermid. The time you took to analyze and constructively critique my project through all stages was extremely helpful and gave me the benefit of different points of view and backgrounds to generate a more well-rounded knowledge of my topic. I would also like to think Dr. Rosaline Godbout for agreeing to be a member of my examining committee.

Jocelyn Bischof, Dr. Jason Bush, Julia Devos, Xiao Li, Becky Mercer, Qasim Rasi and Alysa Tennese are the wonderful members of the Wevrick lab who I was fortunate to spent my days surrounded by. They made the experience of coming to work every day that much better and have contributed so much to the completion of this work. I especially appreciate the guidance and friendship of Dr. Jason Bush, Joselyn Bischof, and Alysa Tennese. From my first day as a nervous inexperienced student with absolutely not idea of where to begin, Jason was there to kindly and appropriately direct by experiments. Anytime I was

confused about an technical approach or analysis of results, I knew immediately that I could turn to Jason and he would always stop what he was doing a lend me an ear. I will greatly miss our non-work related chats about music, books or life in general and even your jokes that I often found myself the butt of. The bottomless knowledge that Jocelyn provided to all my questions both concerning this project and other aspects of science was indispensible to me. I looked forward to our humor-filled chats everyday and I am so appreciative of having someone I knew I could turn to for honest and constructive advice on any topic. Finally thank you to Alysa for a great friendship and advice about all the lab and medicine questions I approached you with. Your willingness to listen to my anxieties and tirades on any topic means so much to me and your candid and supportive feedback helped me through many a problem.

The information contained in this thesis on sleep and Prader-Willi syndrome largely came out of a directed learning course taught by Dr. Andrea Haqq. I greatly enjoyed this course and the great experience would not have been possible had I not had as fantastic as a person to guide me. I really appreciate all the time she took out of her schedule to help me through the course.

Finally I would like to thank my family who has always been an unfaltering and tremendously positive support in all my academic endeavors. Their consistent belief in my ability to succeed and achieve what I often thought not possible played a vital role in what I have accomplished and means so much to me.

Abbreviations

5-HT	Serotonin
AVP	Arginine vasopressin
bHLH-PAS	Basic helix-loop-helix period aryl single-minded-domain
BR	Blocking reagent
BSA	Bovine serum albumin
CCG	Clock controlled genes
CHX	Cycloheximide
Co-IP	Co-immunoprecipitation
CREB	Cyclic-adenosine monophosphate response element binding protein
CRE	cAMP response elements
CS	Calf serum
CSF	Cerebrospinal fluid
CSNK	Casein family of kinases
CT	Circadian time
DMEM	Dulbecco's modified Eagles's medium
DRN-LC	Dorsal raphe nuclei locus coerulus
DSPS	Delayed sleep phase syndrome
ECL	Enhanced chemiluminescence
EDS	Excessive daytime sleepiness
EEG	Electroencephalogram
ENU	*N*-ethyl-*N*-nitrosourea
EST	Expressed sequence tags
eVLPO	Extended aspect of the ventrolateral preoptic nucleus
FASPS	Familial advanced sleep phase syndrome
FBS	Fetal bovine serum
GABA-A	γ-aminobutyric acid type A
HAT	Histone acetyltransferases
HDAC	Histone deacetylases
GSK-3β	Glycogen synthase kinase-3β

IC	Imprinting centre
LARII	Luciferase Assay Reagent
LH	Lateral hypothalamus
LPT	Lateral pontine tegmentum
MAGE	Melanoma antigen-associated gene
MHD	MAGE homology domain
MSLT	Multiple sleep latency test
NB	Nuclear body
NREM	Non-REM
NPY	Neuropeptide Y
PACAP	Pituitary adenylate-cyclase activating polypeptide
PBS	Phenol buffered saline
PBSX	PBS with 0.05% Triton-X
PC	Precoeruleus
pRGC	Photosensitive retinal ganglion cells
PML	Promyelocytic leukemia nuclear bodies
PPT-LDT	Pedunculopontine tegmentum laterodorsal tegmentum
PSG	Polysomnograph
PVH	Paraventricular hypothalamus
PWS	Prader-Willi Syndrome
REM	Rapid eye movement
RHT	Retinalhypothalamic tract
S&G	Stop & Glo
SCN	Suprachiasmatic nucleus
SDS-PAGE	SDS-polyacrylamide gel electrophoresis
SFM	Serum free media
SLD	Sublaterodorsal nucleus
snoRNA	small nucleolar RNA
SON	Supraoptic nucleus
SOREM	Sleep onset REM
SUMO	Small ubiquitin-related modifier

SWS	Slow wave sleep
UPD	Uniparental disomy
VIP	Vasoactive intestinal peptide

List of Tables

List of Figures

Chapter 1. Introduction

1.1 Prader-Willi Syndrome

1.1.1 Characteristics of Prader-Willi syndrome

Prader-Willi syndrome (PWS) is a genetically complex human obesity syndrome estimated to affect between 10,000 and 25,000 live births, with more recent studies predicting a rate of 1 in 15,000. This makes PWS to date the most common cause of morbid genetic obesity (Goldstone, 2004). The disorder was first documented in the literature in 1956 by Dr. Andrea Prader, Dr. Alexis Labhart, and Dr. Heinrich Willi. The physicians documented similar symptoms in nine patients seen at their clinic and established PWS as a newly defined disorder (Prader et al. 1956, Wevrick 2009). Subsequent to this publication, several case studies, an examination of prevalence of symptoms, and finally a review article in 1968 were published. It was not until 1981, however, that a set of diagnostic criteria was available (Holm et al., 1993; Holm and Laurnen, 1981). An understanding of the genetic basis of this disorder was also published in 1981 but use a diagnostic tool was not available at this time and as a result, underdiagnosis in children and overdiagnosis in obese mentally handicapped adolescents and adults commonly occurred (Holm et al. 1993, Ledbetter et al. 1981). The genetics of Prader-Willi syndrome and its usefulness in diagnosis will be discussed in a later section. Since this information has become more readily available, a new set of diagnostic criteria were established by consensus with a variety of clinical experts and the final criteria published in 1993 by Holm et al.

Three categories of diagnostic criteria subdivide syndrome characteristics into major, minor, and supportive groupings, which include both mental and physical abnormalities (Figure 1). Major criteria include hypotonia, feeding problems in infancy, hyperphagia or obsession with food often leading to obesity, characteristic facial dysmorphia, hypogonadism, global developmental delay, and a deletion on chromosome 5, region q11-13 (5q11-13) (Gunay-Aygun et al., 2001; Holm et al., 1993). Babies

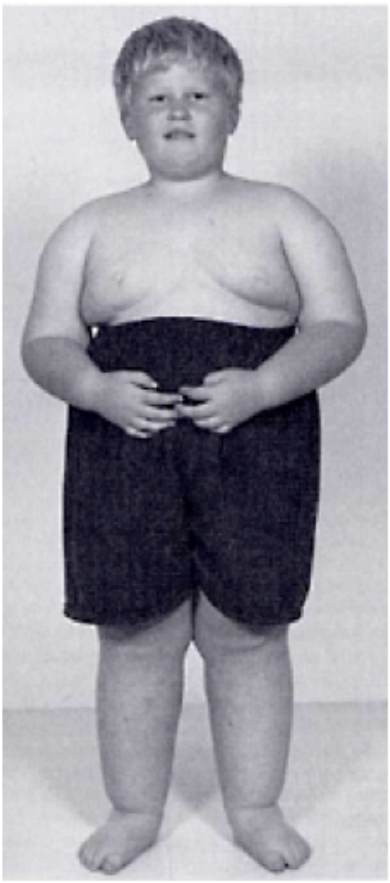

Figure 1. A young boy with the archetypal morphology observed in individuals with Prader-Willi Syndrome (http://medgen.genetics.utah.edu/photographs/diseases/high/420a.gif).

with PWS first present with central hypotonia of varying degrees in the neonatal period and infancy. Hypotonia is pronounced to a degree that babies are often described as "floppy" (Burman et al., 2001). Interestingly, though these individuals may have a normal body mass index, reduced muscle mass is complemented by excess adipose tissue (Kennedy et al., 2006). These symptoms can abate with age but often persist. Feeding problems observed during infancy stand in sharp contrast to the hyperphagia that subsequently manifests and is the most prominent component of PWS. Due to problems with poor suck reflex and apparent lack of hunger, babies gain weight slowly and often require special feeding techniques (Holm et al. 1993). Obesity is a trademark characteristic of PWS, and begins with sudden weight gain at age 1 to 6 years, increasing with age so that one third of PWS patients are more than twice their ideal weight. Characteristic facial features observed in PWS are described as a narrow bifrontal diameter, almond-shaped eyes, and a down-turned, small mouth with a thin upper lip (Goldstone, 2004; Holm et al., 1993). In males, hypogonadism manifests as scrotal underdevelopment, cryptorchidism or lack of testis, or small penis and/or testes. Females present with severe hypoplasia of labia minora and/or of the clitoris. Both sexes also experience delayed or incomplete gonadal maturation causing delayed puberty which manifests as small gonads, decreased facial and body hair, lack of voice change in boys and amenorrhea/oligomenorrhea after age 16 in girls (Crino et al., 2003; Eiholzer et al., 2006). While there are two reports of successful pregnancies in women with PWS following hormone induction, fertility in males has never been documented (Burman et al., 2001; Eiholzer et al., 2006). Hyperphagia and obsession with food is a significant factor in the development of obesity in PWS. Behavioural modification serves as the most effective means to counter these tendencies.

Other minor diagnostic findings include observance of infant lethargy or weak cry that improves with age, behavioural problems, sleep problems and apnea, hypopigmentation, short stature and small hands or feet, narrow hands with straight ulnar borders, esotropia or myopia, thick viscous saliva, difficulties articulating speech, and tendency to skin-pick. The characteristic behaviour

problems encountered with PWS develop during childhood and consist of at least five of: temper tantrums, obsessive and autistic-like behaviours, violent outbursts, manipulative behaviour, perseveration, psychosis, stubbornness, tendency to be argumentative or oppositional, stealing, and lying (Holm et al. 1993, Gunay-Aygun et al. 2001, Wevrick 2009).

Finally, there are a small number of supportive findings which, though not included in scoring during diagnosis, facilitate the identification of PWS. Individuals with PWS may exhibit high pain threshold, decreased vomiting, altered sensitivity to temperature, scoliosis or kyphosis, early adrenarche, osteoporosis, particular unexpected skill with jigsaw puzzles, and normal neuromuscular studies (Gunay-Aygun et al., 2001; Holm et al., 1993). Patients are scored with each major criteria weighing 1 point, and each minor criteria weighing ½ a point. A total of 5 points with at least 4 coming from the major group in children 3 or under, or 8 with 5 or more major group points for those over 3 are required for the diagnosis of PWS. Overall, various features of PWS, namely persistent appetite, altered metabolism, disrupted reproductive ability, and sleep disturbances are indicative of a central hypothalamic developmental defect. The hypothalamus is a cluster of neurons located in the ventral midbrain and serves as a relay centre which integrates information on energy balance through autonomic and sensory feedback (Schwartz, 2004). It is also the location of the body's central clock which plays a critical role in the timing of eating, metabolic activity and sleep (Takahashi et al., 2008).

1.1.2 Sleep abnormalities in Prader-Willi Syndrome

Sleep disruption in PWS is relevant to the study of *Magel2* since loss of this gene leads to a faulty circadian rhythm. The details of the rhythm dysfunction will be described in detail in later sections. However a review of the PWS sleep phenotype will be of relevance in connecting the molecular consequences of *Magel2* loss to a clinical manifestation in the disorder. Excessive daytime sleepiness (EDS) has typically been the characteristic sleep abnormality described

in PWS, reportedly affecting 70 to 85% of individuals. The quality and quantity of sleep is assessed using an electroencephalogram (EEG), which measures brain electrical activity. Non-rapid eye movement sleep (NREM) is the first stage of sleep and occurs in between phases of rapid eye movement (REM). REM sleep is characterized by decreased muscle tone, low-voltage, fast EEG activity, and theta activity (4-7 Hz). Polysomnographs (PSG) examine nighttime sleep, while multiple sleep latency tests (MSLTs) are used to study daytime sleep. A review of a number of studies in which these tests were performed additionally revealed a number of defects in REM sleep in PWS (Goldstone, 2004). These consist of decreased REM sleep latency, sleep onset REM (SOREM), reduced percentage of REM sleep and decreased NREM sleep instability consistent with generalized hypoarousal (Camfferman et al., 2008; Manni et al., 2001; Priano et al., 2006; Verrillo et al., 2009; Vgontzas et al., 1996). Sleep latency indicates the amount of time from lights out to REM sleep onset and is considered abnormal if it is less than 70 minutes. Some individuals with PWS will also fall directly into REM sleep and this is what is meant by SOREM (Carskadon et al., 1986). Narcoleptic-like symptoms, such as sleep attacks, cataplexy, sleep paralysis and hypnagogic hallucinations have been reported at higher than normal levels in PWS patients though there is a great deal of variabilty in the occurrence and presentation of these symptoms.

Various explanations, suggesting a role of sleep apnea or obesity, have been put forth regarding the physiological or neurobiological underpinnings of these sleep problems. These studies, however do not account for the full spectrum of PWS sleep problems as absence or treatment of these symptoms does not completely ameliorate sleep abnormalities (Camfferman et al. 2008, Vgontzas et al. 1996). An alternative explanation of the observed sleep phenotype proposes an association with hypothalamic dysfunction, specifically hypothalamic control of circadian rhythm and NREM/REM cycling (Hertz et al., 1993; Vela-Bueno et al., 1984). I theorize that the sleep dysfunction seen in PWS is based in a defect of circadian rhythm output and hypothalamic neuronal output control of the REM-NREM switch mechanism.

Implicit in the understanding of how the sleep phenotype observed in PWS results from improper regulation of the movement between NREM and REM sleep, is an understanding of the neurobiology of NREM and REM sleep. The most recently proposed model localizes the switch to the mesopontine tegmentum. REM-off neurons are located in the ventrolateral periaqueductal grey matter (vlPAG) and the lateral pontine tegmentum (LPT) receive inhibitory and activating inputs from the extended aspect of the ventrolateral preoptic nucleus and orexin neurons, which promote arousal, respectively. The GABAergic REM-off neurons mutually inhibit GABAergic REM-on neurons located in the precoeruleus (PC) and sublateraodoral nucleus (SLD), forming the flip-flop switch. These two regions may also receive modulatory input from the DRN-LC and PPT-LDT neurons, regions formerly thought to be the location of the REM switch. During NREM sleep, GABAergic REM-off neurons, activated by orexin, inhibit the action of SLD-PC REM-on neurons. This process is reversed during REM sleep, where SLD-PC localized neurons inhibit vlPAG-LPT neurons (Lu et al., 2006).

The sleep phenotype observed in PWS suggests a malfunctioning of the flip-flop switch. Loss of functioning of neurons in both the REM-on and REM-off regions, observed following lesions to these areas, disrupts the correct transitioning pattern between NREM sleep and REM sleep, causing more transitions at inappropriate times (Lu et al., 2006). However, REM-off neurons also receive excitatory input from the orexin neurons in the LH and inhibitory input from the eVLPO. Conceivably then, PWS patients may suffer from improper functioning of these projections. Orexin neurons discharge during active waking, less during quiet waking (lack of movement), and abolish firing during sleep (Lee et al., 2005a). Loss of orexin, orexin neurons or the orexin receptor thus results in narcolepsy, characterized hypersomnolence, SOREMs, and cataplexy or loss of muscle tonus, reminiscent of those observed in PWS.

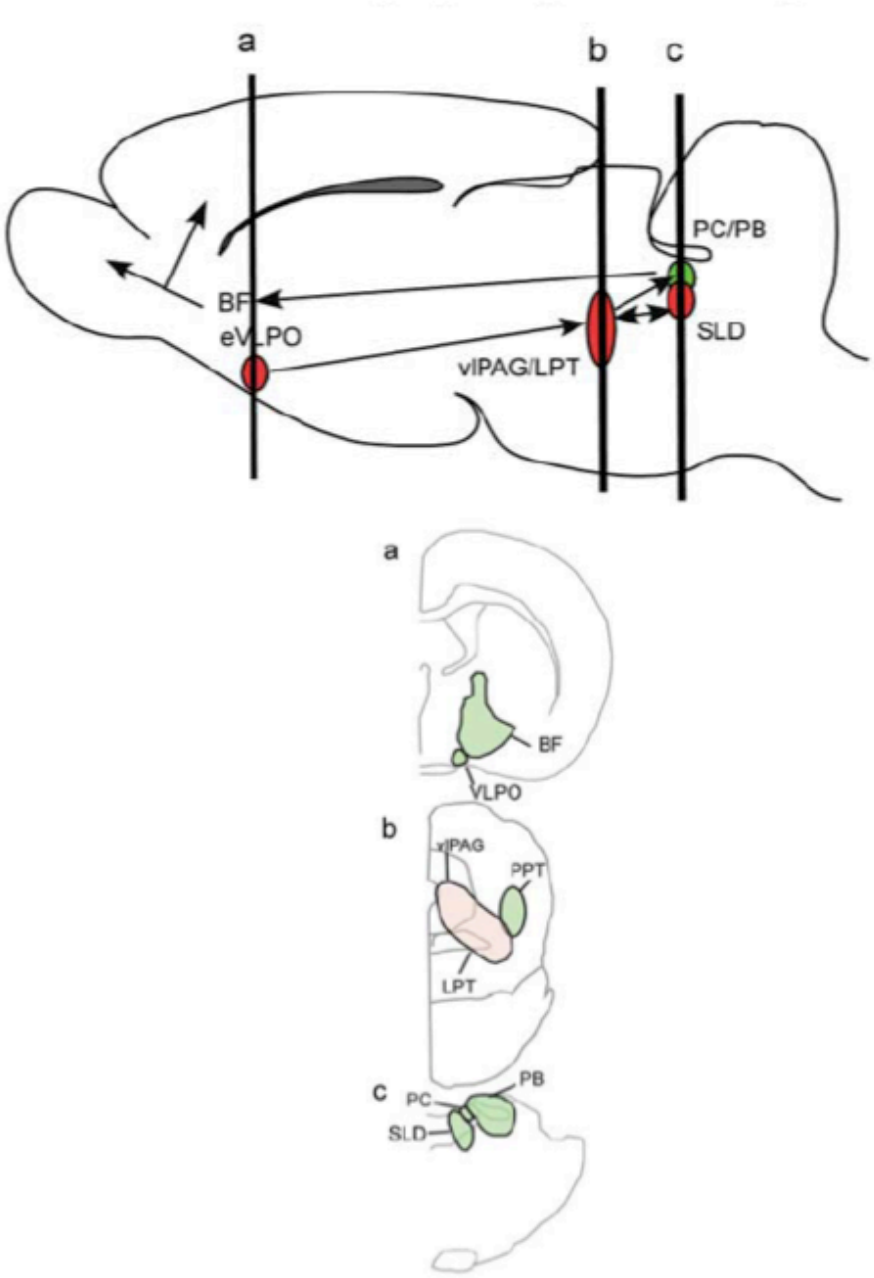

Figure 2. Brain regions involved in transitions between NREM and REM sleep. The REM flip-flop switch is localized to the mesopontine tegmentum. GABAergic REM-off neurons are located in the ventrolateral periaquductal grey matter (vlPAG) and then lateral pontine tegmentum (LPT). These neurons inhibit the REM-on neurons in the procoerulus (PC) and the sublaterodorsal nucleus (SLD). The REM-off region also receives inhibitory and excitatory input from the extended aspect of the ventrolateral preoptic nucleus (eVLPO) and orexin neurons in the lateral hypothalamus (LH). Adapted from Fuller et al. 2007.

While there is no difference in the number of orexin neurons in patients with PWS, a significant decrease in the levels of CSF orexin was found in three different studies (Arii et al., 2004; Fronczek et al., 2005; Mignot et al., 2002; Nevsimalova et al., 2005). Additionally of interest is the fact that mice null for Magel2, one of the genes lost in PWS, exhibit decreased numbers of orexin neurons and orexin peptide (Kozlov et al., 2007). These studies illustrate that improper activation of the REM-off region by orexin neurons, whether due to decreased neurons or orexin peptide, may contribute to the PWS sleep phenotype, however more studies are necessary for this to be determined conclusively. A similar quantitative analysis of the REM-active inhibitory neurons in the eVLPO has not been undertaken in PWS patients.

It is also plausible that PWS patients have abnormal activation of the orexin and eVLPO neurons, which in turn would alter the functioning of the NREM/REM switch. An important regulator of hypothalamic nuclei is the suprachiasmatic nucleus (SCN), and both orexin neurons of the LH and the eVLPO receive input from the SCN (Takahashi et al., 2008). Furthermore, the timing of sleep and the specific stages of sleep are regulated by circadian rhythm, in addition to homeostatic mechanisms. While the homeostatic process functions as a gauge of sleep need, increasing through the wake period and decreasing through the dark period, the circadian clock exerts control over the timing and gating of sleep and the movement through different sleep stages (including entrance into REM sleep) (Franken and Dijk, 2009; Kilduff et al., 2008). The SCN is particularly important for the regulation of the circadian aspects of REM sleep. Rats exhibit increased tendency for REM sleep (homeostatic regulation) in both sham-lesioned and SCN lesioned (SCNx) animals, which do not have a functional SCN, regardless of the phase of the circadian cycle following REM sleep deprivation, circadian processes modulate the proneness for REM sleep depending on the particular phase of the cycle. Sham-lesioned rats exhibited two times the REM tendency in the rest phase, when REM sleep propensity is greatest, compared to SCNx (Wurts and Edgar, 2000). Forced desynchrony protocols in humans, which misalign the endogenous circadian cycle and a forced rest-activity

cycle demonstrate that the sleep-wake cycle and the SWS aspect of NREM sleep align to the new rest-activity cycle, while REM sleep continues to run with the endogenous circadian period for multiple cycles before aligning as well (Dijk and Czeisler, 1995). Similar protocols in rats have since revealed that anatomically and functionally distinct subsets of SCN neurons control REM and NREM sleep. Observation of clock gene expression revealed that neurons in the ventrolateral (vl) SCN align their output to the forced rest-activity cycle, mimicking the response of NREM sleep to desynchronization. In contrast, those in the dorsalmedial (dm) SCN neurons express according to the free-running rhythm, realigning only 3 to 6 cycles following desychronization, as was the case in REM sleep cycling. The specific desynchrony response patterns were observed in NREM and REM sleep indicate their control by vlSCN and dmSCN neurons respectively (Lee et al., 2009b).

1.1.3 Genetics of Prader-Willi Syndrome

PWS results from loss of activity of genes on chromosome 15 in the region q11-q13. The specific molecular mechanisms that underlie this loss are varied but stem from an inherent instability in this genomic region, making PWS part of a set of sporadic human genetic disorders termed "genomic disorders" (Figure 3). Segmental duplication-like structures flank the area of interest and inherently predispose this area to deletions and duplications (Sharp et al., 2006). In addition to PWS, other disorders associated with this genomic region include the supernumerary isodicentric marker 15 syndrome and Angelman syndrome (Wang et al., 2004). A form of epigenetic gene regulation termed genomic imprinting normally silences the expression of the maternal PWS genes in the proximal portion of chromosome 15. The process marks particular genes in the germline state and affects their level of expression. The 15q11-q13 PWS region is differentially regulated depending on the parent of origin. Expression of genes from the maternal chromosome is imprinted and silenced through methylation, leaving only the paternally derived genes for transcription and production of gene

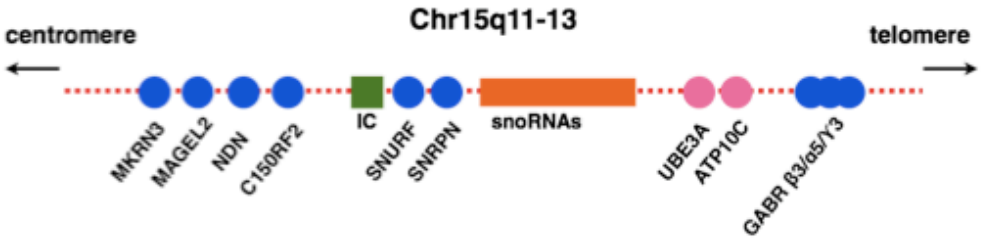

Figure 3. Region on chromosome 15q11-13 associated with Prader-Willi Syndrome (PWS) and the genes found therein. Both maternally imprinted (blue) and paternally imprinted (pink) genes are found in the region. Silencing is controlled by the imprinting centre (green). A set of intronic small nucleaolar RNAs (snoRNAs) (orange) are located telomeric to their host genes, *SNURF* and *SNRPN* (Wevrick 2009).

products (Horsthemke and Buiting, 2006). PWS arises when there is loss of the paternal chromosome 15q11-q13 region, which can result from a number of genetic alterations. Deletion of this paternal chromosome region is the most common cause of PWS, being responsible for approximately 70% of cases (Wang et al., 2004). Second to deletion, is a phenomenon termed uniparental disomy (UPD), which occurs in about 25% of cases, whereby an individual will possess either two maternal or two paternal chromosomes (Nicholls et al., 1989). UPD associated with PWS results from nondisjunction during meiosis in the mother with loss of the paternal copy, ultimately causing an individual to inherit two copies of the maternal chromosome 15. In this case, since the expression of 15q11-q13 genes in both maternal copies would be silenced, PWS again results despite normal gene content. Additionally, an individual may suffer from a mutation or microdeletion of the regulatory element termed the imprinting centre (IC). Such a disruption can cause either familial PWS or Angelman syndrome depending on whether the PWS (Perk et al., 2002). Finally, a small percentage of PWS cases are caused by parental chromosome translocations (Goldstone, 2004). The result of any of these modifications to genes in the 15q11-q13 region is a disruption of proper fetal and postnatal development ultimately manifesting as PWS.

1.1.3.1 PWS candidate genes

The region of chromosome 15 deleted in PWS varies around two different proximal end break points and shares a common distal end break. These two different subtypes of deletion, type 1 and type 2 respectively, range from 4 to 6 Mb in size. With both rearrangements there is loss of all imprinted genes within the 1.8 Mb imprinted domain, while some non-imprinted genes are included in the larger type 1 deletion. When it is the paternal allele that is deleted, PWS results due to lack of expression of maternally imprinted genes from early in embryogenesis onwards. Depending upon the genetic cause of PWS, individuals will have variation in the expression of non-imprinted genes. With a paternal

deletion, genes that are normally expressed from both copies of chromosome 15 will have reduced or potentially normal expression. In contrast, in UPD or an IC mutation, there would be no expression from imprinted genes but normal expression would be expected from nonimprinted genes. It is thought that the prominent shared features of PWS result from the imprinted genes (Wevrick 2009).

With this in mind a set of candidate genes have been linked to the phenotype of PWS, consisting of four protein-coding imprinted genes and several imprinted genes producing noncoding RNAs (Figure 4). Imprinting is controlled by the *SNRPN-IC* transcription unit, which encodes the SNURF and SmN splicesomal protein (SNRPN). The IC establishes and maintains imprinting on the paternal alleles in this region. *SNRPN-IC* is alternatively spliced and the resulting products include the untranslated exons *IPW* and genes for a set of intronic small nucleolar RNAs (snoRNAs). The function of snoRNAs are to process RNA, typically ribosomal RNA. There have been cases of PWS described in which individuals have rearrangements affecting only the *HBII-85* cluster of snoRNAs and no other imprinted genes. From this, it has been suggested that loss of the snoRNAs is sufficient to cause PWS. It is still unknown however, how the expression of other genes during development is affected in these cases and thus it remains to be seen whether this is true. The four imprinted genes lie centromeric to the IC and include *MKRN3* (encoding Makorin3), *MAGEL2*, *NDN* (encoding necdin), and *C150RF2* (Lee et al., 2003). Makorin3 is a RING zinc finger family transcription factor and is expressed widely. The Magel2 and necdin proteins are both members of the melanoma antigen-associated gene (MAGE) family and thus both share the MAGE homology domain (MHD). Magel2 will be described in more detail in the next section. Necdin is involved in cell survival, neurotrophin signaling, cytoskeletal rearrangement in neurons and neurite outgrowth. Without proper expression of *NDN* in PWS, it is theorized that abnormalities of nervous system development and function may result and contribute to the disorder's phenotype. The function of the last, *C150RF2* remains unknown.

Four nonimprinted genes are found centromeric to the imprinted gene cluster and are included in the type 1 PWS deletion. It is thought that these genes (*CYFIP1*, *NIPA1*, *NIPA2*, and *GCP5*) contribute to phenotypic variation seen in PWS (Chai et al., 2003). Another set of nonimprinted genes is located telomeric to the snoRNA encoding genes. *OCA2* is involved in pigmentation and a mutant form is known to cause oculocutaneous albinism and similarly, reduced pigmentation is observed in PWS individuals where only one maternal allele is expressed. An additional three genes code for γ-aminobutyric acid type A (GABA-A) receptor subunits α_5, β_3, γ_3 and their partial deletion may contribute to the PWS phenotype. Increased expression of the Angelman syndrome gene *UBE3A* occurs in individuals with UPD and thus two maternal copies of the gene because it is normally imprinted and silenced on the paternal chromosome.

1.1.3.2 Magel2

The human *MAGEL2* gene and its murine homologue, *Magel2*, are both located in the PWS critical region on human chromosome 15 and the conserved region on murine chromosome 7 respectively. *MAGEL2* is expressed from the paternal allele at relatively high levels in the brain, specifically the hypothalamus. The protein encoded by the intronless *MAGEL2* gene belongs to the MAGE family of proteins, so termed because of the large central region of the proteins called the MAGE homology domain involved in protein-protein interactions. This characteristic region has been identified in a variety of multicellular organisms, including *Drosophia* and *Aspergillus*, but is not present in *Caenorhabditis elegans* and unicellular organisms. While little is known concerning the functional role of this family, the first protein, MAGE-A1 was identified as a tumor-specific peptide. MAGE-A, along with MAGE-B and MAGE-C, are all expressed on the X chromosome and are designated type I MAGE genes due to their restricted pattern of expression in male germ cells and the placenta as well as many histologically distinct tumors. A second class of phylogenetically distinct MAGE

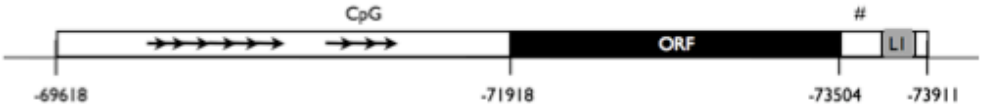

Figure 4. Organization of the mouse Magel2 gene. The black box represents the open reading frame (ORF), open arrows are the upstream CpG repeats, and the grey box indicates the L1 repeat and # indicates the location of the single nucleotide polymorphism (modified from Lee et al. 2000).

genes, the type II MAGE genes, are expressed outside the chromosome X cluster. While necdin, MAGE-F1, and MAGE-G1 are primarily composed of their MHDs much like type I MAGE-A and –B proteins, other type II proteins exhibit more extended N- or C- termini outside of the MHD. Type II MAGE proteins are widely expressed during development, however a clear understanding of a physiological role is lacking for most. Studies point towards an importance of MAGE proteins in cell survival, cell cycle progression, and apoptosis. Incidentally, of all the MAGE genes, most is known about *NDN* and *MAGEL2*, the two MAGE genes found in the PWS critical region (Barker and Salehi, 2002).

MAGEL2 is located 41 kb telomeric to *NDN* and murine *Magel2* ortholog is 150 kb from *Ndn* in the syntenic region. In the 5' to 3' direction, beginning at position 69618 in mice. The mouse *MAGEL2* gene consists of a region of 27 copies of 30 bp head-to-tail tandem repeats, followed by CpG island, followed by a spacer region (Figure 4). The open reading frame then runs from position 71 918 to 73 504. The human and mouse MAGEL2 proteins are approximately 70% homologous and 529 and 525 amino acids respectively. *MAGEL2* contains an extended N-terminal domain that is roughly conserved between it and *MAGED1-4* and *MAGE-E1*. This terminus exceeds that in *NDN* by 188 amino acids, and also unlike necdin, is not proline-rich or acidic (Barker and Salehi, 2002; Lee et al., 2000). *MAGEL2* expression is monoallelic. Specifically, the gene in both humans and mice is expressed from the paternal allele while the maternal copy is silenced following regulation by the imprinting centre (Lee et al., 2000).

1.1.4. *Magel2* Expression Patterns

The expression profile of *Magel2* suggests a role of this gene in the development of specific brain regions. Northern blot analysis of adult human brain and fetal tissue revealed high levels of *MAGEL2* in the putamen, temporal lobe, frontal lobe, occipital lobe, medulla, cerebral cortex and spinal cord of the adult brain as well as in fetal brain, kidney, liver, and lung (Lee et al., 2000). Subsequent whole mount RNA *in situ* hybridization experiments using mouse

pups at embryonic day 9 to 12.5 demonstrate that Magel2 exhibits its strongest expression in the developing hypothalamus (Figure 5A-C). Within this region, intense *Magel2* expression is observed in the ventral thalamus, anterior hypothalamus, supraoptic nucleus (SON), paraventricular hypothalamus (PVH), and suprachiasmatic nucleus (SCN) at E12.5. At this stage of prenatal development, neuronal precursors of the PVH and SON are generated, and thus *Magel2*'s expression occurs before terminal differentiation. At later stages of embryonic development, *Magel2* continues to exhibit its strongest expression in the dorsal medial SCN, SON and preoptic regions (Figure 5D-G). Low levels of *Magel2* are also observed throughout the forebrain, infundibulum at E12.5, which develops into the posterior lobe of the pituitary, and metencephalon area of the hindbrain. *Magel2*'s expression in the forebrain is localized to the ventral thalamus, specifically to the migrating cells of the zona incerta. These expression results are in agreement with the expression defined using a *lacZ* knock-in allele (Lee et al., 2003). At mid-gestation of embryogenesis, the transcript was localized to the central nervous system, specifically the neural tube, forebrain, midbrain and embryonic hypothalamus. Once in adulthood, *Magel2* is observed in various hypothalamic nuclei, in particular, the SCN, PVN, SON, the lateral geniculate nuclei and the amygdala (Figure 6B-C). Outside of the hypothalamus, LacZ histochemistry revealed expression in the external capsule, the lateral and triangular septal nuclei (Figure 6A) (Kozlov et al., 2007).

Hypothalamic expression of Magel2, specifically within the SCN, is of particular interest because many of the symptoms observed in PWS are indicative of hypothalamic and circadian dysfunction. The SCN is the location of the body's core circadian clock and the functioning and importance of this region will be described in more detail in later sections. Transcripts in the SCN often exhibit a discernable rhythm of expression characterized by a single peak and trough in mRNA and protein levels over the course of the 24 hour day. The robustness of this rhythm is indicative of proximity to the core circadian transcriptional machinery in this nucleus and suggests a role in the propagation of circadian

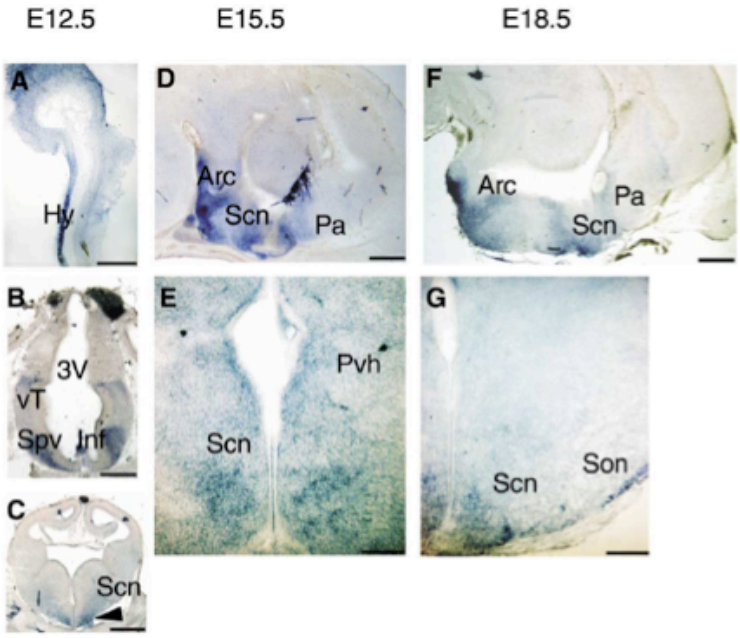

Figure 5. Expression of *Magel2* in the developing murine hypothalamus visualized byRNA in situ hybridization. The E12.5 embryo demonstrates strong staining in the anterior hypothalamus (Hy) in a sagittal section (A) and in the mantle layer of the hypothalamus, ventral thalamus (vT) (B), and in the presumptive suprachiasmatic nucleus (SCN) (C). in transverse sections. At E15.5, expression is localizaed to the arcuate nucleus (Arc), SCN and preoptic area (Pa) regions of the hypothalamus (D), and this staining pattern continues into E18.5 (F). Coronal sections at these embryonic stages again indicate expression in the SCN (E-G) as well as in the supraoptic nucleus (Son) at E18.5 (G). PVH, paraventricular hypothalamus. Sagittal sections are oriented with the anterior to the right. Scale bars: (a and F) 250 μm, (B) 400 μm, (C, D, and G) 500 μm, (E) 150 μm. Reproduced from Lee et al. 2003).

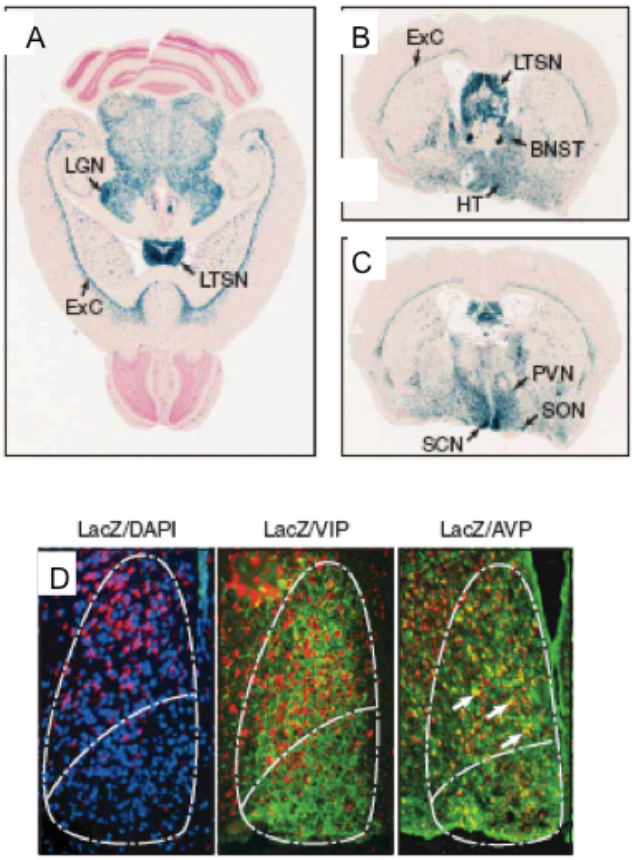

Figure 6. Expression of *Magel2* in the adult murine brain visualized with LacZ histochemistry. A midlevel horizontal section indicates expression in the external capsule (ExC), lateral and triangular septal nuclei (LTSN), and lateral genucleate nucleus (LGN) (A). (B-C) Coronal sections at the level of the anterior commissure (B) and optic chiasma (C). Magel2 is expressed in the bed nucleus of stria terminalis (BNST), the paraventricular nucleus (PVN), supraoptic nucleus (SON) and the suprachiasmatic nucleus (SCN). HT, hypothalamus. (D) Within the SCN, Magel2 expression is specifically localized to a subset of neurons in the dorsolateral SCN. LacZ specific immunostaining of Magel2-positive cells (magenta) was combined with DAPI (blue), vasoactive intestinal peptide (VIP) or arginine vasopressin (AVP) immunoreactive neurons. Reproduced from Kozlov et al. 2008.

information vital to the regulation of other physiological processes (Panda et al., 2002). To aid in a more comprehensive understanding of circadian control over various peripheral systems, high-density oligonucleotide arrays in such species as *Arabidopsis*, *Drosophila* and rodents have been performed to discover transcripts with strong circadian expression profiles (Grundschober et al., 2001; Harmer et al., 2000; McDonald and Rosbash, 2001). Panda et al. (2002) performed a similar high-density oligonucleotide experiment in the SCN and liver over the course of two circadian days. Of the 7000 plus genes and 3000 expressed sequence tags (ESTs) analyzed, 650 transcripts were found to be circadianly regulated. *Magel2* was one of this set of genes with circadian expression. Specifically, *Magel2*'s expression peaks at circadian time (CT) 30, which approximately corresponds to the middle of the day or 6 hours following the exposure to light or endogenous resetting. The trough in expression was observed 12 hours later at CT12. The robustness of the expression was demonstrated by the over 2-fold change in mRNA levels between the lowest and highest levels of expression. *Ndn* in comparison only exhibited a 1.2-fold difference in expression. A later study by Kozlov et al. (2007) using *in situ* hybridizations of brain sections builds off the expression profile performed by Panda et al. (2002). *Magel2* was shown to peak in the late day and trough in the late night, exhibiting a 3.7-fold change in expression. This pattern persisted in constant darkness, with *Magel2* levels increasing until the middle of the subjective day.

1.1.5. Characteristics of mice null for *Magel2*

The potential contribution of Magel2 in the functioning of the circadian cycle was investigated based on the strong levels of *Magel2* expressed in the SCN region of the hypothalamus and its identification as a circadian transcript. The SCN is functionally and anatomically separated into a dorsomedial and ventrolateral region recognized by AVP- and VIP-expressing neurons respectively. A knockout mouse was constructed that replaced part of the Magel2 open reading frame with an in-frame cDNA encoding beta-galactosidase. In this

way, expression of a lacZ fusion protein in the knockout mouse recapitulates the endogenous expression of Magel2. *Magel2-lacZ*-positive neurons were found to be predominantly located in the dorsomedial region and over-lapped with AVP-expressing neurons (Figure 6D). This suggests that Magel2 may have a role in SCN output, sending circadian information to target organs and tissues. The importance of Magel2 in the circadian cycle was assessed using a mouse lacking the paternal copy of the gene (Kozlov et al., 2007). Since the maternal copy is within the PWS imprinted region, it is not expressed and these mice are thus effectively null for *Magel2*. This is confirmed by a complete lack of ß-galactosidase activity in both mid-gestation embryos and adult brains. Though mice were weaned at a frequency 10% lower than expected, the pups that did survive did not exhibit any negative effects on early postnatal viability. Circadian rhythm functioning was assessed in both 8 month or older wildtype and *Magel2* null mice ($Magel2^{m+/p-}$) via wheel-running activity (Figure 7). Mice were entrained for 1 week to a 12 h/12 h light/dark schedule and the number of wheel revolutions per minute was recorded. From this raw data, the daily onset of activity, free-running period, average daily activity and amplitude of rhythmicity were determined. When exposed to constant darkness, wildtype and $Magel2^{m+/p-}$ mice exhibited a similar period of close to 24 hours. However, the $Magel2^{m+/p-}$ mice were significantly less active, running with an average of 3,047 ± 930 wheel revolutions compared to 12,770 ± 2.343 revolutions for wildtype mice. The characteristics of this running were also different in the $Magel2^{m+/p-}$ mice. These mice ran more frequently (8.5 versus 4.9 bouts per day) but for shorter periods (21.8 versus 83.1 minutes) compared to wildtype and exhibited a significantly smaller amplitude in their cycle, which measures mean counts per minute. Perhaps most striking, is the distribution of this locomotor activity throughout the day. Since mice are nocturnal, a healthy wildtype mouse exhibits a distinct block of activity during the dark portion of circadian time. $Magel2^{m+/p-}$ mice in contrast, exhibit frequent short bursts of activity all through the cycle even during light periods. This behavior suggests improper output from the SCN regarding the time

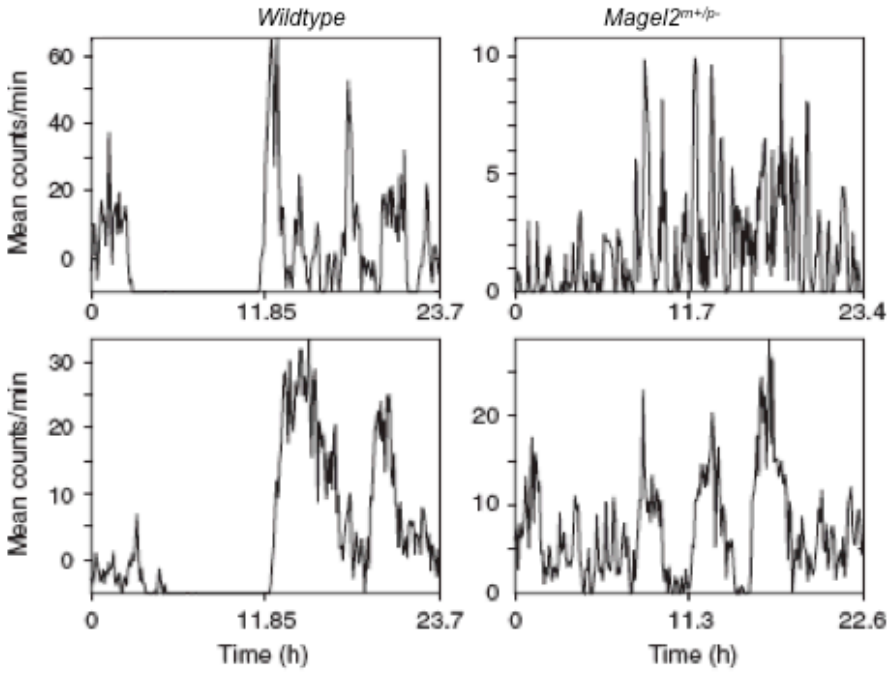

Figure 7. Loss of *Magel2* expression alters the circadian cycling of locomotor activity. Mice were entrained to a 12 h/12 h light/dark cycle for 1 week and then released into constant darkness. Their activity profiles were obtained from days 26-35 in constant darkness. The profiles of two wildtype mice (left) were compared to those of two *Magel2*$^{m+/p-}$ mice. *Magel2*$^{m+/p-}$ mice exhibited increased activity during the "light period" when wildtype mice were not active. *Magel2*$^{m+/p-}$ mice also exhibited more fragmented activity patterns than their wildtype counterparts. Note the scale on each diagram is not the same, so the activity of the wildtype is much higher than that of *Magel2*$^{m+/p-}$.

of day or improper processing of circadian information when no light resetting or zeitgeber information is available. Therefore an understanding of the functional role of Magel2 and its dysfunction in PWS requires an understanding of the clock itself as well as the molecular mechanisms that generate and maintain its rhythm.

1.2 Circadian Rhythm

1.2.1 Functioning of the central clock in the suprachiasmatic nucleus

A diverse range of organisms, from bacteria to humans, exhibits temporal organization of biological processes, which oscillate with a range of periodicities. This coordination not only maintains proper integration of internal operations, but also serves to accurately and flexibly respond to external environmental cycles. The steadfast rotation of the earth about its axis lasting 24-hours has molded the evolution of a similar rhythm within a wide range of species. The daily oscillation between day and night is one environmental indicator that is mimicked by an internal cycle that gives organisms the ability to anticipate and promptly respond to daily environmental changes. This endogenous cycle termed circadian, *circa* meaning about and *dies* meaning day, was coined by Franz Halberg in 1959. Processes following a circadian rhythm exhibit a single crest and trough of activity over the course of 24-hours. The ebb and flow of this activity is realigned, or entrained, with the corresponding environmental time, through resetting mechanisms known as zeitbergers. Since the daily fluctuation between light and dark is a largely consistent variable for most organisms, this is the primary zeitberger. Yet even without an external signal, the approximate 24-hour period biological rhythm is pervasive enough to function endogenously.

Though circadian clocks are now understood to exist in all eukaryotes and some prokaryotes, they were initially recognized in isolated cells from unicellular organisms and were thus first understood to function in a cell-autonomous manner. In unicellular organisms, such as cyanobacteria, *N. crassa* and *G.*

polyedra, a marine dinoflagellate, circadian cycles are currently understood to exist as multiple oscillators within an individual cell. The oscillators can be thought of both as slave-oscillators, synchronized by a pacemaker, and as pacemakers themselves, which coordinate independent outputs. Multicellular organisms in contrast, have only one oscillator, which functions using the same molecular machinery in multiple synchronized cells and cell types. Since my focus is on the biological causes of circadian deregulation in Prader-Willi syndrome in humans, I was largely interested in the circadian rhythm in the mammalian context. Regardless of the organism however, the basic model of circadian clock functioning is the same, consisting of an input-oscillator-output structure. Organisms received input from the external or internal environment that serves as a cue regarding the phase of the environmental and inner cycle. The oscillator then drives the rhythm of the organism, affecting various processes. In mammals, the internal clock exists within every cell, but is centrally located in a region of the hypothalamus termed the suprachiasmatic nucleus (SCN). The SCN consists of bilateral nuclei of approximately 20,000 neurons situated just above the optic chiasm. The SCN can be separated into parts determined by the subsets of neurons found in those regions. The ventrolateral portion is largely made up of small oval or round neurons with axosomatic synapses. Smaller neurons are distributed throughout the dorsomedial area and this region is made up of both axosomatic and axodentitric synapses. While several peptides are synthesized by neurons in the SCN, the main components observed are arginine vasopressin (AVP) and vasoactive intestinal peptide (VIP) as deduced by light and electron microscopic immunocytochemistry with anti-AVP and –VIP antibodies. Such studies have found AVP and VIP neurons to be localized to the dorsomedial and ventrolateral portions of the SCN respectively and as such served as anatomical and functional markers for the parameters of these areas (Ibata et al., 1999). Axons of the VIP neurons make connection with the AVP neurons and thus are proposed to be intrinsic SCN communicators (Ibata et al. 1993). Most input, both direct and indirect, to the SCN is received in the ventral portion. This input is

from retinal ganglion cells, serotonin neurons (5HT) of the raphe nuclei, and neuropeptide Y (NPY).

The hypothalamus is involved in regulation of the body's homeostatic processes, so it makes sense that this region would contain a nucleus where external time cues can guide the timing of feeding and digestion, sleeping and temperature regulation. As previously mentioned, light is the central zeitgeber of the clock. Entrainment input from light reaches the SCN by first activating a subset of photosensitive retinal ganglion cells (pRGCs) separate from rods and cones (Figure 8) (Hankins et al., 2008). The unique retinal cells were originally isolated in *rd/rd* mice, which have no functional rods and only 5% cone survival. Even without these photoreceptors, the mice exhibit normal circadian responses to light. The same functioning photoentrainment was observed in mice that possessed no rods or cones known as *rb/rb cl* mice (Freedman et al., 1999; Lucas et al., 1999). pRGCs detect variations in the quantity and quality of light, but are much less sensitive than cells involved in image detection. Light must be of brighter intensity (200 times brighter in the hamster) and of durations lasting longer than 30 seconds. The photopigment within the pRGCs is melanopsin linked to the vitamin A chromophore 11-*cis* retinal with a peak sensitivity at 479 nm. This opsin photopigment gene, *Opn4* is expressed within the subpopulation of RGCs necessary and sufficient for photoentrainment, working in concert with rods and cones. When a photon strikes these cells, the energy is translated to an intracellular chemical signaling cascade that depolarizes the RGCs and sends signal down their axon projections, known as the retinal-hypothalamic tract (RHT), to the core region of the SCN. The core region is located in the ventrolateral SCN. The RHT terminals release excitatory pituitary adenylate-cyclase-activating polypeptide (PACAP) and glutamate. The SCN also receives indirect photic and brain state information via input from the geniculohypothalamic tract, the pretectum, and the median Raphe nucleus. The RHT signals cause an influx of calcium and the downstream activation of cyclic-adenosine monophosphate response element binding protein (CREB) and binding of this phosphorylated CREB to cAMP response elements (CREs) in responsive

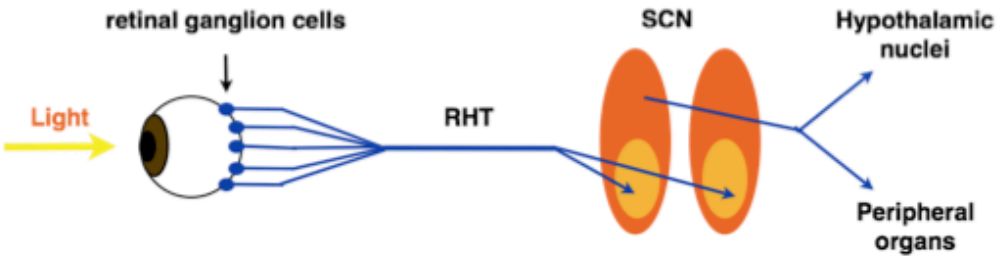

Figure 8. The endogenous circadian clock is reset by light, the primary zeitgeber of the rhythm. Light hits retinal ganglion cells in the eye and these cells transmit the information to the core region of the suprachiasmatic nucleus (SCN) via the retino-hypothalamic tract (RHT). The core region (light orange) of the SCN sends projections to the shell (dark orange), which transmit the information to other hypothalamic nuclei and peripheral organs.

genes, including *Period1* (*Per1*). Per1 is a core circadian protein which thus serves as the point of connection between input and oscillation.

1.2.2 Cell autonomous transcription-translation feedback loop

As mentioned, even without environmental entrainment, the SCN functions as the body's pacemaker, generating self-sustaining oscillations and sending time-keeping information to the peripheral organs. Each neuron within the SCN generates an endogenous rhythm, which is synchronized through communication. Within each cell, the timekeeping cycle exists as a transcription-translation feedback loop. All circadian oscillators are composed of positive elements that activate clock genes that in turn activate negative elements. These negative elements complete the circle, by inhibiting the positive elements (Bell-Pedersen et al. 2005). In mammals, the positive elements are the proteins circadian locomoter output cycles kaput (Clock) or its paralog neuronal PAS domain protein 2, Npas2, and brain-muscle Arnt-like protein 1 (Bmal1). The negative elements are composed of the Period (Per) proteins, Per1/2/3, and the Cryptochromes (Cry), Cry1/2. Together these components form the primary negative feedback loop. At the beginning of the day, the basic helix-loop-helix period aryl single-minded-domain (bHLH-PAS) containing transcription factors Bmal1 and Clock heterodimerize and bind to E-box *cis*-regulatory elements in clock controlled genes (CCGs) including the *Per* and *Cry* genes, initiating their transcription. As day progresses, the Per and Cry proteins form heterocomplexes and accumulate in the nucleus of SCN neurons, peaking in the beginning of circadian night. Per and Cry proteins heterodimerize and inhibit the activity of Bmal1/Clock and thus their own transcription, which reaches a nadir by the end of circadian night (Lee et al., 2001; Takahashi et al., 2008). Subsequent degradation of Per and Cry proteins reduces their levels throughout the night and the cycle gradually begins anew as the repression of Bmal1 and Clock is ablated.

A secondary transcription-translation feedback loop exists and though not essential, adds robustness to the primary loop by determining period length and

phase-shifting properties. The loop consists of the orphan nuclear hormone receptor, Rev-erbα and Rora, which are members of the retinoic acid-related orphan receptor family. Rev-erbα inhibits the transcription of *Bmal1* by antagonizing the activities of the *Bmal1* transcriptional activator, Rora, which binds to the Ror response element in the *Bmal1* promoter (Preitner et al., 2002; Sato et al., 2004). It is itself inhibited by Per2 and in this way, Per2 functions as a positive regulator of the circadian clock (Preitner et al., 2002). Thus, as Per2 levels increase through the circadian day and into the early night, the inhibition of *Bmal1* transcription abates and levels of Bmal1 increase in preparation for the decreased levels of Per and Cry inhibitors.

1.2.2.1 Clock

The first protein recognized in mammals for its crucial role in circadian rhythm functioning, and incidentally before its *Drosophila* homolog, was the bHLH-PAS protein Clock. Prior to this point, a spontaneous semi-dominant mutation in the golden hamster called *tau*, unrelated to Clock, was known to result in an approximate 2 and 4 hour shortening of the circadian period in heterozygous and homozygous mutants respectively (Ralph and Menaker, 1988). While helpful in focusing studies of circadian processes towards the genetic contribution, the lack of detailed genetic information for the hamster limited the contribution of this mutation towards a molecular understanding (King et al., 1997). Vitaterna et al. (1994) screened the progeny of mice treated with *N*-ethyl-*N*-nitrosourea (ENU) for circadian clock mutations. They discovered a semi-dominant mutation that resulted in longer periods of 24.5 to 24.8 hours (*Clock*/+ heterozygous mice) or more extremely long periods of 26 to 29 hours (*Clock*/*Clock* homozygous mice) compared to the 23.3 to 23.8 hour period observed in wildtype mice. *Clock*/*Clock* mice were also found to be arrhythmic under conditions of constant darkness. The authors concluded that *Clock* defines a circadian rhythm gene associated with regulation of the intrinsic circadian period and maintenance of this rhythmicity under conditions of constant darkness (Vitaterna et al., 1994). The mutation,

hereafter referred to as *Clock*$^{\Delta 19}$, results from exon skipping and deletion of 51 amino acids in the protein's putative transcriptional regulatory domain (King et al., 1997). Rescue of the circadian phenotype following expression in the mutant mice of a *Clock* gene-containing bacterial artificial chromosome confirmed this protein's role in the circadian clock (Antoch et al., 1997). Clock was subsequently identified as a bHLH-PAS transcription factor expressed most highly in the hypothalamus and eye (King et al., 1997; Vitaterna et al., 1994).

1.2.2.2 Bmal1

Bmal1, also known as Mop3, Jap3 or Arnt3, was separately identified as a novel bHLH-PAS protein as part of an iterative search of ESTs for bHLH-PAS protein like sequences. *Bmal1* was described as a 2.9 kb single transcript that generates a 624 amino acid protein with close homology to Ah receptor nuclear translocator (Arnt) and Arnt2, although Bmal1's expression patterns were distinct from these proteins (Hogenesch et al., 1997; Ikeda and Nomura, 1997). Early work hinted that Bmal1 and its homolog Mop9 were the functional partners of the already identified Clock in the proper maintenance of circadian rhythm. Bmal1 was shown to form heterodimers that co-express with Clock in SCN neurons and to drive transcription from circadian gene E-box elements (Hogenesch et al., 1998; Hogenesch et al., 2000; Honma et al., 1998; Ikeda et al., 2000; Jin et al., 1999). Confirmation of Bmal1's, but not Mop9's, role as an indispensible component of the mammalian circadian clock was established using a comparative genetics approach. The highly conserved *Drosophila* circadian oscillator functions with a heterodimeric transcriptional activator complex involving two bHLH-PAS proteins, dCLOCK and dCYCLE (Rutila et al., 1998). There are two mammalian homologs of dCYCLE known as Mop3 and Mop9, also known as Bmal1 and Bmal2, but the latter has been shown not to be functionally redundant and it's biological role has not been well defined. Mice lacking Bmal1 most dramatically display complete loss of circadian rhythmicity under conditions of constant darkness. Additionally, the *Bmal1*$^{-/-}$ mice are significantly less active

as measured by wheel-running but are significantly more active during the light phase of the circadian cycle. Bmal1 acts as a positive regulator of gene expression as demonstrated by the nonrhythmic baseline levels of *mPer1/*2 and mouse albumin D-element binding protein (*mDbp)* gene expression in *Bmal1*$^{-/-}$ mice (Bunger et al., 2000). The *mDbp* gene is under circadian regulation but is not part of the central clock (Lopez-Molina et al., 1997). The transcription of *Bmal1* follows a robust circadian cycle and, as described above, is under the control of *Rev-erba*. The period of its mRNA peaks and troughs approximately antiphase that observed for the *Per1* and *Per2* (Shearman et al., 2000).

1.2.2.3 Bmal1-Clock dimerization and transcriptional activation

Upon discovery of Clock and Bmal1, an understanding of the tendency for bHLH-PAS proteins to heterodimerize and act as transcription factors already existed. As such, researchers investigated the possibility that this too was how those two circadian proteins functioned in the mammalian system. Potential Clock-interacting proteins were identified by two research groups independently with a yeast two-hybrid screen and the results of these experiments revealed strong interaction with Bmal1 as well as co-expression in the brain and retina (Gekakis et al., 1998; Hogenesch et al., 1998; Takahata et al., 1998). Through the use of luciferase reporter assays, Clock-Bmal1 heterodimers were found to activate transcription by binding to an E-box element (CACGTG) within the *mPer1* promoter. This ability was observed only when the two proteins were present together and not alone. The Clock-Δ19 mutant protein, while still able to bind its heterodimeric partner and bind to the E-box site, lacks the capability to activate transcription (Gekakis et al., 1998).

1.2.2.4 Period proteins

Per proteins, as noted above, are involved in the transcriptional repression through inhibition of the activity of Bmal1-Clock heterodimers (Sun et al., 1997;

Tei et al., 1997). The *Drosophila* circadian system has served as a well-defined and convincing model of the molecular mechanisms of the circadian feedback loop. The first mammalian gene cloned with sequence similarity to its *Drosophila* counterpart was *mPer1*, separately discovered and originally named *RIGUI* and *hper* (Sun et al., 1997; Tei et al., 1997). Per1 exhibits self-sustained circadian expression in the SCN, which is reset by light cues at CT22 and is thus currently understood to be the link between zeitbergers and the endogenous clock (Albrecht et al., 1997; Shearman et al., 1997; Takumi et al., 1998a). The entire family of distinct mouse *Per* genes was soon after revealed through database searches to include *mPer1*, *mPer2*, and *mPer3*. Per proteins are PAS proteins, lacking a bHLH domain (Zylka et al., 1998). The *mPer2* gene was uncovered using BLAST and FASTA searches for the Genbank database and the human *PER1* gene sequence. Expression of *mPer2* oscillates with a 24 hour rhythm that peaks approximately 4 hours later in the day than *mPer1*. Additionally, *mPer2* was demonstrated to be responsive to light exposure during the subjective night. (Albrecht et al., 1997; Shearman et al., 1997; Takumi et al., 1998a). The final member of the mammalian *per* gene family to be isolated was *mPer3*. While the gene shows a circadian cycling in SCN expression, it is not induced by light during any phase (Takumi et al., 1998b; Zylka et al., 1998).

Mouse models with mutations in the various *Per* genes reveal functionally distinct roles as negative elements of the clock. A deletion mutation in the PAS domain of Per2 leads to arrhythmicity in mice under conditions of constant darkness (Zheng et al., 1999). Alternatively, mice with a targeted disruption of *Per2* were found to exhibit complete arrhythmicity under conditions of constant darkness as well as reduced levels of clock gene expression in the SCN (Bae et al., 2001). This result is consistent with its proposed role as a positive regulator of circadian gene expression (Shearman et al., 2000; Zylka et al., 1998). A mutation in human *PER2*, affecting the ability of casein kinase Iε to phosphorylate PER2, has also been described which results in familial advanced sleep phase syndrome (Toh et al., 2001). Mice with a targeted disruption in *Per1* were also found to have a severely disrupted circadian locomotor rhythm in extended exposure to

constant darkness but SCN gene rhythms were unaffected. *Per1*/*Per2* double-mutant mice were immediately arrhythmic demonstrating that Per1 impacts the circadian cycle through interaction with other clock proteins. In the case of Per3, mice with a mutation in this gene suffer a slight shortening of cycle period as measured by free-running rhythm (Bae et al., 2001).

1.2.2.5 Cryptochromes

While the other core clock proteins were discovered based on comparison with *Drosophila* counterparts, for the Cry proteins, this was not the case. In *Drosophia*, the Per co-repressor is encoded by *Timeless* (*Tim*), which is a similarly rhythmically regulated clock gene. A mammalian homolog of *Tim* does exist but is not necessary or sufficient to fill a transcriptional inhibitory role (Kume et al., 1999). Cry proteins, in contrast, were identified as part of an attempt to find mammalian versions of photolyase, a DNA-repair enzyme that undergoes photoreactivation, requiring light energy captured by blue-light collecting chromophores. van der Horst et al. (1999) found two genes with high homology to class I photolyases also possessing a carboxy-terminal extension similar to crytochromes or pterin/flavin-containing proteins but lacking DNA repair activity. As such the two genes were termed *Cry1* and *Cry2*. *Cry1* and *Cry2* mutant mice were generated to decipher the proteins' function and were initially hypothesized to be circadian photoreceptors due to their expression within the ganglion and inner nuclear retinal layer and because of the involvement in entrainment of circadian cycles in plants. *Cry1*-knockout mice possess a free-running rhythm significantly shorter than the approximate 24 hour rhythm of wildtype mice while that of *Cry2*-knockout mice is significantly longer. Heterozygous mice show no discernible phenotype. Double knockout mice, lacking both *Cry1* and *Cry2*, are completely arrhythmic (van der Horst et al., 1999). The Cry proteins play a crucial role in the negative feedback of the circadian clock as they are the repressors that bind directly to the Clock/Bmal1 heterodimers and can alone abolish Clock/Bmal1 driven E-box transcription. They interact with all of the

mPer proteins and move them from the cytoplasm to the nucleus and may have a role in Per2 stability (Kume et al., 1999; Shearman et al., 2000). Towards this, the rhythm of Cry1/2 expression is coincident with that of Per1/2 (Reppert and Weaver, 2001).

1.2.3 Posttranslational modifications in the circadian clock

Proper functioning of self-sustaining circadian rhythm is dependent on a variety of posttranslational modifications which fine-tune and temporally organize the central transcription-translation feedback loop. In fact, circadian regulation of gene expression appears to be of less importance in preservation of the daily rhythm than alterations to the proteins themselves (Gallego and Virshup, 2007). Out of phase expression or overexpression of Clock does not adversely alter cycle functioning and neither does nonrhythmic expression of *Per* (Kim et al., 2002; Yang and Sehgal, 2001). Most significantly, maintenance of the endogenous 24 hour oscillation is critically conserved via a time delay between the generation of Per and Cry inhibitory proteins and their action on the core transcriptional activators (Vanselow and Kramer, 2007). Additionally, of importance is the timely degradation of all circadian proteins at appropriate times through the cycle.

1.2.3.1 Phosphorylation

Phosphorylation within the circadian molecular machinery is perhaps the most important and best understood modulator of the circadian oscillator. It is the posttranslational modification with the indispensible duty of maintaining the approximate 24 hour period by delaying the action of the repressor proteins. If no such delay occurred, transcripts of *Per* and *Cry* would be translated and active proteins generated in the course of a few hours. All core circadian proteins are phosphorylated, serving to regulate their subcellular localization, activity, and stability. The casein family of kinases (CSNK) and glycogen synthase kinase-3β (GSK-3β) is implicated in both the *Drosophila* and mammalian clockwork

functioning. The Per proteins are phosphorylated by CSNK1ε and CSNK1δ *in vivo* and GSK-3β (Camacho et al., 2001; Eide et al., 2002; Iitaka et al., 2005; Keesler et al., 2000). Mutations in CSNK1ε, which interfere with the ability of this protein to phosphorylate Per proteins, shortens the circadian period in the Syrian hamster. Similarly, when there are alterations to the phosphorylation site in Per2 or the CSNK1 binding site in Per3, familial advanced sleep phase syndrome (FASPS) and delayed sleep phase syndrome (DSPS) result respectively (Ebisawa et al., 2001; Toh et al., 2001). Similarly, CSNK1ε has been show to phosphorylate Bmal1 and the Cry proteins *in vivo* (Eide et al., 2002). Cry1 is phosphorylated only when bound to Per proteins.

The phosphorylation of circadian proteins is related to their stability, specifically through targeting for degradation via the 26S proteosomal pathway. Hyperphosphorylated Per proteins are primed for degradation, as inhibition of CSNK1ε slows Per2 and Per1 breakdown and also lengthens circadian period (Keesler et al., 2000). CSNK1ε phosphorylated Per proteins attract the ubiquitin ligase adaptor F-box protein β-TRCP1 and β-TRCP2, homologs of the *Drosophila* Slimb protein that functions in a similar role to this homolog. As with CSNK1ε, CSKIδ phosphorylates and in turn destabilizes both Per1 and Per2 (Camacho et al., 2001). Phosphorylation of Per proteins also plays a role in their nuclear entry and appropriate timing of the circadian cycle. Per1 is predominantly nuclear when expressed alone in HEK293 cells. Coexpression with CSNK1ε however, restricts entry of Per1 into the nucleus in a phosphorylation-dependent manner by masking the nuclear localization signal (Vielhaber et al., 2000). In contrast, both CSNK1 proteins are able to induce nuclear translocation of mPer3, simultaneous to inducing its degradation (Akashi et al., 2002). Through this posttranslational modification regulating abundance and localization, Per proteins form the rate-limited step of feedback inhibition (Lee et al., 2009a).

Western blot analysis in transfected HEK-293 cells indicated that phosphorylation of Bmal1 and Clock are mutually dependent. The proportion of phosphorylated Bmal1 increases and total levels decrease with increasing Clock and so Clock plays a necessary role in this modification of Bmal1 (Kondratov et

al., 2003; Yoshitane et al., 2009). The same was true in the case of Clock, where increasing levels of Bmal1 are correlated with increasing amounts of phosphorylated but decreasing total Clock. Thus the authors speculate that Bmal1-mediated phosphorylation of Clock is related to its degradation. It has been shown in NIH3T3 cells and mouse liver that Clock is phosphorylated during the day and is hyperphosphorylated during inhibition of E-box transcription (Yoshitane et al., 2009). Since levels of Clock mRNA and protein do not exhibit strong circadian oscillation in the SCN, variations in Clock levels occur due to this modification in additon variations in nuclear levels (Gekakis et al., 1998; Vitaterna et al., 1994). The activity of Bmal1-Clock at a responsive promoter was directly correlated with levels of both phosphorylated Bmal1 and Clock (Eide et al., 2002). In contrast, phosphorylation of Bmal1 by mitogen-activated protein kinase (MAPK), results in decreased transcriptional activity (Sanada et al., 2002). The Cry but not the Per proteins, suppress the phosphorylation of Bmal1 and Clock, which in turn results in increased levels of Bmal1 due to increased stability (Dardente et al., 2007; Yoshitane et al., 2009).

1.2.3.2 Acetylation

Acetylation is a well-studied mechanism of epigenetic modifications. Acetyl groups are added to the ε-amino groups of particular lysine residues on histone N-terminal tails, opening the chromatin conformation through the neutralization of charge and facilitating access of the transcriptional machinery to the DNA, thus inducing transcription. Non-histone proteins can also be acetylated and the alteration can have varying affects on protein activity, including increasing or decreasing DNA affinity, transcriptional activation, protein stability and protein interactions (Glozak et al., 2005). Histone acetyltransferases (HAT) and histone deacetylases (HDAC) are the enzymes involved in adding and removing acetyl groups respectively. Analysis of the protein sequence of Clock revealed that this core circadian transcriptional activator possesses HAT activity involved in chromatin-remodeling events that are essential to the functioning of

circadian rhythmicity (Doi et al., 2006). Clock is also involved in the acetylation of Bmal1. Bmal1 is rhythmically acetylated throughout the circadian cycle, peaking at the time of least transcription of CCG, perhaps through facilitating the recruitment of Cry1 to the Clock-Bmal1 heterodimer (Hirayama et al., 2007). The deacetylated state of histone H3 and Bmal1 is maintained by the HDAC, Sirt1. During periods of Clock-Bmal1 transcriptional activity, Bmal1 is in a deacetylated state while the histone H3 is acetylated. This fits a model whereby Clock-mediated acetylation and Sirt1-mediated deacetylation maintain acetylation and activation of circadian promoters and their subsequent deactivation via Bmal1 acetylation and Cry1 repression (Nakahata et al., 2008).

The stability of Per2 is also regulated through levels of acetylation, which is in part maintained by Sirt1 de-acetylation. Sirt1 binds to Per2 in a circadian manner, peaking when Per2 levels are lowest early in the subjective day. This corresponds to the point where acetylated Per2 levels are lowest, indicating that Sirt1-mediated deacetylation facilitates Per2 degradation via ubiquitination and proteasomal degradation. The researchers also found that Sirt1 activity is required for robust circadian transcription of core circadian genes (Asher et al., 2008).

1.2.3.3 SUMOylation

The addition of small ubiquitin-related modifier (SUMO) to Bmal1 is another way in which both the cellular localization and stability of this protein is regulated. There are three SUMO paralogues in mammals, SUMO1, SUMO2, and SUMO3. The latter two are 95% identical and are thus referred to as SUMO2/3 and share 45% homology with SUMO1. SUMOylation describes the process itself, where SUMO residues are covalently linked to lysines residues (Geiss-Friedlander and Melchior, 2007). Highly conserved lysine residues were noted in the linker region between the two PAS domains in the Bmal1 protein and examined as a potential site for SUMO modification. Bmal1 was found to serve as a substrate for sumoylation in a circadian manner in the mouse liver, with the sumoylated form peaking at ZT9. This pattern parallels Bmal1's activity and is

induced and dependent on the presence of Clock (Cardone et al., 2005). Later work more clearly established the functional role of Bmal1 sumoylation. Addition of the SUMO residue, primarily SUMO2/3, exclusively targets Bmal1 to the promyelocytic leukemia nuclear body (NB) and serves as a prerequisite for ubiquitination. Interestingly, timing of Bmal1 sumoylation coincides with the transcriptional activity of Bmal1-Clock heterodimers at CCGs and is concomitant with Bmal1's degradation via the ubiquitin-proteasome system (Lee et al., 2008).

1.2.4 A model of the circadian clock

As a new day begins at CT 0, the Bmal1-Clock heterodimer is beginning to activate various CCGs, including the transcriptional repressors, *Per* and *Cry* (Figure 9A). The last cycle's inhibitory proteins have been depleted following proteasomal degradation. Throughout the light period, this transcription steadily increases, producing more and more Per and Cry proteins. Bmal1 and Clock are both in their phosphorylated, active forms, with Bmal1 playing the additional role of shuttling between the nucleus and cytoplasm to bring Clock into the nucleus (Figure 9B). Transcription of clock genes is facilitated by the acetylation of histones, by Clock. Coinciding with active transcription, is the robust proteosomal degradation of Bmal1 in PML bodies, following SUMOylation and ubiquitination. Once the day draws to an end, levels of Per and Cry mRNA are reaching their peak and the resulting protein levels are rising (Figure 9C). This is followed by a delay of a number of hours, during which Per and Cry are being phosphorylated and activated. Per is also acetylated and consequently protected from proteosomal degradaton. Per and Cry are able to enter the nucleus. There, they inhibit the activity of Bmal1-Clock. At the same time, Bmal1 is increasingly acetylated by Clock and this modification attracts Cry proteins. The binding of Cry hinders the transcriptional activity of Bmal1-Clock by stabilizing unphosphorylated Bmal1. Cry also protects Bmal1 from SUMOylation and so levels of the protein increase. Clock levels decrease following hyperphosphorylation by CIPC, which targets it for proteasomal degradation. In the late night, decreased generation of the

repressor proteins and their breakdown alleviates the inhibition of Bmal1 and Clock and the cycle begins anew (Figure 9D).

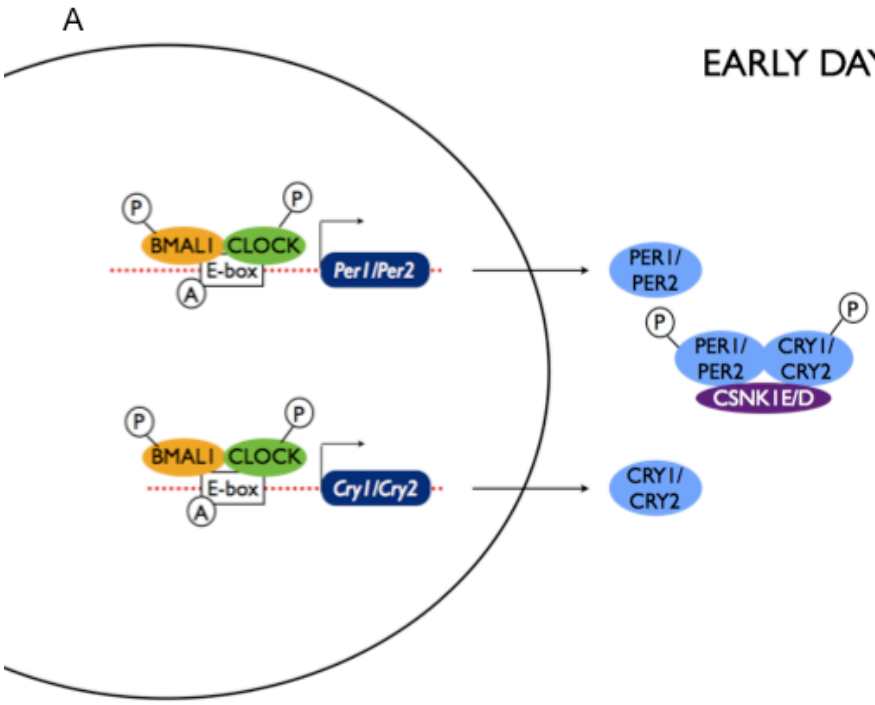

Figure 9. A schematic of the transcription-translation feedback loop which forms the molecular circadian clock.. (A) Early in the day, Bmal1-Clock heterodimers activate the transcription of clock controlled genes including *Per* and *Cry*, the repressive proteins in the cycle. Levels of Per and Cry rise and are phosphorylated by casein kinases. (B) Following a delay of several hours, Per and Cry move into the nucleus and to begin inhbiting transcriptional activity of Bmal1-Clock. During this time, Bmal1 is being rapidly degraded in promyelocytic leukemia nuclear bodies (PML). (C) As evening begins, inhibition takes full effect and levels of *Per* and *Cry* decrease. Levels of Bmal1 also increase as its acetylated form attracts Cry, which in turn protects Bmal1 from degradation. (D) When the night draws to a close, the Per and Cry proteins have been depleted via proteasomal degradation and the inhibiton of Bmal1-Clock mediated transcription is alleviated.

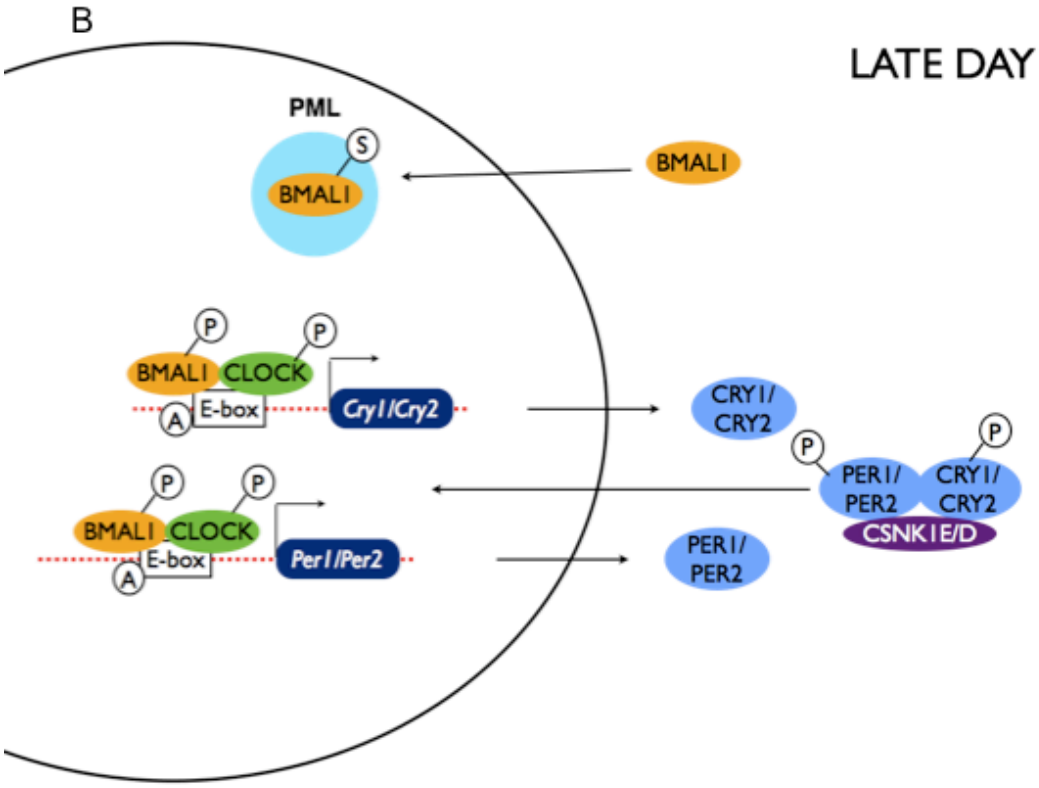
B
LATE DAY
PML
S
BMAL1
BMAL1
P
P
BMAL1
CLOCK
E-box
A
Cry1/Cry2
CRY1/
CRY2
P
P
PER1/
PER2
CRY1/
CRY2
CSNK1E/D
P
P
BMAL1
CLOCK
E-box
A
Per1/Per2
PER1/
PER2

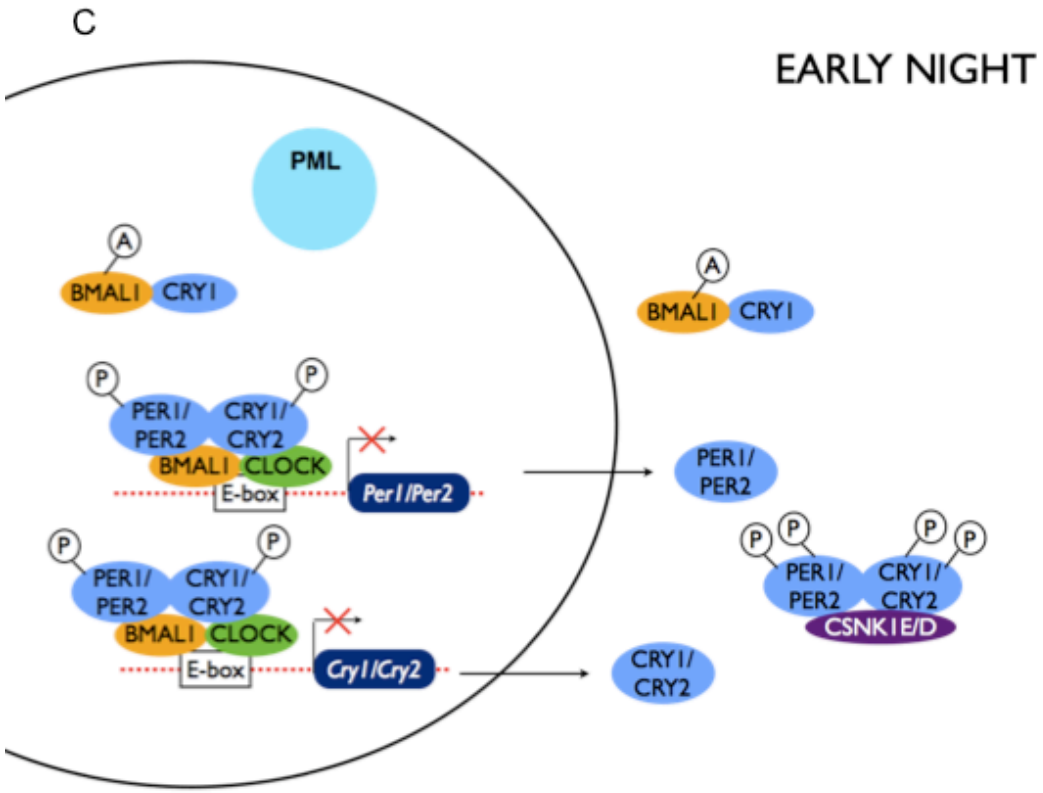
C
EARLY NIGHT
PML
A
BMAL1
CRY1
P
PER1/
PER2
CRY1/
CRY2
BMAL1
CLOCK
E-box
Per1/Per2
Cry1/Cry2
CSNK1E/D

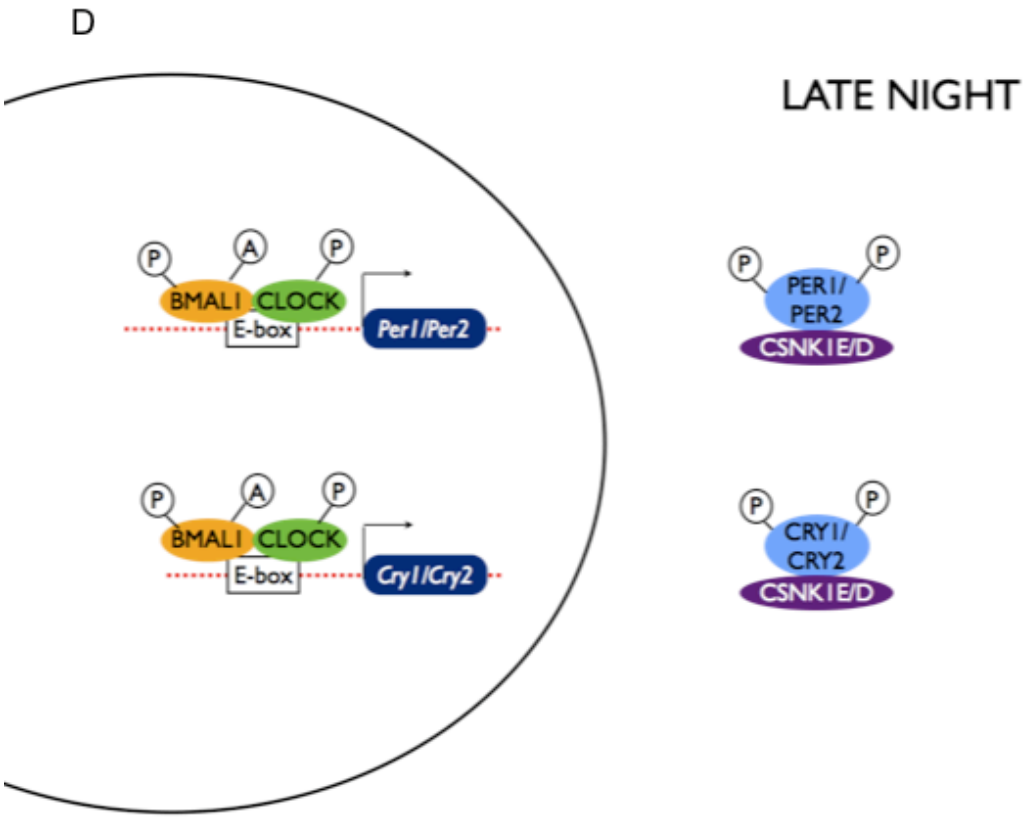
D
LATE NIGHT
P
A
P
BMAL1
CLOCK
E-box
Per1/Per2
P
P
PER1/
PER2
CSNK1E/D
P
A
P
BMAL1
CLOCK
E-box
Cry1/Cry2
P
P
CRY1/
CRY2
CSNK1E/D

1.3 Hypothesis and Aims

Evidence collected from reviewing the symptoms of PWS is indicative of a hypothalamic abnormality, potentially involving the circadian clock. Similarly, mice lacking the PWS gene *Magel2*, exhibit symptoms that suggest a disrupted circadian rhythm. *Magel2* is expressed strongly in the SCN, the location of the central clock, specifically in the shell region that sends information regarding circadian period to other areas of the brain and periphery. From this, I hypothesized that Magel2 plays a role in one of the inter-connecting transcription-translation feedback loops of circadian clock output. Overall I aimed to characterize the nature of this involvement by looking at how Magel2 specifically affects transcription of CCGs, by looking at the localization and stability of circadian proteins, and by determining whether Magel2 can interact with circadian proteins. It is the hope that this work will provide insight into Prader-Willi Syndrome in order to provide better treatment for the disorder.

Chapter 2. Materials and Methods

2.1 Plasmids

A list of plasmids is provided in Table 1. Full-length mouse Magel2 (521 amino acids) was cloned into pcDNA4/HisMaxB mammalian expression vector (Invitrogen, Carlsbad, CA) with an N-terminal Xpress epitope tag to form pcDNA4HisMaxXpressMagel2 (referred to as Xpress-Magel2) (Lee et al., 2005b). Full-length mouse Per2 (1258 amino acids) and full-length mouse Cry1 (607 amino acids) were both cloned into pcDNA3.1/V5His (Invitrogen, Carlsbad, CA) to form pcDNA3.1Per2V5His (referred to as Per2-V5) and pcDNA3.1Cry1V5His respectively, and were obtained from Dr. J. Takahashi at Northwestern University (Kume et al., 1999). Full-length mouse Bmal1 (626 amino acids) and full-length mouse Clock (855 amino acids) were cloned into pcDNA3-HA (Invitrogen, Carlsbad, CA) to generate pcDNA3HABmal1 and pcDNA3HAClock respectively (Kondratov et al., 2003). An alternate Clock construct was used in experiments as well. For this plasmid, full-length Clock was cloned into pcDNA3.1-Myc (Invitrogen, Carlsbad, CA) to generate pcDNA3.1MycClock (Kwon et al., 2006). These three plasmids were obtained from Dr. M. Antoch at the Roswell Park Cancer Institute. To generate the pGL3-E2 box circadian enhancer plasmid, a 3.3-kb *Eco*RI/*Xba*I fragment covering base pairs -1,128 to +2,129 including the noncanonical circadian enhancer (E2) E-box candidate 5'-CACGTT-3' at base pairs -20 to -15 was isolated from *Per2*-positive bacterial artificial chromosome and cloned into pGL3-Basic luciferase reporter (Promega Corporation, Madison, WI) to generate pGL3-E2 and was obtained from Dr. J. Takahashi at Northwestern University (Yoo et al., 2005). The pRL-TK vector was used as an internal control reporter containing a *Renilla* luciferase cDNA cloned from the *Renilla reniformis* (sea pansy) (Promega Corporation, Madison, WI). The negative controls used in the increasing protein level experiments included LacZ cloned into pcDNA3.1/V5His to generate pcDNA3.1LacZV5His (referred to as LacZ-V5) and *PITX2* cloned into pcDNA4/HisMaxBXpress and pcDNA3-HA to generate pcDNA4/HisMaxBXpress*PITX2* (referred to as Xpress-*PITX2*) and

pcDNAHA*PitX2* (referred to as HA-PitX2) respectively. These constructs were all obtained from Dr. M. Walter at the University of Alberta.

2.2 Antibodies

Mouse monoclonal anti-Xpress and anti-V5 antibodies were from Invitrogen (Carlsbad, CA). Mouse monoclonal anti-HA and anti-gamma tubulin antibodies were from Sigma-Aldrich (Oakville, ON). Rabbit polyclonal anti-HA antibody was from Santa Cruz Biotechnologies, Incorporated (Santa Cruz, CA). Rabbit polyclonal anti-Myc antibody was from Sigma-Aldrich (Oakville, ON). Rabbit polyclonal anti-V5 antibody was from Millipore (Billerica, MA).

Secondary enhanced chemiluminescence (ECL) sheep anti-mouse and ECL goat anti-rabbit IgG, Horseradish Peroxidase linked whole antibodies were from GE Healthcare UK Limited (Little Chalfont Buckinghamshire, UK). Goat anti-mouse Alexa Fluor 488 and 594 and goat anti-rabbit Alexa Fluor 488 and 594 secondary antibodies were from Invitrogen (Carlsbad, CA).

2.3 Cell culture and transfections

NIH3T3 cell lines were cultured in Dulbecco's modified Eagle's medium (DMEM) supplemented with 10% calf serum (CS) (Invitrogen, Carlsbad, CA). NIH3T3 cells were used for dual luciferase assays, immunofluorescence experiments, increasing protein effects experiments and half-life experiments. Cells were counted using a hemocytometer. For the luciferase assay, either 2×10^4 cells per well of a 24-well plate in 1 mL of DMEM with 10% CS. For the remaining experiments, 1×10^5 cells per well of a 6-well plate in 2 mL of DMEM with 10% CS. After 18 to 24 hours, cells were transfected using Attractene Transfection Reagent (Qiagen, Mississauga, ON) according to the manufacturers instructions. Specifically, for the cells plated in the 24-well plate, a total of 0.4 μg of appropriate combination of plasmid DNA and 5 ng of pRL-TK *Renilla* control luciferase plasmid were diluted in 60 μL of DMEM serum free media (SFM). One

μL of Attractene Transfection Reagent was added to the diluted DNA and mixed by light tapping. For cells plated on 6-well plates, a total of 1.2 μg of appropriate plasmid DNA was diluted in 100 μL in SFM. Subsequently, 3 μL of Attractene was added. When required, empty vector plasmids were co-transfected in order to keep the total amount of plasmid transfected constant across all transfections. The resulting mixtures were incubated for 15 minutes at room temperature. The appropriate solutions were added drop-wise onto the cells and the plates swirled to evenly distribute the mixture. The plates were then incubated at 37°C and 5% CO_2 for 18 to 24 hours. Protein half-life was measured by treating cells with cycloheximide (CHX) (Sigma-Aldrich Corporation, Oakville, ON). CHX dissolved in DMSO to a concentration of 200 mg/mL was diluted to 100 μg/mL in DMEM with 10% CS at 37°C.

HEK293 cell lines were maintained in DMEM supplemented with 10% fetal bovine serum (FBS) (Invitrogen, Carlsbad, CA). HEK293 cells were used for coimmunoprecipitation experiments. A 85 to 100% confluent T75 flask of cells was de-plated in 14 mL of fresh DMEM with 10% FBS. Two mL of the resulting solution was added to a 100 mm tissue culture dish with 8 mL of DMEM with 10% FBS. Following 18 to 24 hour incubation at 37°C and 5% CO_2, cells were transfected using $CaCl_2$ and HEPES. Specifically, for each 100 mm plate, 72μL of $CaCl_2$ was added to 507 μL of distilled H_2O (dH_2O). To this, a volume of dissolved plasmid corresponding to a total of 4 μg of DNA was added and the resulting solution mixed by light tapping. This solution was added drop wise to another tube containing 590 μL of HEPES buffer (pH 7.4) and the mixture incubated for 5 minutes and tapped lightly to mix. 890 μL of the mixture was then added drop by drop evenly over the plated cells. The plates were then incubated at 37°C and 5% CO_2 for 18 to 24 hours.

2.4 Dual luciferase assays

Dual luciferase assays were performed using the Dual Luciferase Reporter System kit, which provides all solutions utilized in the experiment (Promega

Corporation, Madison, WI). Cells plated in 24-well plates were transfected as described above and incubated for 24 hours. Following two washes with 500 μL of PBS, cells were lysed using 100 μL Passive Lysis Buffer, previously diluted from 5x to 1x in MilliQ water, and left to sit for 20 minutes with occasional shaking. Lysates were then resuspended by pipetting up and down, transferred to a 1.5 mL Eppendorf tube and spun down at 20,800 x g. The Stop & Glo (S&G) solution was made up from the 50x substrate and 1x buffer provided by the kit in a borosilicate glass culture tube. The Luciferase Assay Reagent (LARII) was prepared by resuspending the lyophilized Luciferase Assay Substrate in 10 mL of Luciferase Assay Buffer II. 100 μL of LARII was aliquoted into round plastic cuvettes with one cuvette for each 24-well cell lysate collected.

Luciferase activity was measured using a TD-20/20 Luminometer (Turner Designs, Sunnyvale, CA) set to Dual-Luciferase Reporter (DLR) mode. Firefly (*Photinus pyralis*) luciferase activity of the pGL3-E2 box promoter plasmid was measured by adding 20 μL of lysate to the LARII in the cuvettes, pipetted up and down 3 times and put in the luminometer for reading. The *Renilla* (*Renilla reniformis*) reading was then measured in the same cuvette by adding 100 μL of S&G solution, vortexed for 3 seconds, and put in the luminometer. Within each experiment the assays were replicated 6 times.

2.5 Immunofluorescence

NIH3T3 cells were plated on coverslips in a 6-well plate and transfected as described above. The next day, the cells were washed 2 times for 5 minutes with 37°C PBS, fixed by incubation for 15 minutes with ice-cold 4% paraformaldehyde, and washed 3 times for 5 minutes with room temperature PBS containing 0.05% Triton-X (PBSX). Nonspecific antibody binding was blocked with 2% Blocking Reagent (BR) (Roche Applied Science, Laval, QC) for 15 minutes. The coverslips were then incubated with the appropriate primary antibodies dissolved in 250 μL of BR for 1 hour at room temperature and washed 2 times for 5 minutes with PBSX. Next, coverslips were incubated for 1 hour with

the appropriate fluorescently tagged secondary antibodies dissolved in 250 μL of BR and again washed 2 times for 5 minutes with PBSX and protected from light from this point onward. The antibodies used are described above. DNA was stained with Hoechst 33342 nucleic acid stain (Molecular Probes, Eugene, OR) dissolved in PBSX to a concentration of 0.24 μg/mL for 15 minutes, before 2 final 5 minute washes in PBSX. Coverslips were mounted on glass slides with approximately 5 μL of VectaMount permanent mounting media (Vector Laboratories, Burlington, ON) and sealed with clear nail polish. Two coverslips were prepared for each combination and cells counted from both.

Subcellular distribution was analyzed by examining whether there was an increase in nuclear or cytoplasmic levels. One hundred cells were counted and distinguished as being primarily nuclear, primarily cytoplasmic or evenly nuclear and cytoplasmic. To determine if there was an increase in nuclear levels, the number of cells with primarily nuclear, and nuclear and cytoplasmic were compared to the number of cells with primarily cytoplasmic distrubition in two different assays using a Fischer's exact test. In contrast, the significance of an increase in cytoplasmic levels was determined in the same way except the number of primarily cytoplasmic, and cytoplasmic and nuclear cells were compared to the number of predominantly nuclear.

2.6 Immunoprecipitation

HEK293 cells used for coimmunoprecipitation experiments were transfected as described above. Eighteen to 24 hours following transfection, cells plated in 10 mm cell culture plates were lysed with 300 μL of 150 mM NaCl, 50 mM Tris-HCl at pH 8.0, 0.5% IGEPAL (Sigma-Aldrich, Oakville, ON) and Complete Mini protease inhibitors (1 tablet for 10 mL of lysis solution) (Roche Applied Science, Laval, QC) lysis buffer (ECB). Immediately following collection, the samples were placed on ice and kept at 4°C thereafter. After sitting for approximately 10 minutes, lysates were centrifuged at 4°C for 15 minutes at 20,800 xg. The resulting supernatant was aliquoted with 50 μL for

immunoblotting to confirm protein concentration, and 2 tubes of 100 μL for coimmunoprecipitations. Four hundred μL of an intermediate buffer were added to the 100 μL samples so that the final solution was 100 mM NaCl, 20 mM Tris-HCl, pH 8.0 and 0.5% IGEPAL (the same concentrations as in the "wash buffer" detailed below) with a final volume of 500 μL. The lysates were then pre-cleared by incubation with 50% protein G-agarose slurry for about 1.5 hours to remove anything that would adhere to the beads nonspecifically. For each coIP reaction, 40 μL of 50% protein G-agarose slurry was required. Approximately 400 μL of slurry was made by combining 150 μL of protein G-agarose beads (Sigma-Aldrich, Oakville, ON), 150 μL of a 10 mg/mL solution of bovine serum albumin (BSA) (Sigma-Aldrich, Oakville, ON), and 1.5 mL of a wash buffer of 100 mM NaCl, 20 mM Tris-HCl, pH 8.0, and 0.2% IGEPAL. This solution was mixed end-over-end at 4°C for about 2 hours. The resin was pelleted by spinning at 3000 xg for 1 minute and the beads then washed 5 times with 1.5 mL of wash buffer, mixing end-over-end for 5 minutes, pelleting at 3000 xg for 1 minute in between washes. After the final wash, the beads were dissolved in 200 μL of wash buffer to make the 50% slurry and stored at 4°C until needed. After the lysate solution was pre-cleared, it was pelleted by centrifugation at 3000 xg for 1 minute and the supernatant transferred to a new tube. To this supernatant, the primary antibody of interest was added and the resulting solution mixed end-over-end at 4°C overnight. The next morning, 30 μL of 50% protein G-agarose slurry was added and mixed end-over-end for 3 to 4 hours. Following incubation with the protein G beads, the mixture was pelleted and washed as above four times, 5 minutes each, with 1 mL of wash buffer. The supernatant was removed and discarded and 30 μL of 2x sample buffer (20% glycerol, 4% SDS, and 0.13 M Tris-HCl, pH 6.8) with 2% β-mercaptoethanol and 1% saturated bromophenol blue was added to the samples and boiled for 5 minutes to elute the proteins in preparation for running of the SDS-PAGE gel and immunoblotting. The immunoprecipitation experiments were performed one time.

2.7 Immunoblots

SDS-polyacrylamide gel electrophoresis (SDS-PAGE) and Western blotting was used to separate and visualize proteins from the increasing protein effects experiments, CHX experiments, and coimmunoprecipitation experiments. NIH3T3 lysates from the former two assays were collected in 200 μL of 2x sample buffer and placed on ice and allowed to sit for a minimum of 10 minutes. Each sample was sonicated for 5 seconds and centrifuged at 20,800xg for 15 minutes at 4°C. 0.3 μL of saturated bromophenol blue and 0.6 uL of β-mercaptoethanol was added to 30 μL of the resulting supernatant. The sample was boiled for 5 minutes. Proteins were resolved in a 7.5% gel loaded with 20 μL of sample, electrophoresed at 80 mA in running buffer (25 mM Sigma 7-9, 192 mM glycine, and 0.1% SDS). Gels were transferred to Immobilon P polyvinylidene fluoride membranes (Millipore, Billerica, MA) in 4°C transfer buffer (25 mM Tris base, 192 mM glycine, 20% methanol) at 100 V for 90 minutes. Blots were then incubated 1 hour in 10 mL of TBST (20 mM Tris-Cl, pH 7.5, 137 mM NaCl, 0.1% Tween-20) with 5% skim milk powder (TBST-M) and incubated overnight with the appropriate primary antibody diluted in TBST-M, shaking at 4°C. Membranes were subsequently washed three times, 10 minutes each, in TBST and incubated in HRP-conjugated secondary antibodies diluted in TBST-M for 1 hour, shaking at 4°C, and washed another three times for 10 minutes in TBST. 10 mL of Immobilon Western Chemiluminescent HRP solution made up of 5 mL each of Peroxide Solution and Luminol Substrate (Millipore, Billerica, MA) was added to the membranes for detection on a Kodak image station. Protein intensities were analyzed using Kodak Image Station Software and are reported as ratios of protein of interest signal pixel intensity to γ-tubulin pixel intensity.

Table 1. Plasmids used in transfections of HEK293 and NIH3T3 cells

Name of Construct	Source of Construct	Description	Selection
Xpress-Magel2	Dr. Rachel Wevrick University of Alberta Edmonton, AB	Full-length mouse Magel2 into pcDNA4/HisMaxB-Xpress	Ampicillin
mPer2-V5	Dr. Joseph Takahashi Northwestern University Evanston, IL	Full-length mouse *Per2* cloned into pcDNA3.1-V5-His	Ampicillin
mCry1-V5	Dr. Joseph Takahashi Northwestern University Evanston, IL	Full-length mouse *Cry1* cloned into pcDNA3.1-V5-His	Ampicillin
HA-mBmal1	Dr. Marina Antoch Roswell Park Cancer Institute Buffalo, NY	Full-length mouse *Bmal1* cloned into pcDNA3-HA	Ampicillin
HA-mClock	Dr. Marina Antoch Roswell Park Cancer Institute Buffalo, NY	Full-length mouse *Clock* cloned into pcDNA3-HA	Ampicillin
Myc-mClock	Dr. Marina Antoch Roswell Park Cancer Institute Buffalo, NY	Full-length mouse *Clock* cloned into pcDNA3.1-Myc	Ampicillin
pGL3-E2 box promoter	Dr. Joseph Takahashi Howard Hughes Medical Institute Evanston, IL	3.3-kb *Eco*RI/*Xba*I fragment isolated from *Per2*-positive BAC clone subcloned into pGL3-Basic luciferase reporter	Ampicillin
pRL-TK	Dr. Michael Walter University of Alberta Edmonton, AB	Promega *Renilla* luciferase internal control	Ampicillin
LacZ-V5	Dr. Michael Walter University of Alberta Edmonton, AB	Full-length *LacZ* cloned into pcDNA3.1-V5-His	Ampicillin
PitX2-Xpress	Dr. Michael Walter University of Alberta Edmonton, AB	Full-length mouse *PitX2* cloned into pcDNA4/HisMaxB-Xpress	Ampicillin
PitX2-HA	Dr. Michael Walter University of Alberta Edmonton, AB	Full-length mouse *PitX2* cloned into pcDNA3-HA	Ampicillin

Chapter 3. Results

3.1 Bmal1/Clock heterodimer activity at the Per2 promoter is decreased in the presence of Magel2

In searching for a functional role of Magel2 in circadian rhythm, I looked at the more well documented behaviour of its close homolog Necdin. Necdin is another MAGE protein and the gene also maps to the region associated with Prader-Willi syndrome. Necdin is a neurodevelopmental protein involved in regulation of cell cycle, differentiation and apoptosis. It has been shown to function by altering the activity of a number of transcription factors, including Dlx and Msx (Kuwajima et al., 2006; Kuwajima et al., 2004; Miller et al., 2009). We therefore wondered whether Magel2 might alter the transcriptional activity of the Bmal1/Clock heterodimer at E-box promoters. To investigate this question, we assessed the impact of Magel2 on the activation of the Per2 promoter by Bmal1 and Clock. We performed a dual luciferase assay by transfecting NIH3T3 cells with a *mPer2-E2::Luciferase* (mPer2:luc) construct containing the circadian enhancer (E2) with a noncanonical E-box (Figure 10A). While additional E-box candidate elements have been found in the *mPer2* promoter, mutation of E2 alone caused the greatest reduction in Bmal1-Clock-mediated activation. Thus, this E-box is associated with most cis element activity (Yoo et al., 2005). We also co-transfected cells with a control renilla lucifease reporter construct. As expected, cell transfection with pcDNA3.1 plasmids encoding Bmal1 and Clock caused an approximate 4.5-fold increase in luciferase activity over baseline levels (Figure 10B, assay 2 versus assay 1). Addition of Per2 and Cry1 cloned into pcDNA3.1 repressed this activity, with Cry1, a stronger repressor than Per2, decreasing relative luciferase activity significantly below baseline levels (Figure 10B and C, assay 3 and 4 versus assay 2). This likely occurs because Cry1 is also inhibiting the activity of endogenous Bmal1 and Clock on the transfected mPer2:luc construct. Interestingly, addition of Magel2 also significantly inhibits the activity of Bmal1 and Clock at the Per2 E-box (Figure 10B and C, assay 5 versus assay 2).

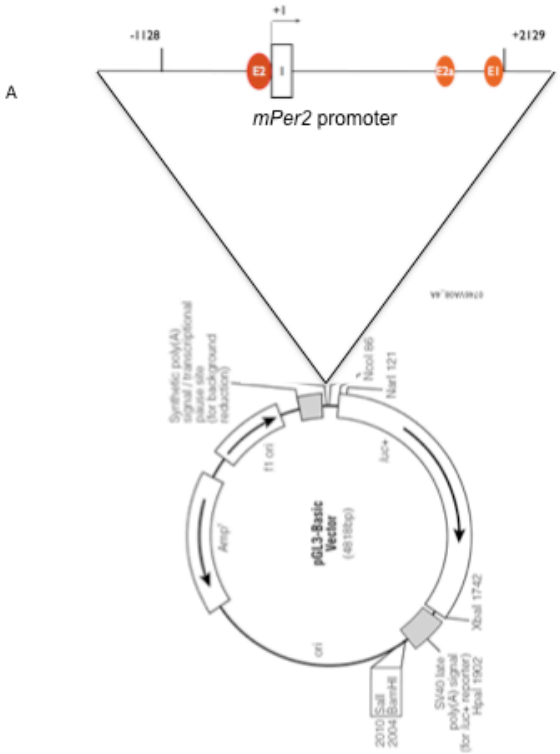

Figure 10. Activity of the Bmal1 and Clock heterodimer is decreased in the presence of Magel2. A dual luciferase assay was performed in NIH3T3 cells transfected with per2:luciferase and various constructs. (A) A schematic of the mPer2::luciferase construct used in the dual luciferase assay. The 3.3 kb mPer2 promoter fragment was subcloned into the pGL3-Basic luciferase reporter vector. The open box represents exon 1 of *mPer2*, +1 is the transcription start site, and open ovals are the E-box enhancer sites, E1, E2, and E2a (modified from Yoo et al. 2005). (B) Increased luciferase activity is observed with addition of Bmal1-HA and Clock-HA and this activity is significantly decreased when Per2-V5 or Cry1-V5 are added. (C) Transfection of Magel2-X also significantly reduces luciferase activity compared to Bmal1-HA and Clock-HA activation and this effect is stronger when cotransfected with Per2-V5 but not Cry1-V5. Note (B) and (C) are from one experiment.

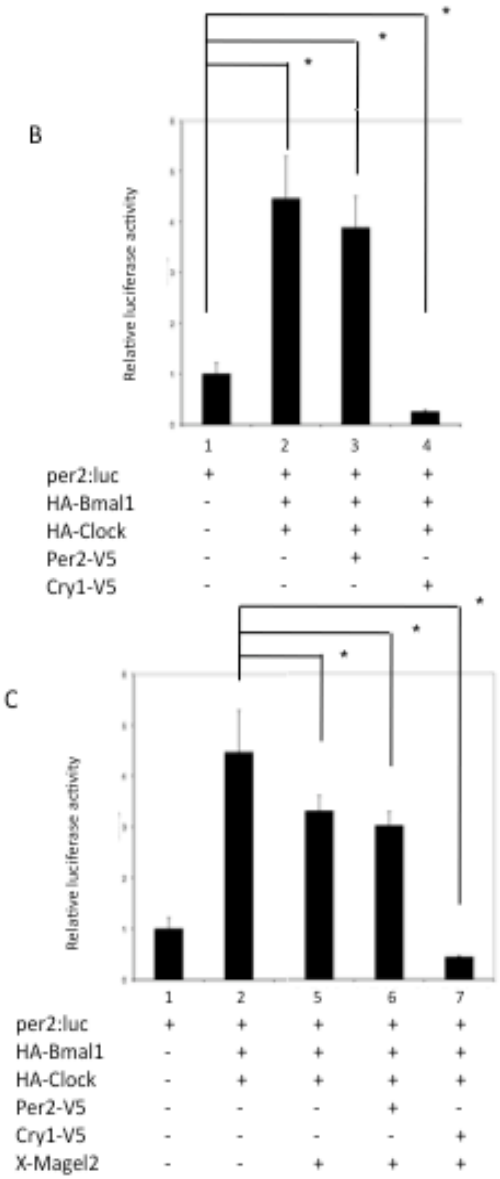

* $p < 0.0001$

Assay 3 versus assay 6
$p = 0.0009$

Assay 5 versus assay 6
$p = 0.03$

Assay 4 versus assay 7
$p < 0.0001$

Assay 5 versus assay 7
$p < 0.0001$

To investigate whether there is an effect of the presence of both Magel2 and the known transcriptional repressors on transcriptional activity, we performed similar experiments in which Magel2 was cotransfected with either Per2 or Cry1 constructs. The addition of Per2 and Magel2 resulted in a significantly stronger repressive effect than either of these proteins alone. Since the total amount of construct was the same in assays 3, 5 and 6, this result indicates that Magel2 and Per2 may function together and facilitate the other's action to inhibit the activity of Bmal1 and Clock (Figure 10B and C, assay 3 versus 6). The same result was not seen with Magel2 and Cry1 as these two proteins produced a level of luciferase activity intermediate to that observed with either construct transfected alone (Figure 10B and C, assay 4 versus 7). These results indicate a potential role of Magel2 as a transcriptional repressor of the Bmal1 and Clock heterodimer in the functioning of the circadian clock.

3.2 Coexpression of circadian proteins and Magel2 alters their subcellular distribution

Subcellular distribution of circadian proteins throughout the cycle is an important mechanism that controls both the transcriptional activity of the Bmal1/Clock heterodimer and stability or degradation of the proteins (Kwon et al., 2006; Lee et al., 2008). We next investigated whether Magel2 exerts its repressive effect by altering cellular localization of circadian proteins. Previously, Bmal1 was found to be predominantly located within the nucleus throughout the cycle whether transfected alone or with Clock (Kondratov et al., 2003). The subcellular distribution of Clock however is dependent on the circadian fluctuations of Bmal1. Movement of Clock is dependent on its binding to Bmal1 as lack of Bmal1 or mutation in this protein's nuclear localizing sequence results in exclusive cytoplasmic accumulation of Clock (Kondratov et al., 2003; Kwon et al., 2006).

Next, I examined the subcellular distribution of Magel2 expressed alone or with various circadian proteins. I transfected NIH3T3 cells plated on coverslips with various combinations of constructs encoding either epitope-tagged circadian constructs or the empty vector. These cells were subsequently fixed and incubated with the appropriate antibody for fluorescence immunocytochemistry. For each combination, 100 cells were counted and the subcellular localization of the recombinant epitope-tagged protein classified as either nuclear, nuclear and cytoplasmic, or cytoplasmic depending upon the subcellular region where the greatest level of fluorescence was observed. Xpress-tagged Magel2 (Xpress-Magel2) was transfected alone into cells and probed with a mouse anti-Xpress monoclonal antibody followed by an AlexaFluor 594 goat anti-mouse secondary antibody. Quantification revealed that 18% of cells exhibited primarily nuclear localization, 38% of cells expressed the protein evenly across the nucleus and cytoplasm, and in 44% of cells, cytoplasmic concentration predominated (Figure 11A). I then co-expressed Xpress-Magel2 with the epitope-tagged circadian proteins Myc-Clock, HA-Bmal1 , Per2-V5 and Cry1-V5 to determine whether co-expression changed the subcellular distribution of Xpress-Magel2. These epitope-tagged circadian proteins were visualized using rabbit anti-HA for HA-Bmal1, rabbit anti-Myc for Myc-Clock, or rabbit anti-V5 for V5-Per2 and V5-Cry1 polyclonal antibodies. Mouse anti-Myc monoclonal antibody, together with rabbit anti-HA polyclonal antibody was used to visualize Myc-Clock and Ha-Bmal1 in cells expressing Myc-Clock, Ha-Bmal1, and Xpress-Magel2. Subsequently, the coverslips were incubated with AlexaFluor 488 or 594 goat-anti rabbit or AlexaFluor 488 or 594 goat-anti mouse, secondary antibody. We compared the number of cells showing predominantly nuclear plus those exhibiting nuclear and cytoplasmic distribution to the number of cells with mostly cytoplasmic localization in order to determine whether coexpression lead to increased nuclear levels of Xpress-Magel2. The subcellular distribution of Xpress-Magel2 was not significantly altered when cotransfected with HA-Bmal1 or Myc-Clock (Figure 11B or C, and G, lane 2 or 3 versus 1). However, when both HA-Bmal1 and Myc-

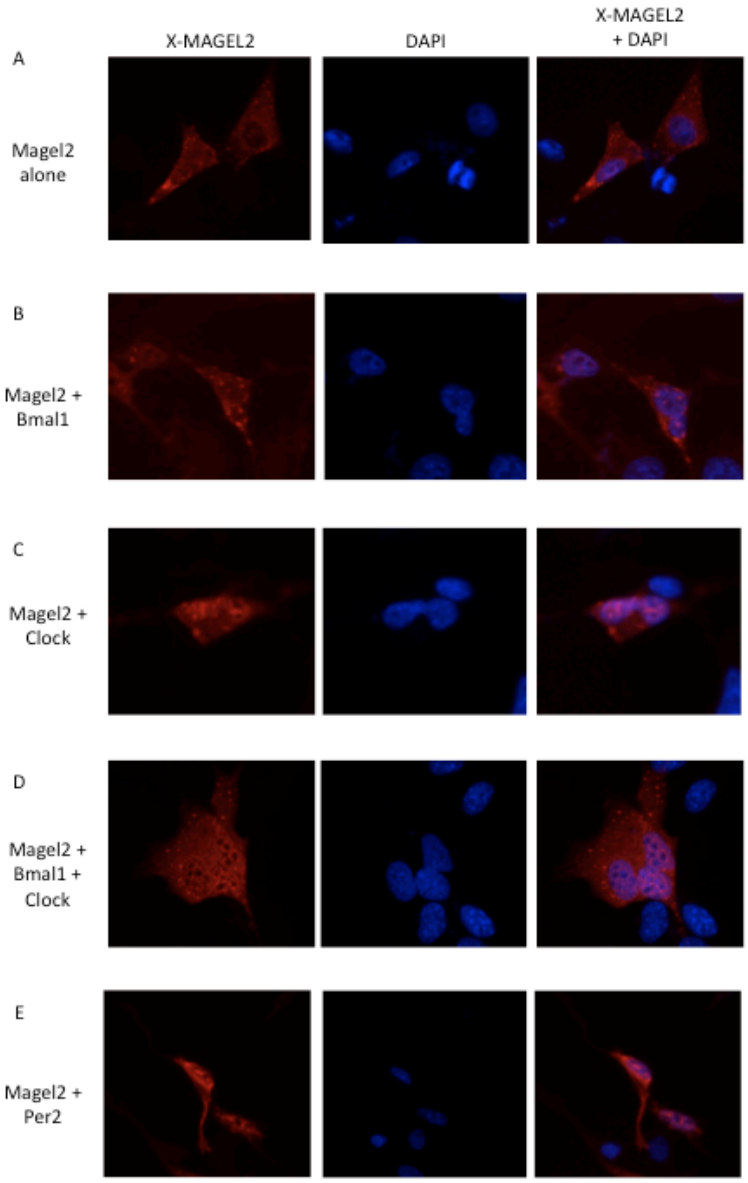

Figure 11. Subcellular distribution of Xpress-Magel2 is altered when coexpressed with circadian proteins. NIH3T3 cells plated on coverslips were transfected with Xpress-Magel2- and tagged circadian proteins-expressing constructs alone and in various combinations. Cells were assayed based on the subcellular region with the greatest expression. (A) Xpress-Magel2 showed predominantly cytoplasmic localization when transfected alone, and (B) with HA-Bmal1 (lane 2 versus 1 in (G)), (C) with Myc-Clock (lane 3 versus 1 in (G)), or (D) with HA-Bmal1 and Myc-Clock together (lane 4 versus 1 in (G)). Xpress-Magel2 became more nuclear localized following coexpression (E) with V5-Per2 (lane 5 versus 1 in (G)) and (F) V5-Cry1 (lanes 6 versus 1 in (G)). Black indicates predominately nuclear, grey indicates evenly nuclear and cytoplasmic, and white, indicates predominantly cytoplasmic.

F

Magel2 +
Cry1

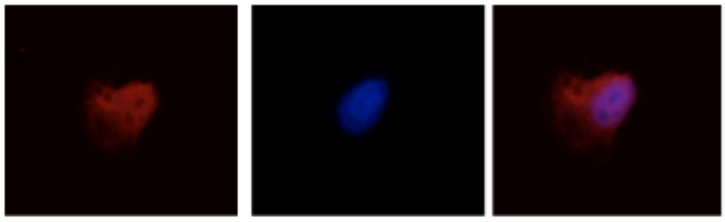

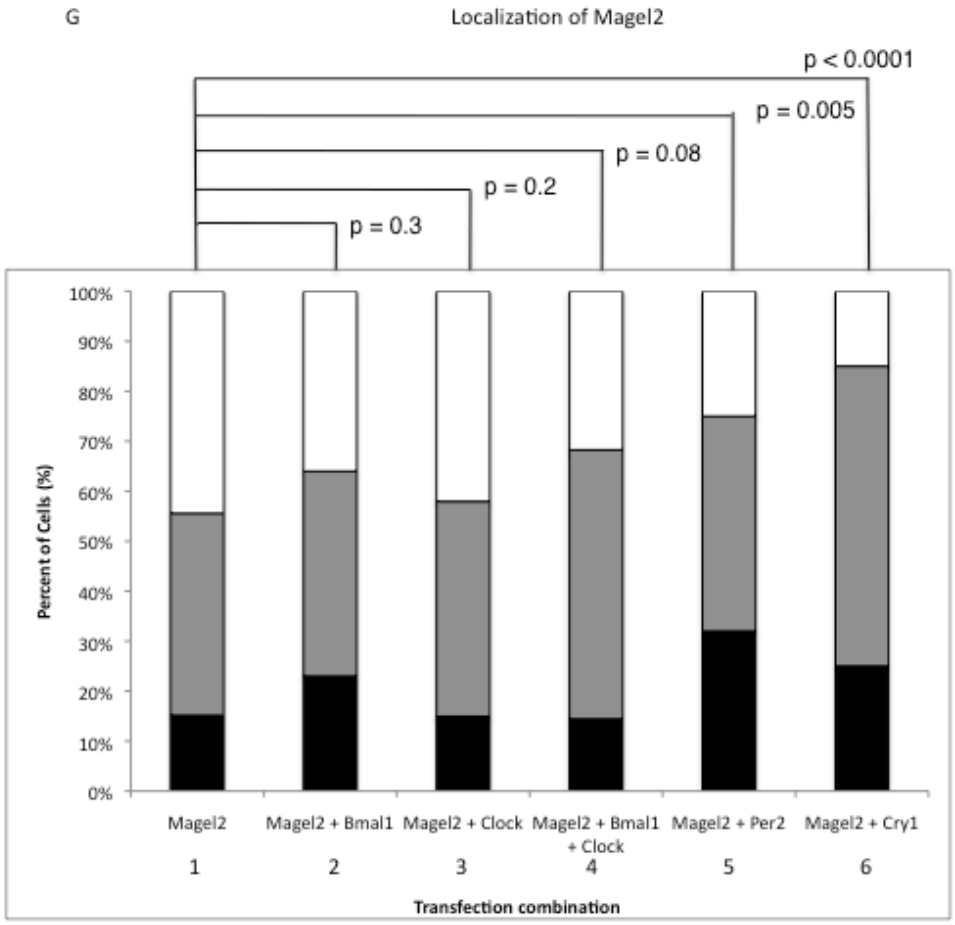
G
Localization of Magel2
p < 0.0001
p = 0.005
p = 0.08
p = 0.2
p = 0.3
100%
90%
80%
70%
60%
50%
40%
30%
20%
10%
0%
Percent of Cells (%)
Magel2
Magel2 + Bmal1
Magel2 + Clock
Magel2 + Bmal1 + Clock
Magel2 + Per2
Magel2 + Cry1
1
2
3
4
5
6
Transfection combination

Clock were present in the cell with Xpress-Magel2, an increase in the number of cells with nuclear or nuclear and cytoplasmic Magel2, from 56% to 71%, was observed, though this effect was not significant (Figure 11D and G, lane 4 versus 1). Similarly, in the presence of Per2-V5 and Cry1-V5 the proportion of cells with nuclear Xpress-Magel2 significantly increased from 55% to 75% and 85% respectively (Figure 11E or F, and G, lane 5 or 6 versus 1). This change in localization upon coexpression with HA-Bmal1 and Myc-Clock, Per2-V5 or Cry1-V5 was demonstrated by an increased number of cells with predominantly nuclear or predominantly nuclear and cytoplasmic distribution respectively.

The reciprocal experiments, in which circadian proteins were expressed alone or with Xpress-Magel2, were also performed. Similar to published results regarding localization of endogenous circadian proteins, we found that HA-Bmal1 is predominantly nuclear in 86% of cells, whereas Clock-Myc is found primarily in the nucleus in approximately 30% of cells alone but in close to 70% of cells when co-expressed with Bmal1 (Figure 12A and G, and 12A, B and G, lane 2 versus 1). The latter result is not in complete agreement to the findings by Kondratov et al. (2003) and Kwon et al. (2006), where close to no Clock was seen in the nucleus of singly transfected cells. However, the significant increase in percent of cells with nuclear Clock in the presence of Bmal1 was in accordance with past results. Levels of cytoplasmic HA-Bmal1 significantly increased when expressed with either Myc-Clock or Xpress-Magel2 compared to when transfected alone. This is demonstrated by the increases from 14% of cells with nuclear and cytoplasmic or cytoplasmic Bmal1 distribution when present alone (Figure 12A) to 60% and 36% of cells when present with Clock and Magel2 respectively (Figure 12B, C, and E, lane 2 and 3 versus 1). In contrast, when Bmal1 is expressed with both Clock and Magel2, it has a nearly identical distribution to when it is expressed alone (Figure 12D and G, lane 4 versus 1). In both cases, 86% of cells show primarily nuclear Bmal1 and either 13% or 14% with nuclear and cytoplasmic distribution when Bmal1 is alone or with Clock and Magel2 respectively. The localization of Clock is significantly more cytoplasmic when cotransfected with Magel2 as shown by

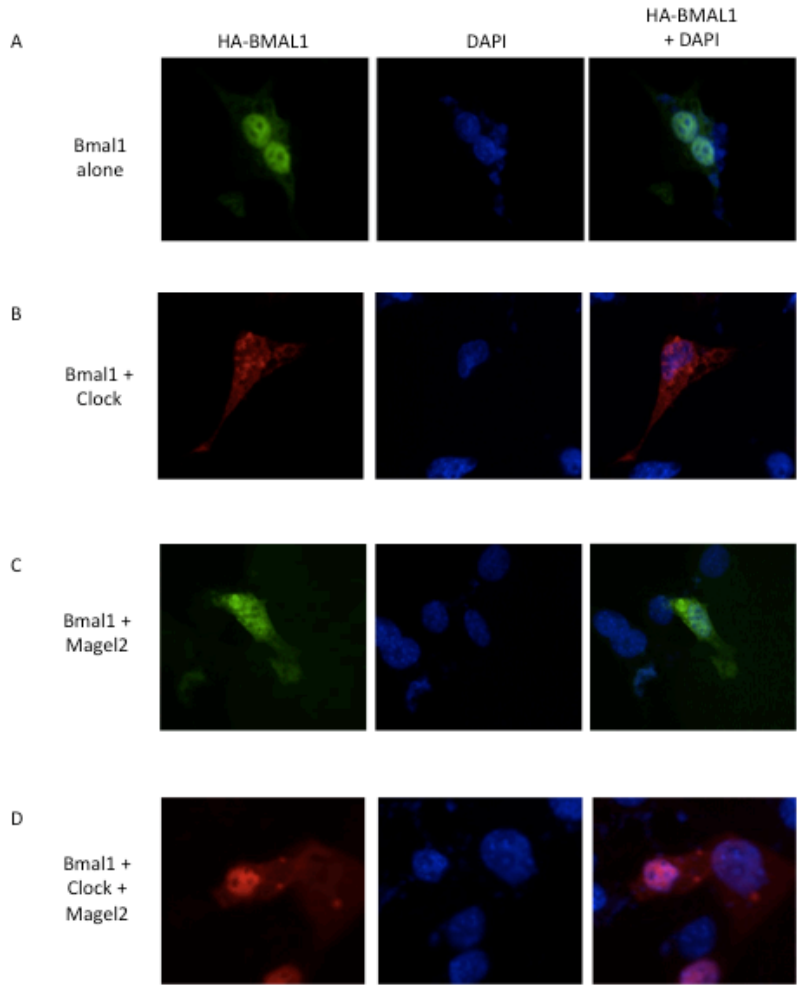

Figure 12. Subcellular distribution of HA-Bmal1 is altered when coexpressed with Clock and Magel2. NIH3T3 cells plated on coverslips were transfected with HA-Bmal1 alone and in various combinations with Xpress-Magel2 or tagged circadian proteins-expressing constructs. Cells were assayed based on the subcellular region with the greatest expression. (A) HA-Bmal1 showed predominantly nuclear localization when transfected alone (lane 1 in (E)). Increased cytoplasmic HA-Bmal1 was observed following coexpression (B) with Myc-Clock (lane 2 versus 1 in (E)) and (C) with Xpress-Magel2 (lanes 3 versus 1 in (E)). Predominantly nuclear localization of HA-Bmal1 was observed following transfection (D) with both Xpress-Magel2 and Myc-Clock (lane 4 versus 1 in (E)). Black indicates predominately nuclear, grey indicates evenly nuclear and cytoplasmic, and white, indicates predominantly cytoplasmic.

E

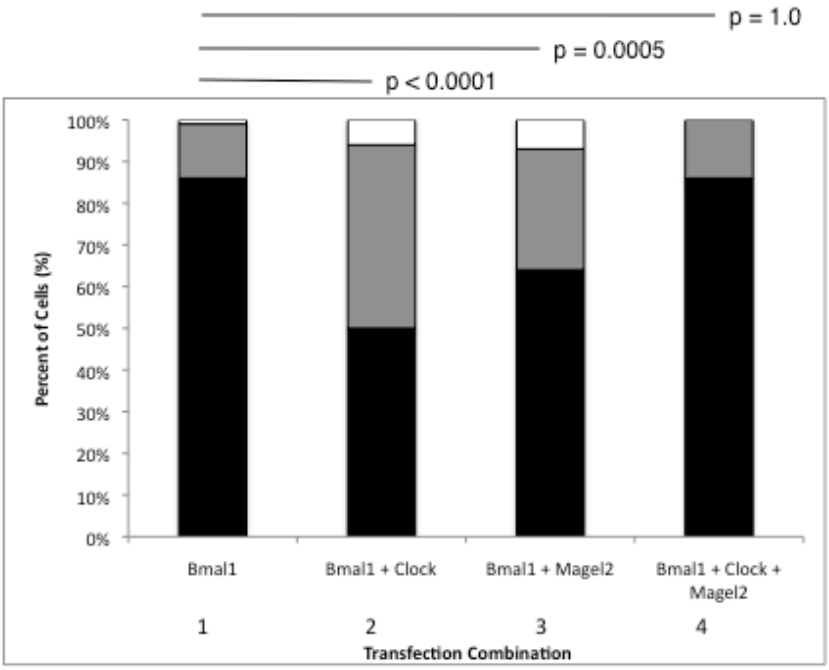
Localization of Bmal1
p = 1.0
p = 0.0005
p < 0.0001
100%
90%
80%
70%
60%
50%
40%
30%
20%
10%
0%
Percent of Cells (%)
Bmal1
Bmal1 + Clock
Bmal1 + Magel2
Bmal1 + Clock + Magel2
1
2
3
4
Transfection Combination

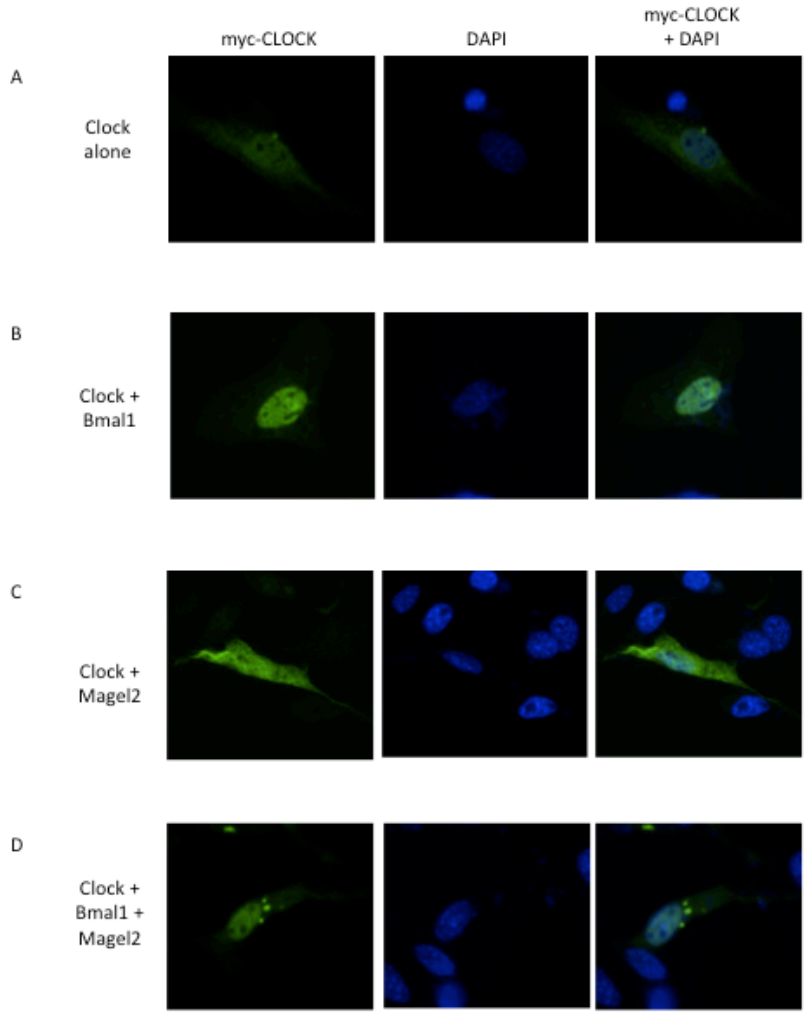

Figure 13. Subcellular distribution of Myc-Clock is altered when coexpressed with Bmal1 and Magel2. NIH3T3 cells plated on coverslips were transfected with Myc-Clock alone and in various combinations with Xpress-Magel2 or tagged circadian proteins-expressing constructs. Cells were assayed based on the subcellular region with the greatest expression. (A) Myc-Clock showed predominantly nuclear and cytoplasmic localization when transfected alone (lane 1 in (E)). Increased nuclear Myc-Clock was observed following coexpression (B) with HA-Bmal1 (lane 2 versus 1 in (E)). HA-Bmal1 was more cytoplasmic when coexpressed (C) with Xpress-Magel2 (lanes 3 versus 1 in (E)). Predominantly nuclear localization of Myc-Clock was observed following transfection (D) with both Xpress-Magel2 and HA-Bmal1 (lane 4 versus 1 in (E)). Black indicates predominately nuclear, grey indicates evenly nuclear and cytoplasmic, and white, indicates predominantly cytoplasmic.

E

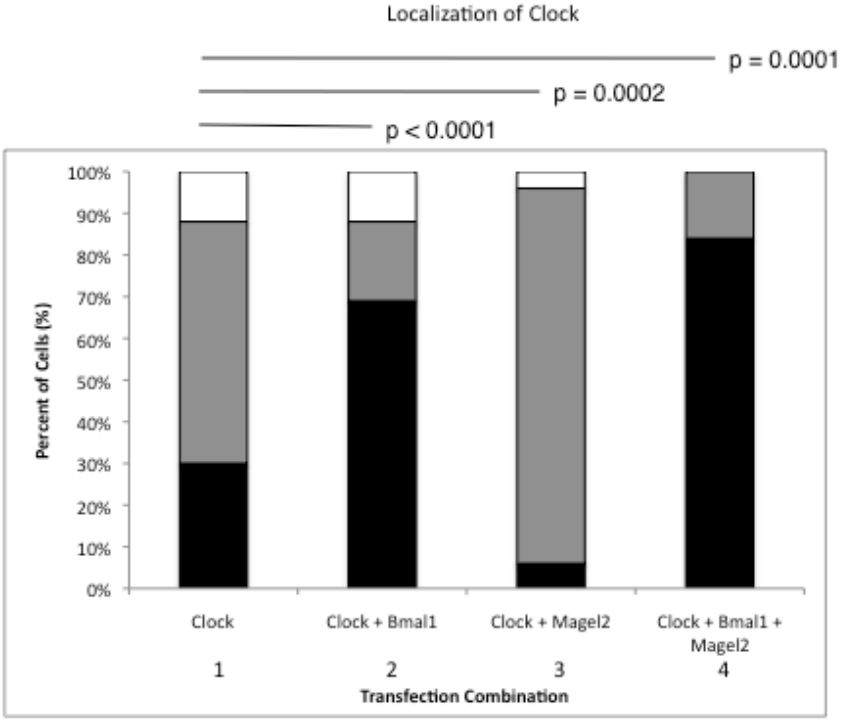
Localization of Clock
p = 0.0001
p = 0.0002
p < 0.0001
100%
90%
80%
70%
60%
50%
40%
30%
20%
10%
0%
Percent of Cells (%)
Clock
Clock + Bmal1
Clock + Magel2
Clock + Bmal1 + Magel2
1
2
3
4
Transfection Combination

the increase from 70% to 94% of cells with nuclear and cytoplasmic or cytoplasmic distribution (Figure 13A and C, and E, lane 3 versus 1). A predominantly nuclear distribution of Clock, 84% of cells, results from the coexpression of Clock with Bmal1 and Magel2 together (Figure 13D and E, lane 4 versus 1). Per2-V5 is found throughout the cell, with 36% and 21% of cells showing primarily nuclear and cytoplasmic localization respectively and the remaining 43% exhibiting nuclear and cytoplasmic distribution. This expression pattern is not altered by Magel2 (Figure 14A, B and C, lane 2 versus 1). Ninety percent of cells transfected with Cry1-V5 alone show greatest expression within the nucleus. Cotransfection with Magel2 causes a significant increase in the cytoplasmic levels of Cry1, from 10% to 25% of cells (Figure 15A, B, and C, lane 2 versus 1). These results indicate that the both Magel2 and core circadian proteins can alter the subcellular location of one another.

3.3 Coexpression of circadian proteins and Magel2 in increasing quantities alters their levels

Subcellular location is an important factor affecting the targeting of circadian proteins for degradation (Kwon et al., 2006; Lee et al., 2008). We examined whether Magel2 and core circadian proteins alter each other's levels when coexpressed. The stability of both Bmal1 and Clock are mutually affected by the presence of the other through alteration of subcellular localization followed by SUMOylation and ubiquitin-dependent proteolysis in promyelocytic leukemia nuclear bodies (PML) (Lee et al., 2008). Because the subcellular location of Bmal1 and Cry1 was altered in the presence of Magel2, we sought to determine if the presence of Magel2 additionally affects the levels of these and other circadian proteins. NIH3T3 cells were transiently transfected with constant amounts of HA-Bmal1, V5-Per2 constructs and increasing amounts of Xpress-Magel2 and decreasing amounts of empty pcDNA4b vector so that the total DNA added to the cells remained the same. As a negative control we also transfected cells with

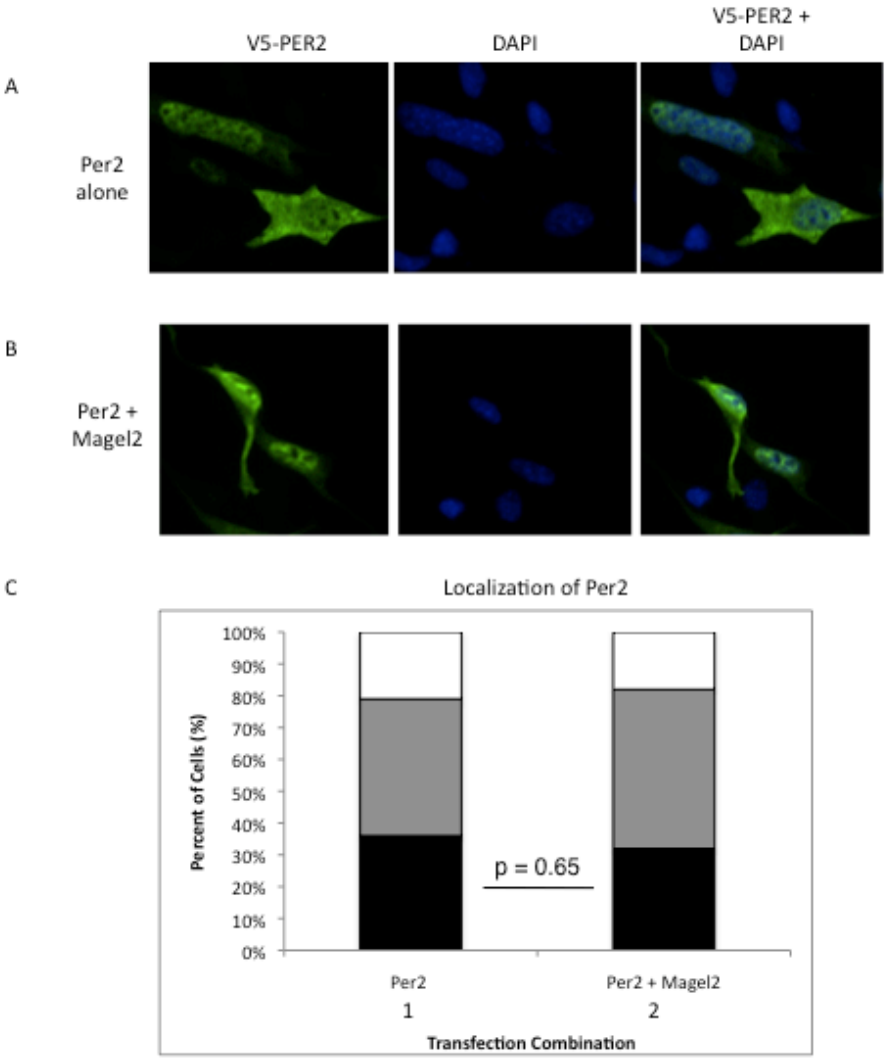

Figure 14. Subcellular distribution of Per2-V5 is not altered when coexpressed with Magel2. NIH3T3 cells plated on coverslips were transfected with Per2-V5 alone and with Xpress-Magel2. Cells were assayed based on the subcellular region with the greatest expression. (A) Per2-V5 showed predominantly nuclear, and nuclear and cytoplasmic localization when transfected alone (lane 1 in (C)) or (B) with Xpress-Magel2 (lane 2 versus 1). Black indicates predominately nuclear, grey indicates evenly nuclear and cytoplasmic, and white, indicates predominantly cytoplasmic.

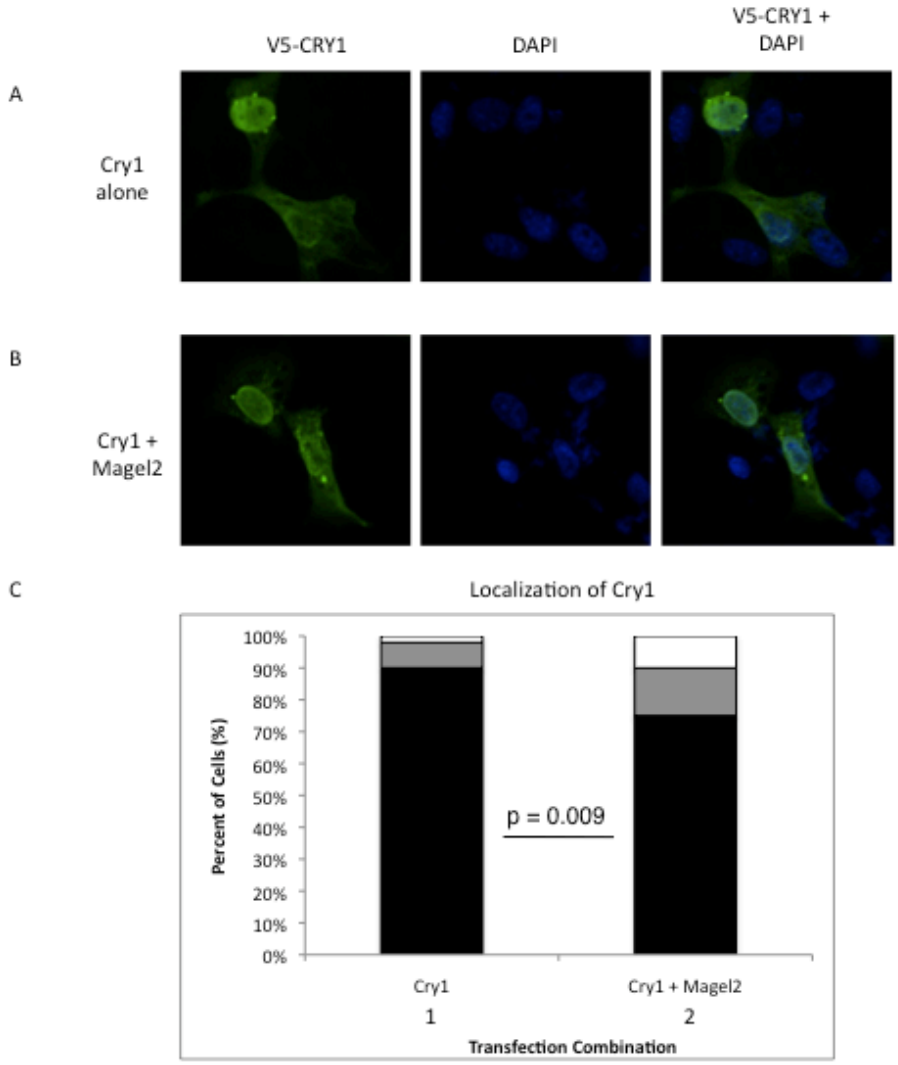

Figure 15. Subcellular distribution of Cry1-V5 is altered when coexpressed with Magel2. NIH3T3 cells plated on coverslips were transfected with Cry1-V5 alone and with Xpress-Magel2. Cells were assayed based on the subcellular region with the greatest expression. (A) Cry1-V5 showed predominantly nuclear localization when transfected alone (sample 2 versus 1). Increased cytoplasmic levels were observed following cotransfection of Cry1-V5 with Xpress-Magel2 (B) (sample 2 versus 1). Black indicates predominately nuclear, grey indicates evenly nuclear and cytoplasmic, and white, indicates predominantly cytoplasmic.

Xpress-tagged PitX2 and found that levels of all proteins were not affected by the presence of a similarly tagged control protein. Lysates were collected and the proteins detected with immunoblot analysis with signal intensities normalized to gamma tubulin. We then calculated the rate of change in protein levels as a function of increasing cotransfected protein. A slope of 0 indicated no significant effect of increasing cotransfected protein. Steady-state levels of Bmal1 were found to increase 2.6 μg^{-1} over the course of progressively greater amounts of Magel2, an amount significantly higher than the zero change expected (Figure 16A). Levels of Per2 were not affected by increasing levels of Magel2 (Figure 17A). There was a trend towards increasedi Per2 levels as amount of Magel2 plasmid transfected was increased from 0 μg to 0.6 μg, however this increase was not significant. Levels of Cry1 were found to significantly decrease as increasing amounts of *Magel2* was transfected into cells (Figure 18A). This result must be explored further however, since transfection of Cry1 with increasing levels of a negative control construct, Xpress-tagged PitX2, also significantly decreased observed Cry1 protein levels (Figure 20).

Though the mechanism by which Magel2 is degraded is not yet understood, we also sought to establish whether its levels were affected by the presence of circadian proteins. Similar experiments to those described above were performed except that cells were transfected with constant amounts of Xpress-Magel2 and increasing amounts of HA-Bmal1, Per2-V5, or Cry1-V5. Magel2 was also transfected with either 0 μg or 0.6 μg of HA-tagged *PitX2* or V5-tagged *LacZ* plasmids as a negative control for HA-Bmal1, and Per2-V5 or Cry1-V5, respectively. Levels of Magel2 protein were not significantly altered by the presence of increasing Bmal1 (Figure 16B). However, the amount of Magel2 protein was found to decrease as more Per2 was present in cells. Magel2 levels declined 1.6 μg^{-1} as *Per2* levels were increased from 0 μg to 0.6 μg of transfected plasmid (Figure 17B). Similarly, as levels of Cry1 protein are increased, Magel2 levels are found to decrease significantly by 0.6 μg^{-1} (Figure 18B). To further establish whether Per2 diminishes Magel2 levels by negatively affecting its

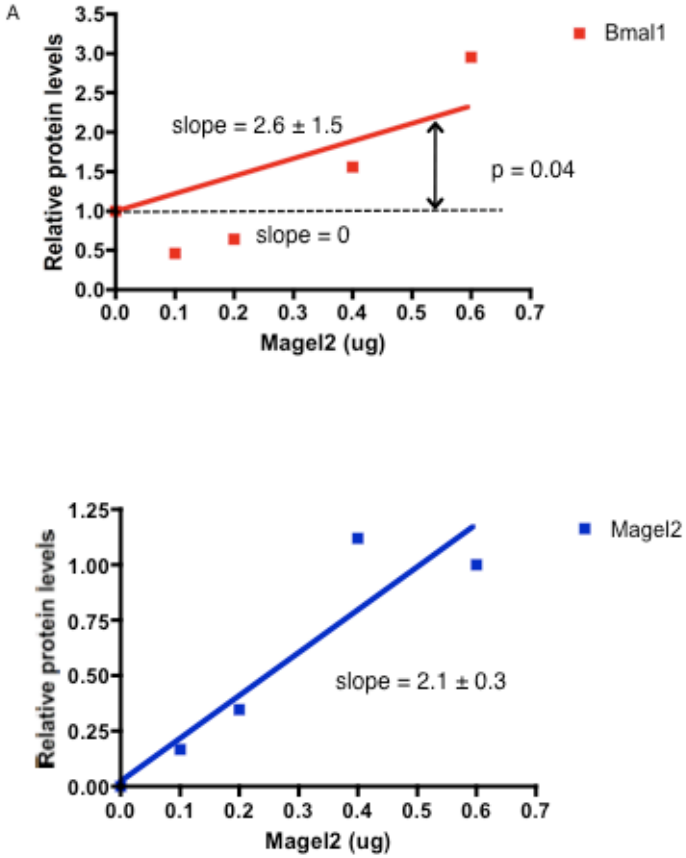

Figure 16. The levels of Magel2 and Bmal1 are altered when coexpressed. NIH3T3 cells were transfected with constant amounts of HA-Bmal1 and increasing amounts of Xpress-Magel2 or constant amounts of Xpress-Magel2 and increasing amounts of HA-Bmal1 protein-expressing constructs. (A) Levels of HA-Bmal1 significantly increase (red graph) as levels of Xpress-Magel2 increase (blue graph). (B) Levels of Xpress-Magel2 are not significantly affected (red graph) by increasing levels of Ha-Bmal1 (blue graph).

B

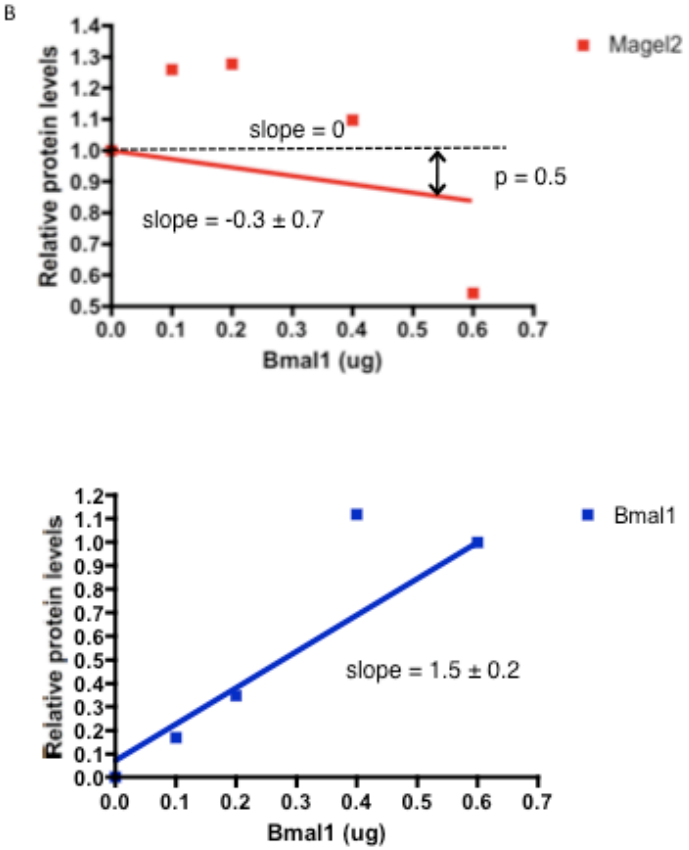
Magel2
Relative protein levels
slope = 0
p = 0.5
slope = -0.3 ± 0.7
Bmal1 (ug)
Bmal1
Relative protein levels
slope = 1.5 ± 0.2
Bmal1 (ug)

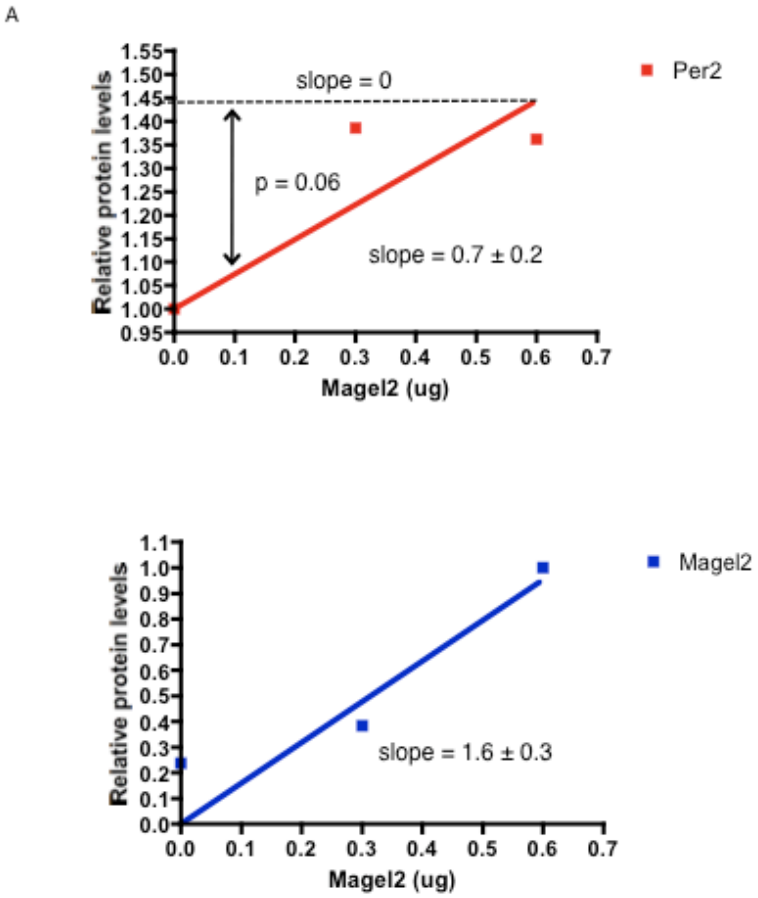

Figure 17. The levels of Per2 and Magel2 are altered when coexpressed. NIH3T3 cells were transfected with constant amounts of Per2-V5 and increasing amounts of Xpress-Magel2 or constant amounts of Xpress-Magel2 and increasing amounts of Per2-V5 protein-expressing constructs. (A) Levels of Per-V5 are not significantly affected (red graph) by increasing levels of Xpress-Magel2 (blue graph). (B) Levels of Xpress-Magel2 significantly decrease (red graph) as levels of Per-V5 increase (blue graph).

B

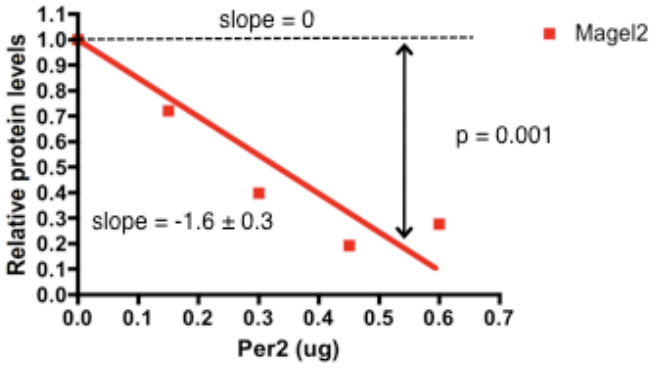
slope = 0
Magel2
p = 0.001
Relative protein levels
slope = -1.6 ± 0.3
Per2 (ug)

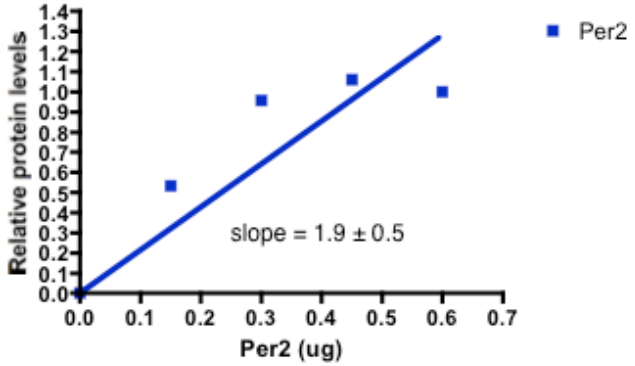
Per2
Relative protein levels
slope = 1.9 ± 0.5
Per2 (ug)

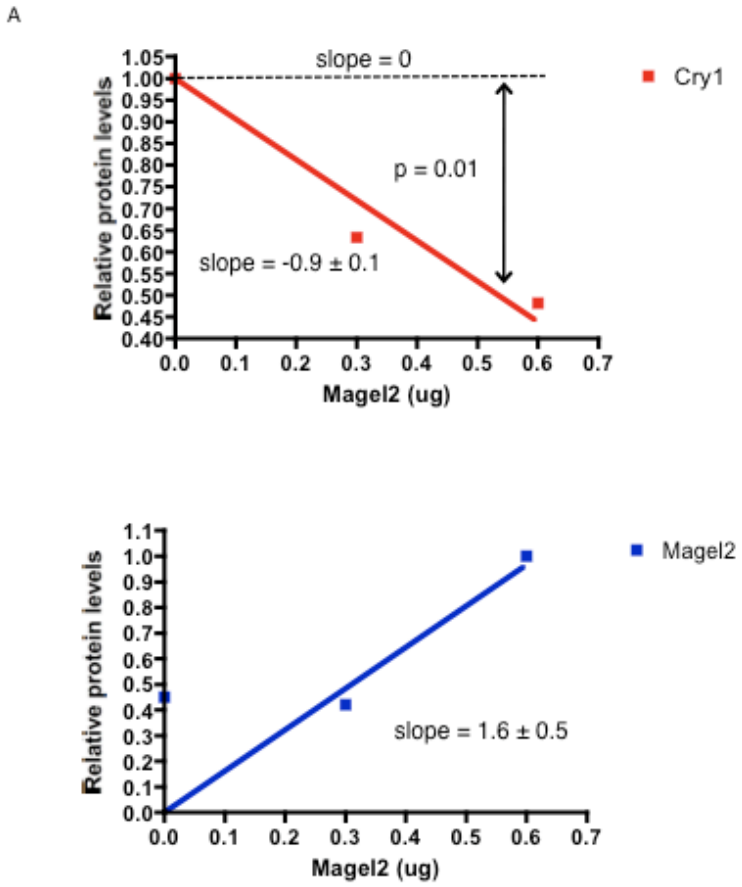

Figure 18. The levels of Cry1 and Magel2 are altered when coexpressed. NIH3T3 cells were transfected with constant amounts of Cry1-V5 and increasing amounts of Xpress-Magel2 or constant amounts of Xpress-Magel2 and increasing amounts of Cry1-V5 protein-expressing constructs. (A) Levels of Cry1-V5 significantly decrease (red graph) as levels of Xpress-Magel2 increase (blue graph). Levels of Xpress-Magel2 do not increase significantly. (B) Levels of Xpress-Magel2 are not significantly affected (red graph) by increasing levels of Cry1-V5 (blue graph).

B

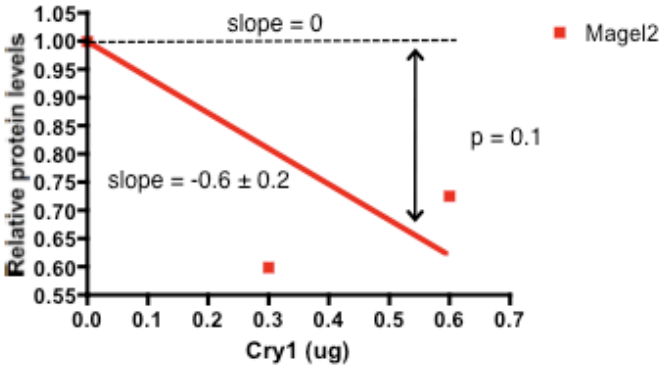
slope = 0
Magel2
p = 0.1
slope = -0.6 ± 0.2
Relative protein levels
1.05
1.00
0.95
0.90
0.85
0.80
0.75
0.70
0.65
0.60
0.55
0.0 0.1 0.2 0.3 0.4 0.5 0.6 0.7
Cry1 (ug)

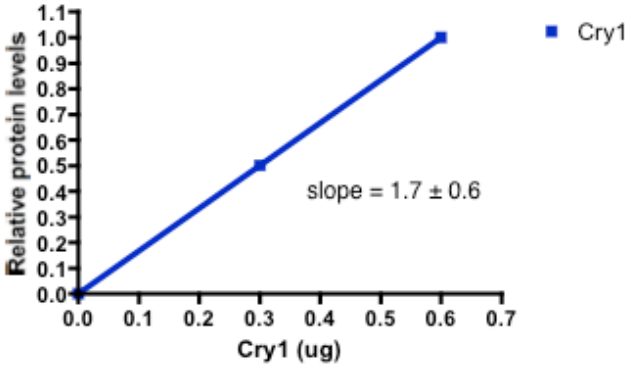
Cry1
slope = 1.7 ± 0.6
Relative protein levels
1.1
1.0
0.9
0.8
0.7
0.6
0.5
0.4
0.3
0.2
0.1
0.0
0.0 0.1 0.2 0.3 0.4 0.5 0.6 0.7
Cry1 (ug)

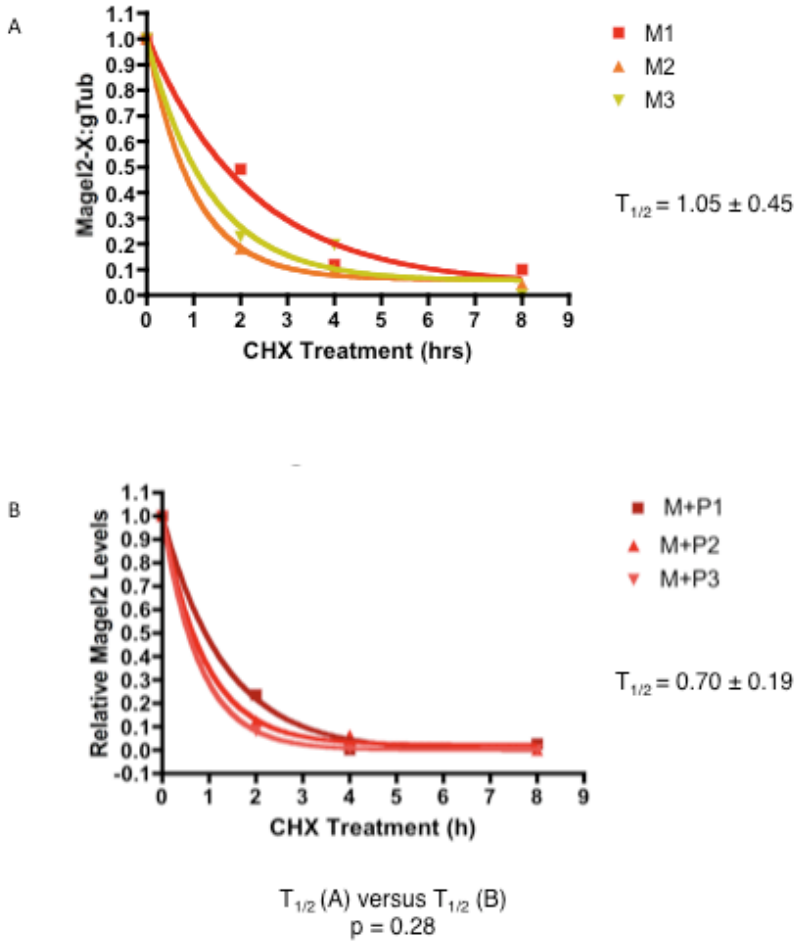

Figure 19. The halflife of Magel2 is not altered by the presence of Per2. NIH3T3 cells were transfected with Xpress-Magel2 (M) and either empty vector or V5-Per2 (P). Following treatment with CHX for the times indicate, lysates were collected and Xpress-Magel2 detected via immunoblotting. Analysis of the rate of degradation of Xpress-Magel2 when transfected alone revealed a halflife of 1.5 hours (A). When co-transfected with V5-Per2, the halflife of Magel2 was found to be reduced to 0.70 hours, though this change was not significant.

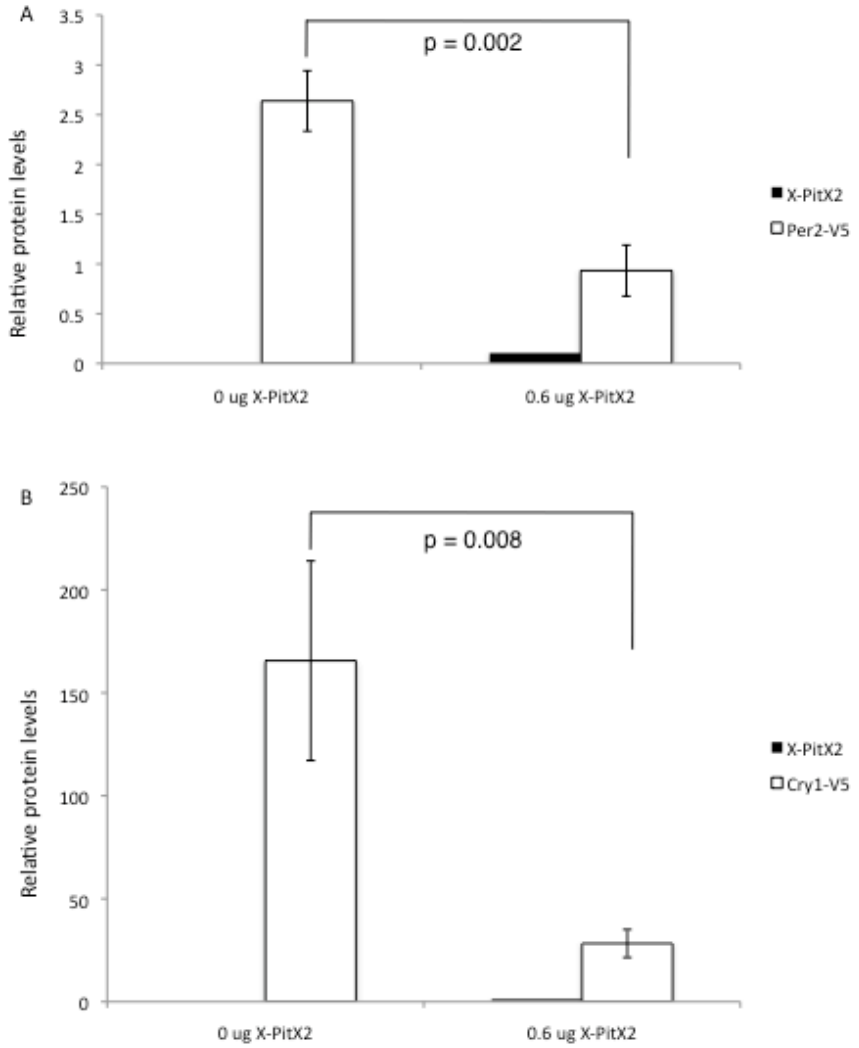

Figure 20. Co-expression with the Xpress-tagged control protein lowers levels of V5-tagged circadian proteins. NIH3T3 cells were transfected with constant amounts of Per2-V5 or Cry1-V5 and either empty vector or Xpress-PitX2. (A) Levels of Per2-V5 significantly decrease (white) in the presence of X-PitX2 (black). (B) Levels of Cry1-V5 significantly decrease (white) in the presence of X-PitX2 (black).

stability, we examined the half-life of Magel2 in the presence or absence of Per2. Cells were transfected with 0.6 μg of Xpress-Magel2 and V5-Per2 and subsequently treated with CHX to arrest mRNA translation and protein production. Lysates were collected at time points up to 8 hours and the proteins were detected via immunoblotting and normalized to gamma tubulin. When Magel2 was expressed alone, its half-life was 1.05 hours (Figure 19A). The turnover of Magel2 was increased in the presence of Per2. Its half life was reduced from 1.05 to 0.70 hours, however this effect was not significant with a p value of 0.28 (Figure 19B). Magel2 and circadian proteins alter the levels of one another, an effect which may be related to the changes observed in subcellular localization.

3.4 Magel2 can interact with core circadian proteins

Since we found that Magel2 represses activity of Bmal1 and Clock at the Per2 promoter and alters the subcellular distribution and levels of Bmal1, we tested whether Magel2 could physically interact with circadian proteins, using a co-immunoprecipitation experiment. HEK293 cells were transiently transfected with epitope-tagged full-length genes encoded by plasmid expression cDNAs. The first potential interaction examined was between Magel2 and Bmal1. Cells were transfected with Xpress-Magel2 and HA-Bmal1 together or alone with the corresponding empty vector. After 24 hours, cell lysates were collected and incubated with either mouse anti-Xpress monoclonal antibody or mouse anti-HA monoclonal antibody over night. Subsequently, the lysates were mixed end-over-end with a 50% protein G-agarose and then run on an SDS-PAGE gel to separate the proteins.Western blots of resulting precipitate were probed for HA-Bmal1 or Xpress-Magel2 using rabbit anti-HA polyclonal antibody or mouse anti-Xpress monoclonal antibody respectively (Figure 21A). Sample lysates were also run without antibody incubation to confirm the expression of the transfected proteins. Although a band does appear in the lane representing lysate from cells transfected with HA-Bmal1 and empty vector, this band is weaker than that observed in the

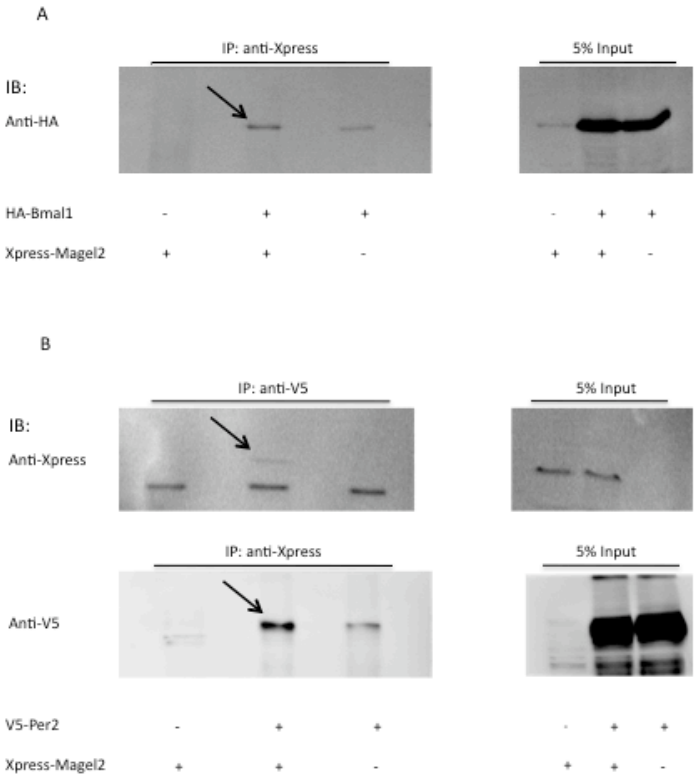

Figure 21. Magel2 can interact with core circadian proteins. (A) HEK293 cells were transfected with expression constructs encoding Xpress-Magel2 and HA-Bmal1 individually or together. HA-Bmal1 was immunoprecipitated with the anti-HA antibody and the resulting protein complexes immunoblotted with anti-Xpress antibody to detect Magel2. The band observed indicates Magel2 can interact with Bmal1. (B) HEK cells were transfected with expression plasmids encoding Xpress-Magel2 and V5-Per2 individually or together. V5-Per2 or Xpress-Magel2 were immunoprecipitated with either anti-V5 or anti-Xpress antibody and the resulting protein complex immunoblotted with either anti-Xpress or anti-V5 antibodies to detect Xpress-Magel2 or V5-Per2. The resulting bands indicate that Magel2 can interact with Per2. In both (A) and (B), 5% of the volume of cell lysate used for immunoprecipitation was immunoblotted to confirm the presence of the proteins.

lane with lysate from cotransfected cells. This suggests that there is nonspecific binding of HA-Bmal1 to the protein G agarose beads used in the assay. The reciprocal experiment was performed in which lysate from HEK293 cells again transfected with X-Magel2 and HA-Bmal1 were immunoprecipitated with rabbit anti-HA polyclonal antibody and immunoblotted with mouse anti-Xpress monoclonal antibody. No X-Magel2 was pulled down and observed in the blot co-transfected with HA-Bmal1. Still, these results indicate that Magel2 can interact with the circadian protein Bmal1.

We also performed co-immunoprecipitation experiment to detect a physical interaction between Magel2 and Per2. Similar to the experiment described above, HEK293 cells were transfected with cDNA-expression constructs containing X-Magel2 and full-length V5-tagged Per2 together or alone with the appropriate empty vector. The collected lysates were incubated with either mouse anti-Xpress monoclonal antibody or mouse anti-V5 monoclonal antibody and the next day incubated with 50% protein G-agarose bead slurry. The resulting supernatant was run on an SDS-PAGE gel and following Western blotting, incubated with anti-Magel2 monoclonal antibody or rabbit anti-V5 polyclonal antibody. A band was observed following immunoblotting with mouse anti-V5 monoclonal antibody in cells co-transfected with plasmids expressing X-Magel2. As was seen in the co-immunoprecipitation experiment with X-Magel2 and HA-Bmal1, a nonspecific band was observed following immunoblotting the lane representing cells transfected with V5-Per2 alone. This band was weaker than that seen in the lane representing the lysate of cells co-transfected with plasmids expressing V5-Per2 and X-Magel2 (Figure 21B). The reciprocal experiment in which lysates from *X-Magel2* and *V5-Per2* singly and cotransfected HEK293 cells were immunoprecipitated with rabbit anti-V5 polyclonal antibody revealed the presence of X-Magel2 following immunoblotting with anti-Xpress monoclonal antibody. This band was only observed in cells cotransfected with the two constructs, indicating that X-Magel2 and V5-Per2 can interact.

Chapter 4. Discussion and Conclusions

4.1 Introduction

In this study, I have begun to piece together a functional role for Magel2 in the proper functioning of circadian rhythm. Up to this point, loss of *Magel2* and its corresponding protein product, as occurs in Prader-Willi Syndrome, has been shown to disrupt the proper function of circadian rhythm. Studies of transfected cells suggest that Magel2 plays a role in fine-tuning the proper timing and magnitude of the repression of transcriptional activation by the Bmal1-Clock heterodimer. A discernable pattern in clock controlled gene expression cycling over the course of 24 hours is present within all cells and tissues in the mammalian body. These organs receive information regarding the proper entrainment of this cycle from the central timekeeping locus of the SCN. Since Magel2 expression is strongest within the hypothalamus and quite pronounced in the dorsomedial region of the SCN, this protein may play a role in output of central clock information. Since the protein does not appear to play as essential a role in the peripheral tissues, it is conceivable that Magel2 complements the other repressive proteins completing the feedback loop of the clock, adding robustness and strength to its perpetual rhythm.

4.2 Magel2 functions as a repressive protein in the circadian clock

The most significant support of this hypothesis comes from the mPer2:luc experiments in transfected NIH3T3 cells. Addition of transcription activators Bmal1 and Clock resulted in the expected increase in luciferase activity. Bmal1-Clock heterodimers increased luciferase activity just over 4-fold compared to background levels (Figure 10A, lane 2 versus 1). Characteristically, Per2 and Cry1 repressed the transcriptional activity of the dimer (Figure 10A, lane 3 and 4 versus 2). The repressive activity of Per2 is known to be weaker than that of Cry1, and was found to inhibit heterodimer driven luciferase activity by 1.1-fold. Cry1

in contrast, is a potent inhibitor of Bmal1-Clock activity as demonstrated by the 17-fold decrease in luciferase activity. This repression lowered the observed luciferase activity below that of the Per2:luc construct alone. Since this is a transfected system, I speculate that this is the result of Cry1 inhibiting not only the transfected Bmal1 and Clock on the promoter, but also the activities of their endogenous counterparts.

Addition of Magel2 to this system revealed that it too inhibits the activity of Bmal1-Clock at the Per2 promoter. Its repressive effect was approximately 1.4-fold (Figure 10B, lane 5 versus 2), an effect significantly stronger than Per2 and weaker than Cry1. I next added combinations of Magel2 and either Per2 or Cry1 to cells and examined luciferase activity once again. The purpose of this experiment was to examine the possibility that Magel2 or the other transcriptional inhibitors could be mutually affecting the activity of the other. Throughout all the luciferase assays, the total amount of DNA added to the cells was kept the same through the addition of empty vector DNA in place of the protein-coding plasmids. Therefore, when two transcriptional repressors were added to the cells instead of one, the amount of 'repressive DNA' added was doubled. From this I assumed that if the proteins were not functioning together, I would see a further decrease in the luciferase activity over that observed when each protein was present alone. Such was the case when Magel2 and Per2 were added. Magel2 and Per2 inhibited Bmal1 and Clock significantly more than either protein present alone (Figure 10A and B, lane 6 versus 5 and 3). The effect was not additive however as the decrease in luciferase activity was 1.5-fold, only slighty more than the decrease caused by Magel2. One reason this occurs may be because of an over-abundance of repressive protein such that effectively all the Bmal1 and Clock are repressed to a given extent by Per2 and Magel2 and there is no role for the excess repressive proteins present in the cell. It is also conceivable that Magel2 and Per2 may affect either the subcellular localization or stability of one another, which results in a less than expected level of repression. In order to further explore this however, Per2:luc assays would need to be performed where

the effect of doubling the amount of Per2 or Magel2 alone is compared to the effect of the same amount of a Per2 and Magel2 combination.

A different result was obtained when Magel2 and Cry1 were both added to the system. The repressive effect observed was significantly less than Cry1 added alone and significantly stronger than Magel2 added alone (Figure 10B, lane 7 versus 5 and 6). Magel2 is perhaps inhibiting the ability of Cry1 to repress the activity of Bmal1-Clock. It is also possible, assuming that Magel2 and Cry1 inhibit Bmal1 and Clock in the same fashion, that a similar situation to that described above is occurring whereby an overabundance of repressive proteins results in competition between Magel2 and Cry1. Since the Cry1 decreased luciferase activity below the background level of the Per2:luc construct alone, the latter explanation is possible. Again the particular mechanisms resulting in the observed effects when Magel2 is present in cells with either Per2 or Cry1 remain to be investigated. Other experiments performed in this project however, specifically those examining subcellular distribution or increasing protein effects, offer clues.

4.3 Magel2 exerts its repressive effect in the cytoplasm

Per proteins are known to be essential for the movement of clock protein complexes into the nucleus at the proper time as part of transcriptional repression and in fact are the rate-limiting component in functional interactions with the Cry proteins. This was demonstrated by *in vivo* studies in which the Cry proteins were nuclear in the repressive phase of the circadian cycle, but otherwise cytoplasmic (Lee et al., 2001). In the transfection studies performed for immunofluorescence, Cry1 was predominantly nuclear, a result contrary to the expected cytoplasmic result described by Lee et al. (2001) (Figure 15A and C, lane 1). However, over-expression of Cry in cultured cells results in predominantly nuclear localization, which is a more appropriate comparison for the experiment performed in this project (Kume et al., 1999). There is in fact a codependence of the Per and Cry proteins in order for proper nuclear translocation to occur. In mice deficient in

Cry, for example, the Per proteins are trapped within the cytoplasm (Lee et al., 2001). As with Cry, Per proteins are predominantly nuclear in overexpression studies (Kume et al., 1999).

Transfected Magel2 was found largely in the cytoplasm (Figure 11E and G, lane 1). When expressed with Per2 or Cry1, a significant increase in nuclear levels was observed (Figure 11G, lane 5 or 6 versus 1). Neither Bmal1 nor Clock nor Bmal1 and Clock together significantly affected the localization of Magel2 in the nucleus Figure 11G, lane 2, 3, or 4 versus 1). These results suggest that Magel2 enters the nucleus to aid in the repression of Bmal1-Clock heterodimer activity at E-box genes as part of the repressive clock protein complex that includes Per and perhaps Cry proteins as well. From these results, one would expect to see a dramatic increase in the repressive action of Magel2 in the Per2:luc assaying where Magel2 was added with Per2 and Cry1. As described above however, this was not the case. Though Magel2 and Per2 added together resulted in increased repression, the decrease in luciferase activity was not as strong as each proteins repressive effect added together, nevermind an even larger increase expected from increased movement of Magel2 into the nucleus. This result suggests that Magel2 may exert its repressive effect in the cytoplasm, in contrast to the Per and Cry proteins which exert their effect in the nucleus. It is also important to note that Magel2 did not to affect the subcellular distribution of Per2, discounting the possibility that the level of repression observed resulted from a decrease in nuclear Per2 (Figure 14).

This explanation is also in line with the Per2:luc results following addition of Magel2 and Cry1. While Cry1 leads to increased levels of nuclear Magel2, levels of nuclear Cry1 decrease in the presence of Magel2. If Magel2 exerts its repressive effect in the cytoplasm while Cry1 acts in the nucleus, a significant weakening in the repressive action of both proteins would be expected when present together. Indeed a subtle but significant increase in luciferase activity is observed. Because the repressive ability of Cry1 is so much stronger than that of Magel2, any effect on Magel2's repression would be overshadowed.

4.4 Magel2 represses the transcriptional activity of Bmal1-Clock by decreasing nuclear levels of Bmal1

The effect of Magel2 on the location of clock proteins within the cell and the response of these proteins to increasing levels of Magel2 provide insight into a means by which Magel2 could inhibit the transcriptional activity of Bmal1-Clock at various clock controlled genes. A great proportion of cells show cytoplasmic Bmal1 when transfected with both Clock and Magel2 (Figure 12E, lane 2 and 3 versus 1). The presence of an effect of Bmal1 localization when co-expressed with Clock is contrary to previous results. Previous work has found that ectopic coexpression of Bmal1 and Clock has no impact on the distribution of Bmal1 within the cell and also that Clock is sequestered exclusively within the cytoplasm when present alone (Kondratov et al., 2003). These immunocytochemical studies were performed in HEK293 cells transfected with 1 µg of DNA using Lipofectamine PLUS reagent. It is possible that proteins have a greater tendency to migrate between the nucleus and cytoplasm in transfected NIH3T3 cells since in my experiments, singly transfected Clock was observed in the nucleus.

In the simplest sense, the presence of less Bmal1 in the nucleus when coexpressed with Magel2 would result in less Bmal1-Clock heterodimer available to transactivate E-box promoters. The per2:luc assays indeed demonstrate less E-box activation. The effect of less nuclear Bmal1 is also interesting to examine in concert with the increasing protein effect experiments. Effects of increasing levels of Magel2 protein in cells with constant amounts of Bmal1 were studied. I found that as levels of Magel2 increase, a reciprocal increase in Bmal1 levels is also observed (Figure 16A). Transfection of cells with a control protein with the same HA-tag as Bmal1, PitX2-HA, with and without Magel2 demonstrated that Magel2 does not significantly alter levels via interaction with the tag. As described in the introduction, Bmal1 is predominately degraded in PML bodies within the nucleus. Within these subnuclear bodies, Bmal1 is conjugated to poly-SUMO2/3. This modification targets Bmal1 for ubiquitination and proteasome-mediated proteolysis (Lee et al., 2008). If the presence of Magel2 either directly

or indirectly leads to a decrease in the levels of nuclear Bmal1, I speculate that this results in less SUMOylation and in turn less degradation of the protein. Bmal1 would thus be present at higher than expected levels within the cells, as is observed. An examination of levels of SUMO2/3-conjugated and ubiquitinated Bmal1 relative to total levels in the presence and absence of Magel2 would allow for confirmation of this hypothesis. If correct, one would observe decreased levels of SUMOylated Bmal1 when Magel2 is present in the system versus without.

Intriguingly, transfection of cells with Bmal1 and both Magel2 and Clock appeared to cancel out any effect of the latter two proteins alone with Bmal1. In the presence of Magel2 and Clock, Bmal1 exhibited a subcellular distribution nearly identical to that observed in cells transfected with Bmal1 alone (Figure 12D and G, lane 4 versus 1). Both Clock and Magel2 lead to decreased levels of nuclear Bmal1, but not when present in the cell together suggesting that Clock and Magel2 affect the activity of one other. The distribution of Magel2 in the cell did not change when co-expressed with Clock (Figure 11C and G, lane 3 versus 1). In contrast, the amount of Clock observed in the nucleus was significantly depleted in the presence of Magel2 (Figure 13C and G, lane 3 versus 1) but this effect was reversed or suppressed when Clock was co-expressed both Bmal1 and Magel2 (Figure 13D and G, lane 4 versus 1). The location of Magel2 is found within the cell does not change when expressed with Bmal1, Clock or Bmal1 and Clock (Figure 11B-D and G, lane 2-4 versus 1). I reason that the apparently contradictory results obtained in the immunofluorescence experiments performed with these proteins is a product of the circadian cycling of proteins. In an *in vivo* system, the relative amounts of Bmal1, Clock and Magel2 will not be present in the unnaturally high amounts and ratios they are when transfected with one another.

How then can the supposed contradictory effect of Clock added to the system make sense in this model of Magel2 activity? One aspect of working with circadian proteins is that their levels, locations, and activities change over the course of the circadian cycle which thus results in differing behaviour depending on the time of day. Since these experiments performed in this project were done

with high levels of all proteins, they were done in a way where the natural relative proportions of proteins were not maintained. Rather, an artificial environment was generated in which the behaviour observed represents not only how the particular proteins behave at their peak levels, but also how they respond to relatively large amounts of the other circadian proteins.

In order to theorize as to what the endogenous behaviour of Magel2 may be, it is helpful to relate the results obtained from the transfected *in vitro* experiments to the endogenous levels of the three proteins at points where each protein peaks in amount. The amount of Clock generated throughout the circadian cycle in the SCN remains largely constant, whereby rather than cycling transcription and translation, circadian behaviour of Clock is generated through post-translational subcellular distribution and phosphorylation (Gekakis et al., 1998; Vitaterna et al., 1994). Bmal1 levels peak at CT 15-21, which corresponds to the late night (Bunger et al., 2000). Bmal1 is most transcriptionally active however at CT 6-10 when its transcript and protein levels are at their lowest. Bmal1 is most susceptible to degradation when it is transcriptionally active within the nucleus early in the cycle because levels of the Cry proteins, which both protect and inhibit the activity of Bmal1, are at their lowest at this point (Kwon et al., 2006). It is not known when Magel2 protein levels peak and trough since there is no antibody available at this point. However, Magel2 transcript levels are known to peak at CT 6-8 (Kozlov et al., 2007; Panda et al., 2002). If as predicted, Magel2 exerts its repressive effect in the cytoplasm, this could occur immediately following translation or at a later point following posttranslational modification. What such posttranslational modification(s) are will be investigated in subsequent studies.

4.5 Circadian proteins affect the levels of Magel2

Clues as to the circadian time of Magel2's action as a transcriptional repressor are provided by studies as to how increasing levels of other circadian proteins affect Magel2. Just as Bmal1 had no significant impact on the subcellular

distribution of Magel2, so too there was no effect on Magel2 levels when present in transfected NIH3T3 cells as greater amounts of Bmal1 were added (Figure 16). There is however, a mutual interaction between Per2 and Magel2. Levels of Per2 were found to significantly increase when co-expressed with increasing amounts of Magel2 (Figure 18A). When expressed with increasing levels of Per2 however, Magel2 levels significantly decreased (Figure 18B). Per2 did not however, significantly alter the half-life of Magel2 (Figure 19). As Magel2 levels increase during the cycle, Per2 levels would also increase, in turn resulting in more and more of the Magel2 moving into the nucleus. Less Magel2 in the cytoplasm means less Magel2 to keep Bmal1 in the cytoplasm, the proposed mechanism of Magel2's inhibitory activity. Magel2 may thus function as a precursor or backup to the inhibitory activity of Per2. Levels of Per2 mRNA reach a peak at CT 8-10, a few hours later than that of Magel2. However there is a delay between the generation of the Per and Cry transcripts and the action of these proteins as repressors within the nucleus. This delay of several hours results from the time required to activate Per and Cry proteins through phosphorylation and subsequent movement into the nucleus (Vanselow and Kramer, 2007). Thus Magel2's action would precede that of Per2. As Per2 levels increase and are stabilized with help of Magel2, Magel2 levels begin to decrease (Figure 17A and B). Cry1 did not impact the levels of Magel2. While levels of Cry1 decreased as more Magel2 was transfected with it, it is not possible to draw conclusions regarding the impact of Magel2 on Cry1 levels (Figure 18A). Expression of Cry1 also decreased significantly when co-expressed with control Xpress-tagged PitX2 (Figure 20).

4.6 A model of the circadian clock with Magel2

Magel2's place within the central circadian clock of the SCN but not in peripheral clocks emphasizes its role in the endogenous timekeeping mechanism of the rhythm. As the day begins, transcription of CCGs by the Bmal1-Clock heterodimer begins to increase, and levels of transcriptional repressor transcripts increase throughout the day. Included in this mix is *Magel2*, as well as the *Per*

and *Cry* mRNAs (Figure 22A). Bmal1 and Clock are in active phosphorylated forms and Bmal1 shuttles between the cytoplasm and nucleus to bring Clock into the nucleus. Clock in turn, acetylates the histones of the CCGs through its HAT activity, relaxing the form to facilitate transcription. The cellular amounts of Bmal1 are simultaneously decreasing as the protein is SUMOylated and ubiquitinated in PML bodies, targeting active Bmal1 for proteosomal degradation.

Following transcription, the levels of Per, Cry and Magel2 mRNAs increase and the repressive proteins are generated in the early evening. Magel2 restricts the movement of Bmal1 into the nucleus, thus initiating repression of the transcription of CCGs. Per and Cry proteins are phosphorylated and activated after a number of hours and enter the nucleus. With higher levels of Per2 and Cry1, a greater proportion of Magel2 is found in the nucleus and overall levels decrease (Figure 22B). Its repressive impact on Bmal1 therefore diminishes. During this time Bmal1 is increasingly acetylated by Clock, which serves to attract the Cry proteins now present in the nucleus. The binding of Cry both decreases the activity of Bmal1-Clock by impairing phosphorylation and also protects Bmal1 from SUMOylation and both Bmal1 and Clock from proteosomal degradation. More *Bmal1* mRNA is transcribed due to the activating impact of Per2. Thus levels of Bmal1 and Clock increase into the late night and the process begins again. Whether Magel2 and circadian proteins exert these affects on one another through direct intereaction remains to be determined, however I did find that Magel2 is capable of interacting with Bmal1 and Per2 (Figure 21A and B).

4.7 From disrupted circadian rhythm to PWS

The question remains how a disruption in circadian rhythm due to the loss of *Magel2* would manifest as some of the symptoms seen in PWS. As reviewed in the introduction, PWS is the summation of abnormalities resulting from the loss of genes within the 11-13q region of chromosome 15. By extension therefore, *Magel2* would account for only a portion of the symptoms observed. The examination of Magel2 at the molecular level revealed that while it functions as a

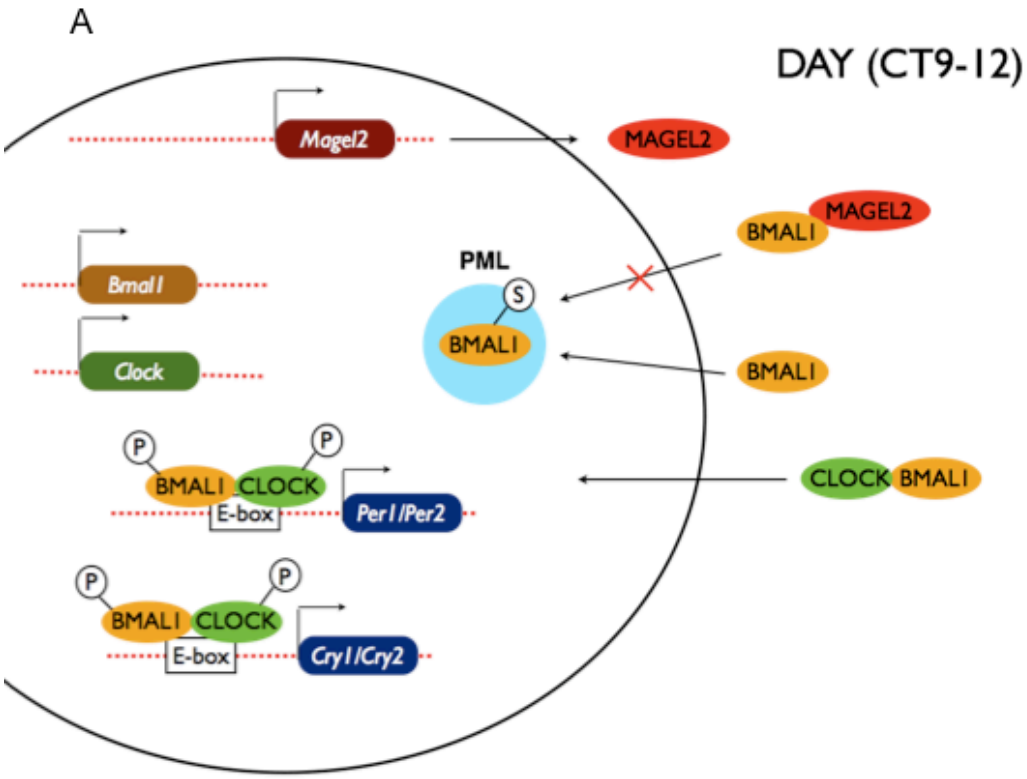

Figure 22. A schematic of *Magel2*'s proposed role in the transcription-translation feedback loop which forms the molecular circadian clock. (A) Early in the day, Bmal1-Clock heterodimers activate the transcription of clock controlled genes including *Per*, *Cry*, and *Magel2,* the repressive proteins in the cycle. Magel2 inhibits transcription by inhibiting the movement of Bmal1 into the nucleus. (B) During the night, Per and Cry move into the nucleus and to starts inhbiting transcriptional activity of Bmal1-Clock. Levels of Magel2 begin to decrease, possibly due to an interaction with Per2 that moves Magel2 into the nucleus to be broken down.

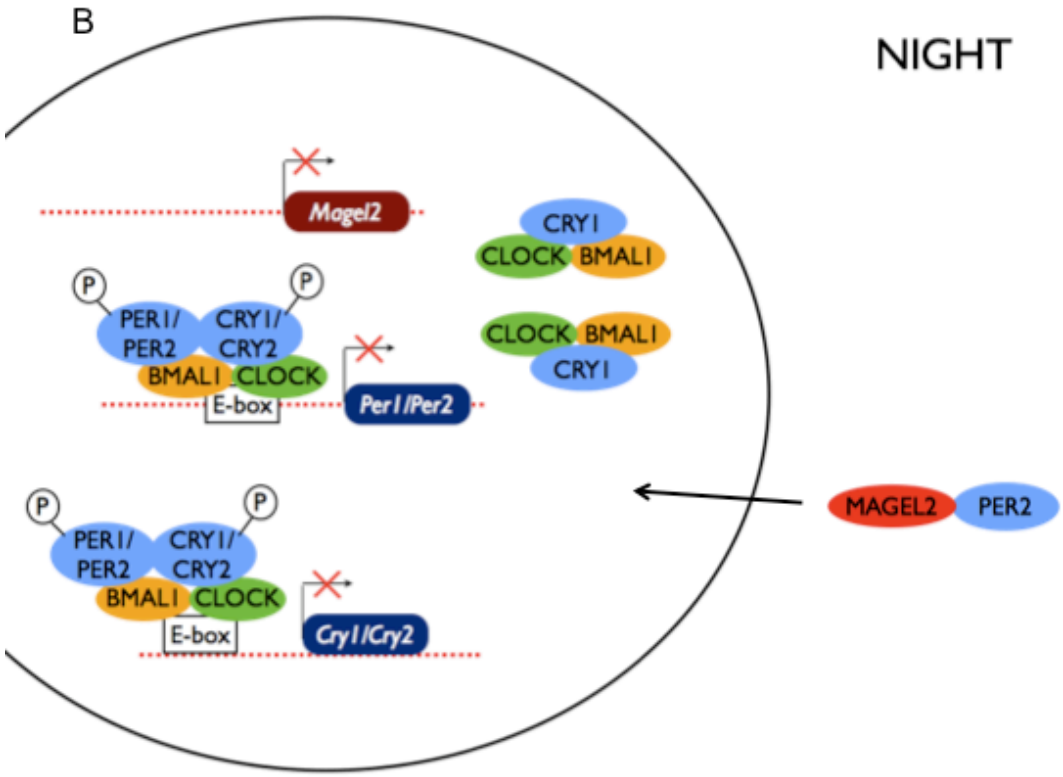
B
NIGHT
Magel2
CRY1
CLOCK
BMAL1
P
PER1/
PER2
CRY1/
CRY2
BMAL1
CLOCK
E-box
Per1/Per2
CLOCK
BMAL1
CRY1
MAGEL2
PER2
P
PER1/
PER2
CRY1/
CRY2
BMAL1
CLOCK
E-box
Cry1/Cry2

repressor protein by restricting Bmal1's movement into the nucleus, this action may preceed that of Per2 and Cry1. Thus without Magel2, Bmal1 would continue to shuttle between the cytoplasm and nucleus and activate transcription. Aside from the core clock genes, Bmal1-Clock would also activate the transcription of other CCGs, which have downstream regulatory effects affecting such processes as the sleep-wake cycle, activity, and hormone secretion (Takahashi et al., 2008). These gene products would have continued expression for longer than normal when Magel2 is not present, leading to an abnormality in the endogenous cycle. Data obtained from locomotor studies of *Magel*$^{m+/p-}$ mice and sleep studies in human patients with PWS suggests that this genetic abnormality manifests as a disruption in the proper resetting of the circadian cycle.

Sleep is intimately connected to the circadian cycle. The cycling of sleep is synchronized by the daily light-dark cycle by phase-advancing or phase-delaying of the rhythm. Thus, since Magel2 has a role in the functioning of the circadian clock, sleep dysfunction in PWS may, at least in part, result due to lack of Magel2 as well. This may occur both directly and indirectly. As previously described, the movement between NREM and REM sleep is under circadian control, suggesting that Magel2 could directly affect this cycling. Additionally, the NREM/REM switch is also controlled by the orexin system, which as an arousal system inhibits REM sleep. Sleep abnormalities in PWS manifest as decreased REM sleep latency, SOREM, reduced percentage of REM sleep and decreased NREM sleep instability consistent with generalized hypoarousal (Camfferman et al., 2008; Manni et al., 2001; Priano et al., 2006; Verrillo et al., 2009; Vgontzas et al., 1996). One explanation for this phenotype suggests a connection with hypothalamic dysfunction, specifically hypothalamic control of circadian rhythm and NREM/REM cycling (Hertz et al., 1993; Vela-Bueno et al., 1984).

Magel2 is expressed from neurons in the dmSCN, the region proposed to be involved in the circadian promotion of REM sleep. Additionally, mice lacking the gene demonstrate a phenotype reminiscent of the characteristic REM dysfunction seen in many PWS patients, namely increased frequency by

decreased length of REM sleep. *Magel2*$^{m+/p-}$ mice are active through circadian time and their activity is characterized by increased frequency and decreased magnitude (Kozlov et al., 2007). From these various experiments, I suggest that improper cycling between NREM/REM sleep results from improper output from the dmSCN resulting in this phenotype that would result from a lack of functional Magel2. Locomoter studies in the *Magel*$^{m+/p-}$ mice suggest that the abnormality is particularly apparent in constant darkness as the mutant mice do exhibit cycling of locomotor activity. It is important to remember however that humans do not live in an environment as tightly regulated as that provided to laboratory animals. Individuals with PWS may be particularly sensitive to various disruptions, such as light during the dark cycle, which can commonly occur in their environment. One way to ameliorate some of the sleep symptoms observed in PWS patients may be to ensure they maintain very well defined sleep-wake stages, with clearly defined and maintained bed and wake times. While growth hormone is often used in the treatment of other symptoms of PWS, it has not been found to significantly improve REM sleep defects (Verrillo et al., 2009). Patients may also be given a wakefulness-promoting drug such as Modafinil, which has been shown to reduce the feelings of daytime sleepiness. How such a drug may affect sleep structure itself remains to be examined.

4.8 Conclusions and Future Work

Much remains to be deciphered in the quest to understand the role Magel2 plays in circadian rhythm and PWS. Specifically, an examination of how loss of *Magel2* affects circadian cycling endogenously is necessary. However, the experiments performed and data collected from the cell culture experiments I have performed provide a number of starting points to confirm and elaborate on. This work has allowed for the generation of a model regarding the functional place of Magel2 as a repressor protein in the transcription-translation feedback loop governing the circadian cycle, as well as theories on how the loss of one gene in

PWS manifests itself in the neurobiological and physiological symptoms of the disorder.

In the immediate future, an experiment exploring the role of Magel2 in levels of SUMOylated Bmal1 would provide support for the theory that Magel2 reduces the transcriptional activity of Bmal1-Clock by restricting the movement of Bmal1 into the nucleus. If this model is valid, lower levels of Bmal1 with a SUMO modification would likely be observed as this event occurs in the nucleus. An experiment that would confirm the immunofluorescence observations concerning subcellular distribution, would be subcellular fractionation followed by analysis on a Western blot. Such an experiment would facilitate the determination of whether decreased levels of a particular protein in a subcellular region are due to increased breakdown or movement out of that region. Possible *in vivo* experiments include a study of the expression of circadian genes in *Magel2*$^{m+/p-}$ mice as compared to wildtype mice over the circadian cycle using RT-PCR or *in situ* hybridization or study of the levels and subcellular localization of circadian proteins in hypothalamic cultures. It is the hope that with continued experimentation at the molecular level and the contextualization of this knowledge in the framework of clinical manifestations, individuals with PWS will be given relief from the persistent distress of their illness.

References

Akashi, M., Tsuchiya, Y., Yoshino, T., and Nishida, E. (2002). Control of intracellular dynamics of mammalian period proteins by casein kinase I epsilon (CKIepsilon) and CKIdelta in cultured cells. Mol Cell Biol *22*, 1693-1703.

Albrecht, U., Sun, Z.S., Eichele, G., and Lee, C.C. (1997). A differential response of two putative mammalian circadian regulators, mper1 and mper2, to light. Cell *91*, 1055-1064.

Antoch, M.P., Song, E.J., Chang, A.M., Vitaterna, M.H., Zhao, Y., Wilsbacher, L.D., Sangoram, A.M., King, D.P., Pinto, L.H., and Takahashi, J.S. (1997). Functional identification of the mouse circadian Clock gene by transgenic BAC rescue. Cell *89*, 655-667.

Arii, J., Kanbayashi, T., Tanabe, Y., Sawaishi, Y., Kimura, S., Watanabe, A., Mishima, K., Hishikawa, Y., Shimizu, T., and Nishino, S. (2004). CSF hypocretin-1 (orexin-A) levels in childhood narcolepsy and neurologic disorders. Neurology *63*, 2440-2442.

Asher, G., Gatfield, D., Stratmann, M., Reinke, H., Dibner, C., Kreppel, F., Mostoslavsky, R., Alt, F.W., and Schibler, U. (2008). SIRT1 regulates circadian clock gene expression through PER2 deacetylation. Cell *134*, 317-328.

Bae, K., Jin, X., Maywood, E.S., Hastings, M.H., Reppert, S.M., and Weaver, D.R. (2001). Differential functions of mPer1, mPer2, and mPer3 in the SCN circadian clock. Neuron *30*, 525-536.

Barker, P.A., and Salehi, A. (2002). The MAGE proteins: emerging roles in cell cycle progression, apoptosis, and neurogenetic disease. J Neurosci Res *67*, 705-712.

Bunger, M.K., Wilsbacher, L.D., Moran, S.M., Clendenin, C., Radcliffe, L.A., Hogenesch, J.B., Simon, M.C., Takahashi, J.S., and Bradfield, C.A. (2000). Mop3 is an essential component of the master circadian pacemaker in mammals. Cell *103*, 1009-1017.

Burman, P., Ritzen, E.M., and Lindgren, A.C. (2001). Endocrine dysfunction in Prader-Willi syndrome: a review with special reference to GH. Endocr Rev *22*, 787-799.

Camacho, F., Cilio, M., Guo, Y., Virshup, D.M., Patel, K., Khorkova, O., Styren, S., Morse, B., Yao, Z., and Keesler, G.A. (2001). Human casein kinase Idelta phosphorylation of human circadian clock proteins period 1 and 2. FEBS Lett *489*, 159-165.

Camfferman, D., McEvoy, R.D., O'Donoghue, F., and Lushington, K. (2008). Prader Willi Syndrome and excessive daytime sleepiness. Sleep Med Rev *12*, 65-75.

Cardone, L., Hirayama, J., Giordano, F., Tamaru, T., Palvimo, J.J., and Sassone-Corsi, P. (2005). Circadian clock control by SUMOylation of BMAL1. Science *309*, 1390-1394.

Carskadon, M.A., Dement, W.C., Mitler, M.M., Roth, T., Westbrook, P.R., and Keenan, S. (1986). Guidelines for the multiple sleep latency test (MSLT): a standard measure of sleepiness. Sleep *9*, 519-524.

Chai, J.H., Locke, D.P., Greally, J.M., Knoll, J.H., Ohta, T., Dunai, J., Yavor, A., Eichler, E.E., and Nicholls, R.D. (2003). Identification of four highly conserved genes between breakpoint hotspots BP1 and BP2 of the Prader-Willi/Angelman syndromes deletion region that have undergone evolutionary transposition mediated by flanking duplicons. Am J Hum Genet *73*, 898-925.

Crino, A., Schiaffini, R., Ciampalini, P., Spera, S., Beccaria, L., Benzi, F., Bosio, L., Corrias, A., Gargantini, L., Salvatoni, A.*, et al.* (2003). Hypogonadism and pubertal development in Prader-Willi syndrome. Eur J Pediatr *162*, 327-333.

Dardente, H., Fortier, E.E., Martineau, V., and Cermakian, N. (2007). Cryptochromes impair phosphorylation of transcriptional activators in the clock: a general mechanism for circadian repression. Biochem J *402*, 525-536.

Dijk, D.J., and Czeisler, C.A. (1995). Contribution of the circadian pacemaker and the sleep homeostat to sleep propensity, sleep structure, electroencephalographic slow waves, and sleep spindle activity in humans. J Neurosci *15*, 3526-3538.

Doi, M., Hirayama, J., and Sassone-Corsi, P. (2006). Circadian regulator CLOCK is a histone acetyltransferase. Cell *125*, 497-508.

Ebisawa, T., Uchiyama, M., Kajimura, N., Mishima, K., Kamei, Y., Katoh, M., Watanabe, T., Sekimoto, M., Shibui, K., Kim, K.*, et al.* (2001). Association of structural polymorphisms in the human period3 gene with delayed sleep phase syndrome. EMBO Rep *2*, 342-346.

Eide, E.J., Vielhaber, E.L., Hinz, W.A., and Virshup, D.M. (2002). The circadian regulatory proteins BMAL1 and cryptochromes are substrates of casein kinase Iepsilon. J Biol Chem *277*, 17248-17254.

Eiholzer, U., l'Allemand, D., Rousson, V., Schlumpf, M., Gasser, T., Girard, J., Gruters, A., and Simoni, M. (2006). Hypothalamic and gonadal components of hypogonadism in boys with Prader-Labhart- Willi syndrome. J Clin Endocrinol Metab *91*, 892-898.

Franken, P., and Dijk, D.J. (2009). Circadian clock genes and sleep homeostasis. Eur J Neurosci *29*, 1820-1829.

Freedman, M.S., Lucas, R.J., Soni, B., von Schantz, M., Munoz, M., David-Gray, Z., and Foster, R. (1999). Regulation of mammalian circadian behavior by non-rod, non-cone, ocular photoreceptors. Science *284*, 502-504.

Fronczek, R., Lammers, G.J., Balesar, R., Unmehopa, U.A., and Swaab, D.F. (2005). The number of hypothalamic hypocretin (orexin) neurons is not affected in Prader-Willi syndrome. J Clin Endocrinol Metab *90*, 5466-5470.

Gallego, M., and Virshup, D.M. (2007). Post-translational modifications regulate the ticking of the circadian clock. Nat Rev Mol Cell Biol *8*, 139-148.

Geiss-Friedlander, R., and Melchior, F. (2007). Concepts in sumoylation: a decade on. Nat Rev Mol Cell Biol *8*, 947-956.

Gekakis, N., Staknis, D., Nguyen, H.B., Davis, F.C., Wilsbacher, L.D., King, D.P., Takahashi, J.S., and Weitz, C.J. (1998). Role of the CLOCK protein in the mammalian circadian mechanism. Science *280*, 1564-1569.

Glozak, M.A., Sengupta, N., Zhang, X., and Seto, E. (2005). Acetylation and deacetylation of non-histone proteins. Gene *363*, 15-23.

Goldstone, A.P. (2004). Prader-Willi syndrome: advances in genetics, pathophysiology and treatment. Trends Endocrinol Metab *15*, 12-20.

Grundschober, C., Delaunay, F., Puhlhofer, A., Triqueneaux, G., Laudet, V., Bartfai, T., and Nef, P. (2001). Circadian regulation of diverse gene products revealed by mRNA expression profiling of synchronized fibroblasts. J Biol Chem *276*, 46751-46758.

Gunay-Aygun, M., Schwartz, S., Heeger, S., O'Riordan, M.A., and Cassidy, S.B. (2001). The changing purpose of Prader-Willi syndrome clinical diagnostic criteria and proposed revised criteria. Pediatrics *108*, E92.

Hankins, M.W., Peirson, S.N., and Foster, R.G. (2008). Melanopsin: an exciting photopigment. Trends Neurosci *31*, 27-36.

Harmer, S.L., Hogenesch, J.B., Straume, M., Chang, H.S., Han, B., Zhu, T., Wang, X., Kreps, J.A., and Kay, S.A. (2000). Orchestrated transcription of key pathways in Arabidopsis by the circadian clock. Science *290*, 2110-2113.

Hertz, G., Cataletto, M., Feinsilver, S.H., and Angulo, M. (1993). Sleep and breathing patterns in patients with Prader Willi syndrome (PWS): effects of age and gender. Sleep *16*, 366-371.

Hirayama, J., Sahar, S., Grimaldi, B., Tamaru, T., Takamatsu, K., Nakahata, Y., and Sassone-Corsi, P. (2007). CLOCK-mediated acetylation of BMAL1 controls circadian function. Nature *450*, 1086-1090.

Hogenesch, J.B., Chan, W.K., Jackiw, V.H., Brown, R.C., Gu, Y.Z., Pray-Grant, M., Perdew, G.H., and Bradfield, C.A. (1997). Characterization of a subset of the basic-helix-loop-helix-PAS superfamily that interacts with components of the dioxin signaling pathway. J Biol Chem *272*, 8581-8593.

Hogenesch, J.B., Gu, Y.Z., Jain, S., and Bradfield, C.A. (1998). The basic-helix-loop-helix-PAS orphan MOP3 forms transcriptionally active complexes with circadian and hypoxia factors. Proc Natl Acad Sci U S A *95*, 5474-5479.

Hogenesch, J.B., Gu, Y.Z., Moran, S.M., Shimomura, K., Radcliffe, L.A., Takahashi, J.S., and Bradfield, C.A. (2000). The basic helix-loop-helix-PAS protein MOP9 is a brain-specific heterodimeric partner of circadian and hypoxia factors. J Neurosci *20*, RC83.

Holm, V.A., Cassidy, S.B., Butler, M.G., Hanchett, J.M., Greenswag, L.R., Whitman, B.Y., and Greenberg, F. (1993). Prader-Willi syndrome: consensus diagnostic criteria. Pediatrics *91*, 398-402.

Holm, V.A., and Laurnen, E.L. (1981). Prader-Willi syndrome and scoliosis. Dev Med Child Neurol *23*, 192-201.

Honma, S., Ikeda, M., Abe, H., Tanahashi, Y., Namihira, M., Honma, K., and Nomura, M. (1998). Circadian oscillation of BMAL1, a partner of a mammalian clock gene Clock, in rat suprachiasmatic nucleus. Biochem Biophys Res Commun *250*, 83-87.

Horsthemke, B., and Buiting, K. (2006). Imprinting defects on human chromosome 15. Cytogenet Genome Res *113*, 292-299.

Ibata, Y., Okamura, H., Tanaka, M., Tamada, Y., Hayashi, S., Iijima, N., Matsuda, T., Munekawa, K., Takamatsu, T., Hisa, Y.*, et al.* (1999). Functional morphology of the suprachiasmatic nucleus. Front Neuroendocrinol *20*, 241-268.

Iitaka, C., Miyazaki, K., Akaike, T., and Ishida, N. (2005). A role for glycogen synthase kinase-3beta in the mammalian circadian clock. J Biol Chem *280*, 29397-29402.

Ikeda, M., and Nomura, M. (1997). cDNA cloning and tissue-specific expression of a novel basic helix-loop-helix/PAS protein (BMAL1) and identification of alternatively spliced variants with alternative translation initiation site usage. Biochem Biophys Res Commun *233*, 258-264.

Ikeda, M., Yu, W., Hirai, M., Ebisawa, T., Honma, S., Yoshimura, K., Honma, K.I., and Nomura, M. (2000). cDNA cloning of a novel bHLH-PAS transcription

factor superfamily gene, BMAL2: its mRNA expression, subcellular distribution, and chromosomal localization. Biochem Biophys Res Commun *275*, 493-502.

Jin, X., Shearman, L.P., Weaver, D.R., Zylka, M.J., de Vries, G.J., and Reppert, S.M. (1999). A molecular mechanism regulating rhythmic output from the suprachiasmatic circadian clock. Cell *96*, 57-68.

Keesler, G.A., Camacho, F., Guo, Y., Virshup, D., Mondadori, C., and Yao, Z. (2000). Phosphorylation and destabilization of human period I clock protein by human casein kinase I epsilon. Neuroreport *11*, 951-955.

Kennedy, L., Bittel, D.C., Kibiryeva, N., Kalra, S.P., Torto, R., and Butler, M.G. (2006). Circulating adiponectin levels, body composition and obesity-related variables in Prader-Willi syndrome: comparison with obese subjects. Int J Obes (Lond) *30*, 382-387.

Kilduff, T.S., Lein, E.S., de la Iglesia, H., Sakurai, T., Fu, Y.H., and Shaw, P. (2008). New developments in sleep research: molecular genetics, gene expression, and systems neurobiology. J Neurosci *28*, 11814-11818.

Kim, E.Y., Bae, K., Ng, F.S., Glossop, N.R., Hardin, P.E., and Edery, I. (2002). Drosophila CLOCK protein is under posttranscriptional control and influences light-induced activity. Neuron *34*, 69-81.

King, D.P., Zhao, Y., Sangoram, A.M., Wilsbacher, L.D., Tanaka, M., Antoch, M.P., Steeves, T.D., Vitaterna, M.H., Kornhauser, J.M., Lowrey, P.L.*, et al.* (1997). Positional cloning of the mouse circadian clock gene. Cell *89*, 641-653.

Kondratov, R.V., Chernov, M.V., Kondratova, A.A., Gorbacheva, V.Y., Gudkov, A.V., and Antoch, M.P. (2003). BMAL1-dependent circadian oscillation of nuclear CLOCK: posttranslational events induced by dimerization of transcriptional activators of the mammalian clock system. Genes Dev *17*, 1921-1932.

Kozlov, S.V., Bogenpohl, J.W., Howell, M.P., Wevrick, R., Panda, S., Hogenesch, J.B., Muglia, L.J., Van Gelder, R.N., Herzog, E.D., and Stewart, C.L. (2007). The imprinted gene Magel2 regulates normal circadian output. Nat Genet *39*, 1266-1272.

Kume, K., Zylka, M.J., Sriram, S., Shearman, L.P., Weaver, D.R., Jin, X., Maywood, E.S., Hastings, M.H., and Reppert, S.M. (1999). mCRY1 and mCRY2 are essential components of the negative limb of the circadian clock feedback loop. Cell *98*, 193-205.

Kuwajima, T., Nishimura, I., and Yoshikawa, K. (2006). Necdin promotes GABAergic neuron differentiation in cooperation with Dlx homeodomain proteins. J Neurosci *26*, 5383-5392.

Kuwajima, T., Taniura, H., Nishimura, I., and Yoshikawa, K. (2004). Necdin interacts with the Msx2 homeodomain protein via MAGE-D1 to promote myogenic differentiation of C2C12 cells. J Biol Chem *279*, 40484-40493.

Kwon, I., Lee, J., Chang, S.H., Jung, N.C., Lee, B.J., Son, G.H., Kim, K., and Lee, K.H. (2006). BMAL1 shuttling controls transactivation and degradation of the CLOCK/BMAL1 heterodimer. Mol Cell Biol *26*, 7318-7330.

Lee, C., Etchegaray, J.P., Cagampang, F.R., Loudon, A.S., and Reppert, S.M. (2001). Posttranslational mechanisms regulate the mammalian circadian clock. Cell *107*, 855-867.

Lee, H., Chen, R., Lee, Y., Yoo, S., and Lee, C. (2009a). Essential roles of CKIdelta and CKIepsilon in the mammalian circadian clock. Proc Natl Acad Sci U S A *106*, 21359-21364.

Lee, J., Lee, Y., Lee, M.J., Park, E., Kang, S.H., Chung, C.H., Lee, K.H., and Kim, K. (2008). Dual modification of BMAL1 by SUMO2/3 and ubiquitin promotes circadian activation of the CLOCK/BMAL1 complex. Mol Cell Biol *28*, 6056-6065.

Lee, M.G., Hassani, O.K., and Jones, B.E. (2005a). Discharge of identified orexin/hypocretin neurons across the sleep-waking cycle. J Neurosci *25*, 6716-6720.

Lee, M.L., Swanson, B.E., and de la Iglesia, H.O. (2009b). Circadian timing of REM sleep is coupled to an oscillator within the dorsomedial suprachiasmatic nucleus. Curr Biol *19*, 848-852.

Lee, S., Kozlov, S., Hernandez, L., Chamberlain, S.J., Brannan, C.I., Stewart, C.L., and Wevrick, R. (2000). Expression and imprinting of MAGEL2 suggest a role in Prader-willi syndrome and the homologous murine imprinting phenotype. Hum Mol Genet *9*, 1813-1819.

Lee, S., Walker, C.L., Karten, B., Kuny, S.L., Tennese, A.A., O'Neill, M.A., and Wevrick, R. (2005b). Essential role for the Prader-Willi syndrome protein necdin in axonal outgrowth. Hum Mol Genet *14*, 627-637.

Lee, S., Walker, C.L., and Wevrick, R. (2003). Prader-Willi syndrome transcripts are expressed in phenotypically significant regions of the developing mouse brain. Gene Expr Patterns *3*, 599-609.

Lopez-Molina, L., Conquet, F., Dubois-Dauphin, M., and Schibler, U. (1997). The DBP gene is expressed according to a circadian rhythm in the suprachiasmatic nucleus and influences circadian behavior. EMBO J *16*, 6762-6771.

Lu, J., Sherman, D., Devor, M., and Saper, C.B. (2006). A putative flip-flop switch for control of REM sleep. Nature *441*, 589-594.

Lucas, R.J., Freedman, M.S., Munoz, M., Garcia-Fernandez, J.M., and Foster, R.G. (1999). Regulation of the mammalian pineal by non-rod, non-cone, ocular photoreceptors. Science *284*, 505-507.

Manni, R., Politini, L., Nobili, L., Ferrillo, F., Livieri, C., Veneselli, E., Biancheri, R., Martinetti, M., and Tartara, A. (2001). Hypersomnia in the Prader Willi syndrome: clinical-electrophysiological features and underlying factors. Clin Neurophysiol *112*, 800-805.

McDonald, M.J., and Rosbash, M. (2001). Microarray analysis and organization of circadian gene expression in Drosophila. Cell *107*, 567-578.

Mignot, E., Lammers, G.J., Ripley, B., Okun, M., Nevsimalova, S., Overeem, S., Vankova, J., Black, J., Harsh, J., Bassetti, C.*, et al.* (2002). The role of cerebrospinal fluid hypocretin measurement in the diagnosis of narcolepsy and other hypersomnias. Arch Neurol *59*, 1553-1562.

Miller, N.L., Wevrick, R., and Mellon, P.L. (2009). Necdin, a Prader-Willi syndrome candidate gene, regulates gonadotropin-releasing hormone neurons during development. Hum Mol Genet *18*, 248-260.

Nakahata, Y., Kaluzova, M., Grimaldi, B., Sahar, S., Hirayama, J., Chen, D., Guarente, L.P., and Sassone-Corsi, P. (2008). The NAD+-dependent deacetylase SIRT1 modulates CLOCK-mediated chromatin remodeling and circadian control. Cell *134*, 329-340.

Nevsimalova, S., Vankova, J., Stepanova, I., Seemanova, E., Mignot, E., and Nishino, S. (2005). Hypocretin deficiency in Prader-Willi syndrome. Eur J Neurol *12*, 70-72.

Nicholls, R.D., Knoll, J.H., Butler, M.G., Karam, S., and Lalande, M. (1989). Genetic imprinting suggested by maternal heterodisomy in nondeletion Prader-Willi syndrome. Nature *342*, 281-285.

Panda, S., Antoch, M.P., Miller, B.H., Su, A.I., Schook, A.B., Straume, M., Schultz, P.G., Kay, S.A., Takahashi, J.S., and Hogenesch, J.B. (2002). Coordinated transcription of key pathways in the mouse by the circadian clock. Cell *109*, 307-320.

Perk, J., Makedonski, K., Lande, L., Cedar, H., Razin, A., and Shemer, R. (2002). The imprinting mechanism of the Prader-Willi/Angelman regional control center. EMBO J *21*, 5807-5814.

Preitner, N., Damiola, F., Lopez-Molina, L., Zakany, J., Duboule, D., Albrecht, U., and Schibler, U. (2002). The orphan nuclear receptor REV-ERBalpha controls

circadian transcription within the positive limb of the mammalian circadian oscillator. Cell *110*, 251-260.

Priano, L., Grugni, G., Miscio, G., Guastamacchia, G., Toffolet, L., Sartorio, A., and Mauro, A. (2006). Sleep cycling alternating pattern (CAP) expression is associated with hypersomnia and GH secretory pattern in Prader-Willi syndrome. Sleep Med *7*, 627-633.

Ralph, M.R., and Menaker, M. (1988). A mutation of the circadian system in golden hamsters. Science *241*, 1225-1227.

Reppert, S.M., and Weaver, D.R. (2001). Molecular analysis of mammalian circadian rhythms. Annu Rev Physiol *63*, 647-676.

Rutila, J.E., Suri, V., Le, M., So, W.V., Rosbash, M., and Hall, J.C. (1998). CYCLE is a second bHLH-PAS clock protein essential for circadian rhythmicity and transcription of Drosophila period and timeless. Cell *93*, 805-814.

Sanada, K., Okano, T., and Fukada, Y. (2002). Mitogen-activated protein kinase phosphorylates and negatively regulates basic helix-loop-helix-PAS transcription factor BMAL1. J Biol Chem *277*, 267-271.

Sato, T.K., Panda, S., Miraglia, L.J., Reyes, T.M., Rudic, R.D., McNamara, P., Naik, K.A., FitzGerald, G.A., Kay, S.A., and Hogenesch, J.B. (2004). A functional genomics strategy reveals Rora as a component of the mammalian circadian clock. Neuron *43*, 527-537.

Schwartz, G.J. (2004). Biology of eating behavior in obesity. Obes Res *12 Suppl 2*, 102S-106S.

Sharp, A.J., Hansen, S., Selzer, R.R., Cheng, Z., Regan, R., Hurst, J.A., Stewart, H., Price, S.M., Blair, E., Hennekam, R.C.*, et al.* (2006). Discovery of previously unidentified genomic disorders from the duplication architecture of the human genome. Nat Genet *38*, 1038-1042.

Shearman, L.P., Sriram, S., Weaver, D.R., Maywood, E.S., Chaves, I., Zheng, B., Kume, K., Lee, C.C., van der Horst, G.T., Hastings, M.H.*, et al.* (2000). Interacting molecular loops in the mammalian circadian clock. Science *288*, 1013-1019.

Shearman, L.P., Zylka, M.J., Weaver, D.R., Kolakowski, L.F., Jr., and Reppert, S.M. (1997). Two period homologs: circadian expression and photic regulation in the suprachiasmatic nuclei. Neuron *19*, 1261-1269.

Sun, Z.S., Albrecht, U., Zhuchenko, O., Bailey, J., Eichele, G., and Lee, C.C. (1997). RIGUI, a putative mammalian ortholog of the Drosophila period gene. Cell *90*, 1003-1011.

Takahashi, J.S., Hong, H.K., Ko, C.H., and McDearmon, E.L. (2008). The genetics of mammalian circadian order and disorder: implications for physiology and disease. Nat Rev Genet *9*, 764-775.

Takahata, S., Sogawa, K., Kobayashi, A., Ema, M., Mimura, J., Ozaki, N., and Fujii-Kuriyama, Y. (1998). Transcriptionally active heterodimer formation of an Arnt-like PAS protein, Arnt3, with HIF-1a, HLF, and clock. Biochem Biophys Res Commun *248*, 789-794.

Takumi, T., Matsubara, C., Shigeyoshi, Y., Taguchi, K., Yagita, K., Maebayashi, Y., Sakakida, Y., Okumura, K., Takashima, N., and Okamura, H. (1998a). A new mammalian period gene predominantly expressed in the suprachiasmatic nucleus. Genes Cells *3*, 167-176.

Takumi, T., Taguchi, K., Miyake, S., Sakakida, Y., Takashima, N., Matsubara, C., Maebayashi, Y., Okumura, K., Takekida, S., Yamamoto, S.*, et al.* (1998b). A light-independent oscillatory gene mPer3 in mouse SCN and OVLT. EMBO J *17*, 4753-4759.

Tei, H., Okamura, H., Shigeyoshi, Y., Fukuhara, C., Ozawa, R., Hirose, M., and Sakaki, Y. (1997). Circadian oscillation of a mammalian homologue of the Drosophila period gene. Nature *389*, 512-516.

Toh, K.L., Jones, C.R., He, Y., Eide, E.J., Hinz, W.A., Virshup, D.M., Ptacek, L.J., and Fu, Y.H. (2001). An hPer2 phosphorylation site mutation in familial advanced sleep phase syndrome. Science *291*, 1040-1043.

van der Horst, G.T., Muijtjens, M., Kobayashi, K., Takano, R., Kanno, S., Takao, M., de Wit, J., Verkerk, A., Eker, A.P., van Leenen, D.*, et al.* (1999). Mammalian Cry1 and Cry2 are essential for maintenance of circadian rhythms. Nature *398*, 627-630.

Vanselow, K., and Kramer, A. (2007). Role of phosphorylation in the mammalian circadian clock. Cold Spring Harb Symp Quant Biol *72*, 167-176.

Vela-Bueno, A., Kales, A., Soldatos, C.R., Dobladez-Blanco, B., Campos-Castello, J., Espino-Hurtado, P., and Olivan-Palacios, J. (1984). Sleep in the Prader-Willi syndrome. Clinical and polygraphic findings. Arch Neurol *41*, 294-296.

Verrillo, E., Bruni, O., Franco, P., Ferri, R., Thiriez, G., Pavone, M., Petrone, A., Paglietti, M.G., Crino, A., and Cutrera, R. (2009). Analysis of NREM sleep in children with Prader-Willi syndrome and the effect of growth hormone treatment. Sleep Med *10*, 646-650.

Vgontzas, A.N., Bixler, E.O., Kales, A., Centurione, A., Rogan, P.K., Mascari, M., and Vela-Bueno, A. (1996). Daytime sleepiness and REM abnormalities in

Prader-Willi syndrome: evidence of generalized hypoarousal. Int J Neurosci *87*, 127-139.

Vielhaber, E., Eide, E., Rivers, A., Gao, Z.H., and Virshup, D.M. (2000). Nuclear entry of the circadian regulator mPER1 is controlled by mammalian casein kinase I epsilon. Mol Cell Biol *20*, 4888-4899.

Vitaterna, M.H., King, D.P., Chang, A.M., Kornhauser, J.M., Lowrey, P.L., McDonald, J.D., Dove, W.F., Pinto, L.H., Turek, F.W., and Takahashi, J.S. (1994). Mutagenesis and mapping of a mouse gene, Clock, essential for circadian behavior. Science *264*, 719-725.

Wang, N.J., Liu, D., Parokonny, A.S., and Schanen, N.C. (2004). High-resolution molecular characterization of 15q11-q13 rearrangements by array comparative genomic hybridization (array CGH) with detection of gene dosage. Am J Hum Genet *75*, 267-281.

Wevrick, R. (2008). Prader-Willi Syndrome. In P.R Beales, I.S. Farooqi, S. O'Rahilly, Genetics of Obesity Syndromes, 223-249. USA: Oxford University Press.

Wurts, S.W., and Edgar, D.M. (2000). Circadian and homeostatic control of rapid eye movement (REM) sleep: promotion of REM tendency by the suprachiasmatic nucleus. J Neurosci *20*, 4300-4310.

Yang, Z., and Sehgal, A. (2001). Role of molecular oscillations in generating behavioral rhythms in Drosophila. Neuron *29*, 453-467.

Yoo, S.H., Ko, C.H., Lowrey, P.L., Buhr, E.D., Song, E.J., Chang, S., Yoo, O.J., Yamazaki, S., Lee, C., and Takahashi, J.S. (2005). A noncanonical E-box enhancer drives mouse Period2 circadian oscillations in vivo. Proc Natl Acad Sci U S A *102*, 2608-2613.

Yoshitane, H., Takao, T., Satomi, Y., Du, N.H., Okano, T., and Fukada, Y. (2009). Roles of CLOCK phosphorylation in suppression of E-box-dependent transcription. Mol Cell Biol *29*, 3675-3686.

Zheng, X.Z., Zhang, Y.P., Zhu, D.L., and Geng, Z.C. (1999). The period gene: high conservation of the region coding for Thr-Gly dipeptides in the Drosophila nasuta species subgroup. J Mol Evol *49*, 406-410.

Zylka, M.J., Shearman, L.P., Weaver, D.R., and Reppert, S.M. (1998). Three period homologs in mammals: differential light responses in the suprachiasmatic circadian clock and oscillating transcripts outside of brain. Neuron *20*, 1103-1110.